Investigating the role of Hsp90 and LRP1 in FN matrix dynamics

A thesis submitted in the fulfilment of the requirements for the degree of

Master of Science in Biochemistry

of

Rhodes University

by

Natasha Marie-Eraine Boël

December 2015

ABSTRACT

Fibronectin (FN), a matrix protein responsible for regulating processes including migration and differentiation, is secreted as a soluble dimer which is assembled into an insoluble extracellular matrix. The dynamics of FN matrix assembly and degradation play a large role in cell migration and invasion contributing to the metastatic potential of cancer cells. Previous studies from our group have shown the direct binding of Hsp90 and FN *in vitro* and that inhibition of Hsp90 with novobiocin (NOV) caused internalisation of the FN matrix. However, the receptor mediating this internalisation is currently unknown. Low density lipoprotein 1 (LRP1) is a likely candidate as it is a ubiquitous receptor responsible for regulating internalisation of diverse ligands and is known to bind both Hsp90 and FN. We used wild type and knockout LRP1 cell lines to study the endocytosis of FN via this receptor. Here, we demonstrate that LRP1-deficient cells accumulated greatly increased levels of FN and were found to be less sensitive to pharmacological inhibition of Hsp90 by NOV. LRP1-expressing MEF-1 and Hs578T breast cancer cells experienced an increase in total FN in response to NOV, at concentrations below the EC50 value, followed by a dose-dependent loss of FN. We attributed greater FN levels to a loss of extracellular FN matrix coupled with increased internalisation of FN. Cell-surface biotinylation and DOC assays showed that loss of extracellular FN was specific to LRP1-expressing MEF-1 cells. Furthermore, we demonstrate that the loss of extracellular FN is not affected by changes in FN mRNA levels as determined by qRT-PCR, and that treatment with NOV resulted in the accelerated degradation of FN in the presence of cycloheximide. Immunoprecipitation studies reveal a putative complex exists between FN, Hsp90 and LRP1 in both cancer and non-cancer cells which is not perturbed by NOV. Western analyses revealed increased proteolytic processing of LRP1 in response to NOV which we proposed, based on literature, to modulate signalling pathways as a potential mechanism for regulating FN turnover. Moreover, using wound healing assays we identified increased migration to be one of the consequences associated with loss of extracellular FN by Hsp90 inhibition but only in cells containing LRP1. In summary, this study provides new insights into the Hsp90-LRP1 mediated loss of FN matrix and also reveals for the first time the functional consequence related to FN turnover by NOV was an increase in migration in LRP1-expressing cells.

DECLARATION

I declare that this thesis is my own, unaided work. It is being submitted for the degree of Master of Science of Rhodes University. It has not been submitted before for any degree or examination at any other university.

Ms Natasha Marie-Eraine Boël

December 2015

Grahamstown, South Africa

TABLE OF CONTENTS

LIST OF FIGURES

LIST OF TABLES

LIST OF ABBREVIATIONS

17-AAG	17-(Allylamino)-17-demethoxygeldanamycin
17-DMAG	17-(Dimethylaminoethylamino)-17-demethoxygeldanamycin
ADAMTs	A Disintegrin And Metalloproteinase with Thrombospondin Motifs
Akt	Protein kinase B
Amp	Ampicillin
ANOVA	Analysis Of Variance
ATCC	American Type Culture Collection
ATP	Adenosine Triphosphate
ATPase	Adenosine 5` Tripohsphatase
BACE-1	β-site of Amyloid precursor protein Cleavage Enzyme-1
BSA	Bovine Serum Albumin
CHX	Cycloheximide
CLQ	Chloroquine
CTD	C-terminal Domain
DMEM	Dulbecco's Modified Eagle Medium
DNA	Deoxyribonucleic Acid
DTSSP	3,3'-Dithiobis[sulfosuccinimidyl]propionate
DOC	Sodium deoxycholate
EC50	Effective Concentration resulting in a 50% reduction in cell viability
ECM	Extracellular matrix
ECL	Enhanced chemiluminescence
EDTA	Ethylenediaminetetraacetic Acid
EGFR	Epidermal Growth Factor Receptor
ERK	Extracellular signal-regulated kinase
ET	Endotoxin
exFN	Extracellular fibronectin
FCS	Fetal Calf Serum
FN	Fibronectin
GA	Geldanamycin
HCl	Hydrochloric acid

HER-2	Human Epidermal growth factor Receptor 2
HIS	Histidine
Hop	Hsp70/Hsp90 organizing protein
HSF	Heat Shock Factor
Hsp	Heat shock protein
HSR	Heat Shock Response
HRP	Horseradish Peroxidase
IB	Immunoblot
Ig	Immunoglobulin
inFN	Intracellular fibronectin
IP	Immunoprecipitation
IPTG	Isopropyl β-D-1-thiogalactopyranoside
kDa	Kilodalton
LDL	Low-density lipoprotein
LPS	Lipopolysaccharide
LRP1	Low density lipoprotein Receptor-related Protein-1
LRP1-58	58 kDa fragment of LRP1
LRP1-85	85 kDa fragment of LRP1
LRP1-ICD	LRP1 intracellular domain
LRPab	LRP1 blocking antibody
LSM	Laser Scanning Microscope
MAPK	Mitogen Activated Protein Kinase
MEF-1	Murine Embryonic Fibroblast-1
MD	Mean distance
MMP	Matrix Metalloproteinase
mRNA	Messenger RNA
MW	Molecular Weight
NHS	N-Hydroxysuccinimide
NOV	Novobiocin
NFkB	Nuclear Factor kappa B
NP40	Nonidet-P-40
NTA	Nitrilotriacetic Acid

NTD	N-terminal Domain
PBS	Phosphate Buffered Saline
PCR	Polymerase Chain Reaction
PMSF	Phenylmethanesulfonylfluoride
q-RT-PCR	Quantitative Reverse Transcriptase-Polymerase Chain Reaction
RAP1	Receptor Associated Protein 1
RGD	Arginine-glycine-aspartic acid peptide
RIPA	Radio-immunoprecipitation assay
RTK	Receptor Tyrosine Kinase
SDS	Sodium-Dodecyl-Sulphate
SDS-PAGE	Sodium-Dodecyl-Sulphate Polyacrylamide Gel Electrophoresis
SN	Supernatant
SMC	Smooth Muscle Cell
TBS	Tris-Buffered Saline
TBST	Tris-Buffered Saline with Tween-20
TGF	Transforming Growth Factor
TIMPs	Tissue Inhibitors of Metalloproteinases
tPA	Tissue-type Plasminogen Activator
TRAP1	Tumor necrosis factor type 1 Receptor Associated Protein
UNT	Untreated
uPA	Urokinase-type Plasminogen Activator
uPAR	Urokinase-type Plasminogen Activator Receptor
UK	United Kingdom
USA	United States of America
UV	Ultra-violet
WB	Western Blot
YT	Yeast Tryptone

LIST OF SYMBOLS

α	Alpha
β	Beta
°C	Degree Celsius
m	Metres
µm	Micrometres
M	Molar
mM	Millimolar
µM	Micromolar
nM	Nanomolar
g	Grams
mg	Milligrams
µg	Micrograms
L	Litres
ml	Millilitres
µl	Microlitres
kDa	Kilodaltons
Da	Daltons
min	Minutes
hrs	Hours
%	Percent or g/100 ml
U	Units
x *g*	Relative centrifugal force to gravity
rpm	Revolutions per minute
v/v	Volume per volume
w/v	Weight per volume
V	Volts
pH	Hydrogen ion concentration

ACKNOWLEDGMENTS

To my supervisor, Dr Adrienne Edkins: I cannot thank you enough for your constant support and encouragement these past three years. Your passion and enthusiasm for what you do have truly been an inspiration for me. I am so grateful for your mentorship.

To Rhodes University and the National Research Foundation: This work would not have been possible without your financial support. Thank you for affording me this opportunity to pursue my dreams.

To my fellow lab members: I am so fortunate to have been part of such an incredible research group, who have come to be my family. Each and every one of you have played such a huge part in my life. Thank you all for your friendship and support.

To Dr Jason Sterrenberg: Yes, you deserve a special mention! You have been my biggest supporter and have always helped me to see the potential in myself. Thank you for all our chats about everything (and nothing), and for your endless advice, encouragement and support.

To my parents, Henny and Tina Boël: You have always had so much faith in me and I hope to continue to make you proud. Thanks mum and dad for your unfailing love and support. I would also like to thank the Lord for his guidance throughout my life. I know all this was made possible through YOU.

Chapter 1. LITERATURE REVIEW

1.2 HEAT SHOCK PROTEINS

Certain heat shock proteins (HSP) belong to a group of proteins called molecular chaperones which are constitutively expressed in cells or accumulate when subjected to stresses, such as heat, hypoxia, nutrient deprivation and carcinogens (Chaudhuri & Paul, 2006; Hartl & Hayer-Hartl, 2002). These are regulatory proteins involved in protein homeostasis in the cell by assisting in maintaining proteins in their correctly folded and active states, as well as preventing their aggregation or denaturation under such stress conditions (Hartl *et al.,* 2011; Röhl *et al.,* 2013). Heat shock proteins were first identified in the early 1970s in *Drosophila* cells upon exposure to heat causing the overexpression of this group of proteins (Ritossa, 1962; Tissières *et al.,* 1974). Thus, when cells are exposed to stress conditions, members of the heat shock transcription factors (HSFs) are activated which induces a heat shock response (HSR) consequently triggering heat shock proteins (Hsps) to become overexpressed (Akerfelt *et al.,* 2010; Fulda *et al.,* 2010). HSF-1 is the one of the main regulators of this HSR (Anckar & Sistonen, 2011; Ruckova *et al.,* 2012). Of the molecular chaperones, the heat shock protein family is the largest and most extensively studied, comprising several subfamilies (Hsp100, Hsp70, Hsp90, Hsp60, small Hsps [Hsp10, Hsp27, Hsp40]), which are primarily classified according to their approximate molecular size (Edkins & Boshoff, 2014). Most Hsps require the free energy of ATP to assist in protein folding, whilst some such as the smaller Hsps have the ability to function independently of ATP (Jakob *et al.,* 1993; Obermann *et al.,* 1998; Chaudhuri & Paul, 2006).

1.2.1 Heat Shock Protein 90 (Hsp90)

Hsp90 is a ubiquitously expressed molecular chaperone responsible for maintaining the active conformation and proteolytic turnover of about 300 intracellular proteins termed ‘clients’ many of which are involved in various signal transduction pathways (Khalil *et al.,* 2011). Hsp90 is constitutively and abundantly expressed in eukaryotic cells under normal conditions, constituting 1-2% of total cellular protein, and functions in facilitating the later stages of protein folding and maintaining clients in easily activated states (Garrido *et al.,* 2001). However, upon exposure to stress cells begin to over express Hsp90 to levels comprising 4-6% of total cellular protein (Garrido *et al.,* 2001; Solit & Chiosis, 2008; Li *et al.,* 2011). A wide range of structurally unrelated client proteins are known to interact with Hsp90, including

transcription factors, kinases and steroid hormones (Whitesell & Lindquist, 2005). A comprehensive and frequently updated list of *bona fide* Hsp90 interacting proteins can be found on the Picard web page (http://www.picard.ch/downloads/Hsp90interactors.pdf). Hsp90 exists as a homodimer with each monomer having three highly conserved domains; a 25 kDa ATP binding N-terminus which is connected via a charged linker region to the 35 kDa middle domain, and the 12 kDa C-terminal dimerization domain which has an alternative ATP binding site (Nemoto & Sato, 1998). There is also an extension at the extreme end of the C-terminus containing a conserved MEEVD amino acid motif to which co-chaperones containing the tetratricopeptide (TPR) repeat (such as Hop, CHIP and DNAJC7) bind (Hartl *et al.,* 2011).

Hsp90 is a central component of the network of molecular chaperones in the cell which cooperates with Hsp70 and other co-chaperones and cofactors to regulate the folding and activity/stability of client proteins (Pratt, 1998; Mayer & Bukau, 2005; Taipale *et al.,* 2012). This multi-chaperone complex was reported in the late 1970s for the group of steroid hormone receptors (Chang *et al.,* 1997). More than 20 co-chaperones have been identified to regulate the function of Hsp90, (Li & Buchner, 2013) the protein Hop (Hsp70-Hsp90 organising protein) being one of the central co-chaperones in the Hsp90 cycle (Chang *et al.,* 1997). Two monomers of Hsp90 associate in an open, inactive form with the C-termini constitutively dimerized and the N-termini separate (Csermely *et al*., 1998; Wandinger *et al.,* 2008). Hsp70 binds the client protein in an ATP-dependent manner assisted by the chaperone activity of Hsp40. This complex then delivers the client protein to Hsp90 via Hop which stabilizes that Hsp90 dimer and inhibits the ATPase activity (Chang *et al.,* 1997; Wegele *et al.,* 2004). The Hsp70-Hop complex consequently dissociates and is replaced by p23 and immunophilins to generate a closed complex whereby the N-termini of Hsp90 dimerises and clamps the client protein (Pratt, 1998). Upon ATP hydrolysis, the client protein is then released and the Hsp90 dimer adopts an open conformation again to accept another substrate (Hendrick & Hartl, 1995; Richter & Buchner, 2001). Two cytosolic Hsp90 isoforms have been identified; the inducible Hsp90α and constitutive Hsp90β, which are encoded for by separate genes and have high sequence similarity (Pepin *et al.,* 2000; Sreedhar *et al.,* 2004). In knockout studies, Hsp90β, but not Hsp90α was shown to be essential for placental development in mice and is embryonic lethal (Voss *et al.,* 2000). Hsp90 isoforms have also been found in the endoplasmic reticulum and the mitochondrial matrix termed glucose regulated protein 94 (Grp94) and

Hsp75/Trap1 respectively. Hsp75 is unique in its LxCxE motif, which binds the SV40 T-antigen binding domain of retinoblastoma protein (Chen *et al.,* 1996), and absence of the highly charged linker region (Felts *et al.,* 2000). A fifth isoform currently under debate is Hsp90N, which is distinct from cytosolic Hsp90 by having a unique 30 amino acid hydrophobic sequence at the N-terminus (which replaces the 25 kDa ATP binding site) (Grammatikakis *et al.,* 2002). It has been suggested that this form of heat shock protein is found on the plasma membrane of cancer cells (Sreedhar *et al., 2*004). Since the Hsp90N lacks the highly conserved N-terminal ATP binding pocket (which is necessary for most chaperone functions) it suggests then that Hsp90N would in fact be non-functional from the traditional perspective of Hsp90 chaperone activity (Schweinfest *et al.,* 1998). Studies by Grammatikakis (2002) have however shown that Hsp90N can carry out functions previously thought to be solely dependent on the N-terminus, such as binding and activating oncogenes independently of co-chaperones. Conversely, it has been argued that Hsp90N is in fact not an additional Hsp90 isoform but rather a chromosomal rearrangement which occurred in a single cell line (Zurawska *et al., 2*008). Thus, there is still much controversy as to whether it should be classified as a distinct gene or whether the isoform arises from processing of one of the other Hsp90 transcripts only in specific contexts.

1.2.2 Hsp90 and cancer

Cancer is a disease which results from the uncontrolled growth of cells and spread around the body and is defined by the six common hallmarks as defined by Hanahan and Weinberg (Hanahan & Weinberg, 2000). Several Hsp90 clients are *bona fide* oncoproteins linked to these six cancer hallmarks, including HER-2, Raf-1, Akt and p53 (Pearl *et al.,* 2008; Whitesell & Lindquist, 2005). Whilst Hsps are essential for normal cell function they also play a pivotal role in maintaining transformation and have been implicated in cancer and cancer metastasis by increasing the survival and growth potential of cancer (Sidera *et al.,* 2008). It is reported that most cancer deaths are as a result of metastases as opposed to the primary tumour (Weigelt *et al.,* 2005; Siegel *et al.,* 2015). Tumours, are often exposed to increased stress conditions including heat shock, hypoxia, nutrient deprivation and acidosis (Bagatell & Whitesell, 2004). This results in larger numbers of destabilised or aggregated proteins, and an increased dependency on Hsp90 chaperoning function in order to survive and maintain homeostasis (Hartl & Hayer-Hartl, 2002; Sreedhar *et al.,* 2004). More than 100 clients of

Hsp90 are mutated or overexpressed in cancers including melanoma, breast, lymphoma and colon carcinomas (Eustace *et al.,* 2004; Sidera *et al.*, 2004; Tsutsumi *et al.,* 2009). Thus the inhibition of Hsp90 has been targeted for development of anticancer drugs (Tsutsumi & Neckers, 2007; Sims *et al., 2*011). Due to the high levels of expression in cancer cells and contribution to cancer cell biology, Hsp90 has consequently been dubbed the "cancer chaperone" (Donnelly & Blagg, 2008). Hsp90 assists in various aspects of the metastatic process, including cell adhesion and motility, making it an attractive target for anti-metastatic therapy. The ongoing challenge faced is minimizing interference of the chaperone function of Hsp90 in normal cells, whilst selectively targeting cancer-related Hsp90 in tumour cells (Bagatell & Whitesell, 2004).

1.2.3 Extracellular Hsp90 (eHsp90)

Numerous studies have focussed on identifying the roles of intracellular Hsp90, but much less is known about the extracellular pool of Hsp90. In 1986, Ullrich and colleagues identified Hsp90 on the surface of mouse cells (Ullrich *et al.,* 1986). Since then Hsp90 has been detected by several groups in the extracellular space and on the surface of cells (Eustace *et al.,* 2004; Hunter *et al.,* 2014; Sidera *et al.,* 2004). The term 'extracellular' is often used interchangeably to describe both membrane-bound and extracellular soluble forms of Hsp90. It is not known by what mechanism it localizes to the extracellular space, but since Hsp90 lacks a secretory signal sequence it must follow an alternative pathway to that of the canonical Golgi transport secretory pathway. Thus, McCready and colleagues (2010) suggested that extracellular Hsp90 (eHsp90) is secreted via exosomes. Alternatively, cell lysis or proteolytic cleavage from the cell surface may release Hsp90 into the extracellular space (Althoff *et al.,* 2001; Calderwood *et al.,* 2007). eHsp90 is thought to derive from the cytosolic Hsp90α and Hsp90β isoforms (Eustace *et al.,* 2004). Some groups have reported the presence of both isoforms in the extracellular space (Hegmans *et al.,* 2004) whilst others have shown that only Hsp90α, and not Hsp90β, exists on the cell surface (Li *et al.,* 2007; Wang *et al.,* 2009). In a study by Eustace *et al.* (2004) it was found that Hsp90α, but not Hsp90β, was secreted to the extracellular space and was able to degrade the matrix by activation of MMP2 (which digests components of the ECM allowing for access to the vasculature system and metastasis). They also showed that Hsp90 inhibition resulted in decreased MMP2 activity which resulted in a loss of cancer invasiveness. Song and colleagues reported that eHsp90 activates MMP2 and also serves as a

substrate for proteolytic cleavage by MMP2 (Song *et al.,* 2010). The predominant function of eHsp90 is suggested to be in the promotion of cell motility and tissue repair, as in the case of wound healing. eHsp90 is thought to chaperone a small group of extracellular client proteins relative to intracellular Hsp90 (McCready *et al.,* 2010; Hunter *et al.,* 2014). Some authors have argued that eHsp90 functions via a receptor mediated induction of signalling pathways, distinct from the chaperoning function of intracellular Hsp90 (Hance *et al.*, 2014). Sidera and colleagues reported eHsp90 binding of HER-2 to increase cell invasion and migration (Sidera *et al.,* 2008). Hsp90 is known to bind low density lipoprotein receptor-related protein-1 (LRP1) (Basu *et al.,* 2001; Gopal *et al.,* 2011), the specific binding site of which has not yet been located on LRP1 (Li *et al.,* 2012). Several groups reported that eHsp90α was able to induce cell migration via its interaction with LRP1 (Chen *et al.,* 2010a; Cheng *et al.,* 2008). It was reported that these pro-motility effects were induced by the binding of a 115 amino acid fragment (termed F-5) located at the boundary between the middle domain and linker region on eHsp90 to LRP1 to activate the various downstream signalling pathways required to initiate cell motility (Cheng *et al.,* 2008; Chen *et al.,* 2010a; Li & Reynolds, 2012). A novel eHsp90 cross-membrane signalling pathway involving the extracellular and intracellular domains of LRP1 has been established to activate Akt kinases stimulating cell migration (Tsen *et al.,* 2013). Although mechanistic reports of eHsp90 functions are scarce and not yet fully elucidated, eHsp90 has been of much interest due to its role in cancer invasiveness. Patsavoudi and colleagues have showed that a cell-impermeable monoclonal antibody, 4C5, was able to reduce breast cancer cell invasion *in vitro* and *in vivo* by selectively binding eHsp90 at the surface of tumour cells (Sidera *et al.,* 2011). The presence of eHsp90 is not exclusive to tumour cells as several groups have reported Hsp90 to reside on the surface of normal cells including neural cells and human dermal fibroblasts (Sidera *et al.,* 2004; Stellas *et al.,* 2007; Li *et al.,* 2007). Additional roles for eHsp90 have also been demonstrated in the pathogenicity of viral and bacterial infections (Zügel & Kaufmann, 1999; Triantafilou & Triantafilou, 2004). This highlights an important role for eHsp90 in both normal and diseases states, however, considering certain tumour cells constitutively express eHsp90 to achieve cell invasion, targeting eHsp90 could prove to be a potential therapeutic strategy for cancer (McCready *et al.,* 2010; Li *et al.,* 2011).

1.2.4 Hsp90 inhibition

Due to the role of Hsp90 as a chaperone of oncogenes and/or tumor suppressors, Hsp90 has become an attractive drug target which has fueled the development of numerous Hsp90 inhibitors for cancer treatment. Hsp90 is in an activated form upon binding of co-chaperones and client proteins. Kamal and colleagues showed that Hsp90 in tumors consists largely of this activated form and that Hsp90 inhibitors selectively accumulate in tumors at least in part due to the high affinity, activated form of Hsp90 in tumor cells versus low affinity, inactive forms in normal cells (Kamal *et al.,* 2003). Inhibition of Hsp90 also renders tumor cells susceptible to treatment by chemotherapy and radiation. The motivation behind targeting Hsp90 inhibition for cancer therapy thus lies in its advantage in both depleting oncogenic proteins and interrupting multiple oncogenic pathways and the increased ATPase activity in cancer cells (Piper & Millson, 2011; Trepel *et al.,* 2010). The development of selective anti-cancer drug targets, such as trastuzumab, has had significant success however the need to target multiple oncogenic proteins and pathways has led to the increased research into Hsp90 inhibitor drugs, since Hsp90 is considered a central node in signalling pathways. Consequently, Hsp90 inhibitors are being tested for their anti-cancer efficacy in combination with these other treatments to create better outcomes (Sidera & Patsavoudi, 2014).

There are effectively two groups of Hsp90 inhibitors which target either the C-terminus or N-terminus of Hsp90. Geldanamycin (GA) was the first identified natural product Hsp90 inhibitors isolated from the fermentation broth of *Streptomyces* in 1970 (Deboer *et al.*, 1970). GA functions by mimicking ATP structure (Prodromou *et al.,* 1997) and preventing ATP binding at the N-terminus of Hsp90 resulting in client degradation (Grenert *et al.,* 1997; Grammatikakis *et al.,* 2002). Since then, various synthetic GA derivatives have been developed, including radicicol, 17-(Allylamino)-17-demethoxygeldanamycin (17-AAG), 17-(Dimethylaminoethylamino)-17-demethoxygeldanamycin (17-DMAG), and retaspamycin (Chiosis *et al.,* 2002). One of the major problems with Hsp90 inhibition has been in the generation of a heat shock response (HSR) brought about by specific binding to the N-terminal ATP-binding site of Hsp90 (Whitesell & Lindquist, 2005; Haggerty *et al.,* 2014). Additionally, many of the N-terminal inhibitors have poor solubility and hepatotoxicity in animal studies. The coumarin-containing antibiotic, novobiocin, was found to bind at a second ATP binding site at the C-terminus of Hsp90 (Marcu *et al.,* 2000). Novobiocin was originally used to treat

bacterial infections by inhibiting topoisomerase II (Burlison *et al.,* 2006). It was initially hypothesized to bind the N-terminal domain (NTD) of Hsp90 due to similarities with ATP, but was later shown to bind within the C-terminal domain (CTD) localized to residues 538-728 (Allan *et al.,* 2006; Kamal *et al.,* 2003). C-terminal inhibitors, in contrast to N-terminal inhibitors, do not induce the HSR (Burlison *et al.,* 2006; Eskew *et al.,* 2011) and are increasingly being pursued due to their better solubility and decreased hepatotoxicity in clinical trials. This type of inhibitor functions by an alternative mechanism, that is, by disrupting the dimerisation of Hsp90, as well as interfering with Hsp90 interaction with co-chaperones and some clients that bind the C-terminus such as HER2, p53 and Raf-1 (Trepel *et al.,* 2010). Several novobiocin analogues have since been developed including taxol and cisplatin created by modification of the core structure of novobiocin allowing for increased Hsp90 inhibition and degradation of client proteins (Donnelly & Blagg, 2008; Kusuma et al., 2011).

The dependency of Hsp90 on its co-chaperones has subsequently also allowed for targeted inhibition of the co-chaperone/Hsp90 interactions. Many of the co-chaperones identified contain a TPR domain which binds to the MEEVD motif of Hsp90. One such example of a co-chaperone type inhibitor is that of a TPR hybrid peptide developed in 2010 which inhibited the interaction of Hsp90 with TPR2A of Hop (Horibe *et al.,* 2011). Targeted inhibition of the Hsp90-client interactions have also been developed. Shepherdin is a compound which inhibits Hsp90 interaction with several clients such as survivin (an inhibitor of apoptosis) and in this way confers a degree of selectivity in tumor cells versus normal cells (Altieri, 2006). Sansalvamide A derivatives developed by McAlpine and colleagues were demonstrated to bind the middle domain of Hsp90 but disrupt the C-terminal interaction with co-chaperones via an allosteric mechanism (Alexander *et al.,* 2009; Vasko *et al.,* 2010). Also, more recently the targeted inhibition of extracellular Hsp90 has been largely explored and two cell-impermeable Hsp90 inhibitors have been described; DMAG-N-oxide (Tsutsumi *et al.,* 2009) and monoclonal antibody, 4C5 (Sidera *et al.,* 2004). Although some Hsp90 inhibitors have shown some clinical activity, none have been approved for clinical application in cancer treatments. The research in this field however is still ongoing and hopes of Hsp90 inhibitors as part of a combinatorial therapy approach are largely being investigated (Sidera & Patsavoudi, 2014).

1.3 EXTRACELLULAR MATRIX

The extracellular matrix (ECM) is the non-cellular component of tissues and organs, which exists to provide essential physical and biochemical cues for the cell. The ECM plays important roles in structural support and cell signalling, and contains proteins involved in regulating cell proliferation, migration, polarity and survival (Lin & Bissell, 1993; Hynes, 2009). The interaction of cells with the ECM is equally important for regulating these processes. Further, the bidirectional communication between the ECM and the actin cytoskeleton, mediated largely by transmembrane integrin receptors is important for cell adhesion and migratory functions (Bridgewater *et al.,* 2012; Frantz *et al.*, 2010). The importance of the ECM is made evident by the large array of diseases that may arise from abnormalities in the ECM including autoimmune and inflammatory diseases, cancer and atherosclerosis. Many factors influence the extracellular environment, including growth factors, ECM proteins, and matricellular proteins. The matricellular proteins are non-structural modulators of extracellular signals and are presumed to assist in providing a linkage between the ECM and cell surface receptors. These include thrombospondins, SPARC (Secreted Protein Acidic and Rich in Cysteine), osteopontins and tenascin-C (Bornstein & Sage, 2002). Some of the ECM proteins include collagen, fibrin, elastin, proteoglycans, fibronectin (FN), laminin, and vitronectin (VN), each of which play distinct roles in the extracellular space (Huang & Greenspan, 2012). Many of these ECM proteins contain multiple domains with specific binding sites for macromolecules or receptors (Hynes, 2009). Some of the functions of fibroblasts include: regulation of inflammation and wound healing, synthesis and deposition of ECM constituents including collagens and fibronectin, secretion of ECM-degrading proteases and growth factors for ECM homeostasis (Kalluri & Zeisberg, 2006). The ECM is highly dynamic and is constantly being remodelled to accommodate for its variety of functions. ECM remodelling occurs in both physiological and pathological cases (Bonnans *et al.,* 2014; Daley *et al.,* 2008). Tissue homeostasis requires a balance between ECM synthesis and degradation. Perturbing homeostasis by loss of function mutations or modifications of ECM molecules and excessive deposition or removal of ECM components results in progression of various disease states including fibrosis, cancer and other developmental abnormalities (Frantz *et al.,* 2010; Lu *et al.,* 2011). The recognised importance of the ECM in mediating disease has increased targeted therapies of the ECM (Theocharis *et al.,* 2015).

1.3.1 ECM and cancer metastasis

Cancer metastases are defined by the movement of tumour cells from its primary location to distant sites in the body where they form secondary tumours (Steeg, 2006). This process requires several steps including degradation of the extracellular matrix, tumour cell detachment from primary tumour and migration of cells in the blood stream, adhesion to tissues at a distant site and growth of secondary tumour (Steeg, 2006; Eustace *et al.,* 2004). Although matrix degradation is required for cancer cell metastasis, this process is also required for normal cellular processes including cell adhesion, differentiation and proliferation where there is a continuous turnover of matrix molecules (Sottile & Chandler, 2005). ECM remodelling can occur through extracellular proteases, including serine proteases, urokinase plasminogen activator (uPA), tissue-type plasminogen activator (tPA), and matrix metalloproteinases (MMPs), or by endocytosis and intracellular degradation (Sottile & Chandler, 2005). However, it is thought that these two mechanisms are not mutually exclusive. Loss of the matrix has been implicated in metastasis of tumours. In particular, the abnormal removal of ECM proteins has been shown to contribute to the onset or development of diseases including cancer (Galante & Schwarzbauer, 2007; Shi & Sottile, 2008). Tissue homeostasis is mediated by the secretion of MMPs, uPA and tPA which in turn are regulated by their corresponding inhibitor proteins: tissue inhibitors of metalloproteinases (TIMPs) and plasminogen activator inhibitors (Egeblad & Werb, 2002; Zhang *et al.,* 2013). Matrix degradation is important for the spread of cancer cells through the body; this degradation event is thought to promote invasion by triggering the activation and recruitment of certain proteases (MMPs, serine proteases, plasmin and cathepsin), all of which degrade the ECM and allow for cancer cells to migrate easily into the bloodstream and colonize tissue at distant sites (Stellas et al., 2010; Zhang et al., 2013). Certain growth factors are also liberated by cells during ECM degradation which further aids in the survival of these tumour cells (Steeg, 2006). The tumour stroma has been shown to exhibit some of the characteristics of a wound such as stiffening induced by ECM deposition and remodelling by fibroblasts (Pickup *et al.,* 2014). The ECM plays dynamic and opposing roles in regulating cell migration. A dense fibrillar network has been shown to serve as a barrier to migrating cells and degradation of the ECM is required to allow for paths in which cells can freely migrate (Egeblad *et al.,* 2010; Friedl & Gilmour, 2009). Others demonstrate that this ECM network

provides a scaffold on which cells can attach and subsequently migrate (McCarthy & Furcht, 1984; Rozario & DeSimone, 2010).

1.3.2 Fibronectin structure

Among the ECM proteins, fibronectin (FN) plays important roles in cell adhesion, motility, wound healing, oncogenic transformation and cell shape maintenance (Schwarzbauer, 1991; To & Midwood, 2011). FN is a 200-250 kDa glycoprotein, with only one FN gene in humans which can give rise to 20 potential FN isoforms through alternative splicing of the gene transcript (Kumazaki *et al.,* 1999). FN is a dimer composed of two large monomeric subunits; each monomer is made up of tandem repeats of three domain types (I-III) (Lemmon *et al.,* 2011) as illustrated in Figure 1. It is so versatile in its functions because it has co-existing binding sites present at its N-terminal domain for various molecules including heparin, actin, DNA and collagen, as well as cell surface proteins (Gutman *et al.,* 1986). Cysteines (indicated by "-S" in Figure 1) present in the C-terminal domain are responsible for joining FN monomers via disulphide bonds (Schwarzbauer, 1991). The 70 kDa N-terminal domain is essential for fibril formation; FN lacking this domain is incapable of assembly (Lemmon *et al.,* 2011; Schwarzbauer, 1991). In particular, the domain type I_{1-5} repeats is considered crucial for FN matrix assembly (Lemmon *et al.,* 2011). The different isoforms of fibronectin are generated by alternative splicing in the regions indicated as A, B and V in Figure 1.

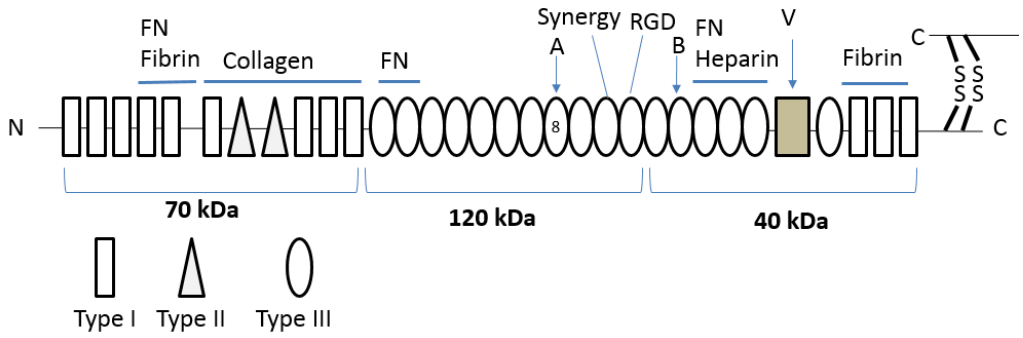

Figure 1: Domain structure of fibronectin with associated binding sites.

The FN glycoprotein is comprised of a series of repeating structures: 12 FN type I, 2 FN type II and 17 type III repeats with an alternatively spliced regions labelled A, B and V. These are organised into functional domains: 70 kDa N-terminal domain, 120 kDa central binding domain (CBD) and 40 kDa heparin binding domain each of which bind multiple partners. Two FN monomers bind by disulphide bonds, S-S, at the C-terminus to form a dimer. (Adapted from Wierzbicka-Patynowski and Schwarzbauer, 2003; Schwarzbauer and DeSimone, 2011).

1.3.3 Fibronectin matrix synthesis

The two forms of fibronectin include its plasma soluble heterodimeric form and cellular insoluble form, which can be separated based on their differential solubility in deoxycholate (Gutman *et al.,* 1986; To & Midwood, 2011). A much larger heterogeneous population exists for cellular FN due to cell-type specific and species-specific splicing. The exact mechanism of fibronectin fibril formation is still unknown, but it is thought that cellular fibronectin is synthesized by various cells (including fibroblasts, myocytes and endothelial cells among others) and secreted by cells as a soluble dimer (Lemmon *et al.,* 2011). FN matrix assembly is a stepwise process which may take as little as 20 minutes (To & Midwood, 2011). Initiation of this process is thought to be the binding of 70 kDa FN domain to cell surface receptors, possibly integrins (McKeown-Longo & Mosher, 1985; Takada *et al.,* 2007). Integrins are the principal transmembrane protein receptors which provide a linkage between the ECM outside the cell and the cytoskeleton inside (To & Midwood, 2011). The binding of FN to integrins induces conformational changes in the actin cytoskeleton which causes receptor clustering. Binding of the RGD (Arg-Gly-Asp) and synergy motifs on FN to $\alpha_5\beta_1$ integrin transmits tension to the fibronectin molecules and stretches them, thereby exposing other FN-association binding sites in the molecule (Mosher *et al.,* 1991; Theocharis *et al.,* 2015). This allows for the FN molecules to bind directly to one another and recruit additional FN molecules to form a fibril, which can be further propagated by the continual addition of FN dimers (Figure 2A) (Erickson, 2002). The exact process of conversion from soluble to insoluble FN and the proteins involved in crosslinking of FN fibrils is still under investigation (Wierzbicka-Patynowski & Schwarzbauer, 2003; Ohashi & Erickson, 2009). Interaction of FN with other ECM proteins is also required in the formation of fibrils between adjacent cells to create a meshwork, resulting in an insoluble matrix (Rozario & DeSimone, 2010). This process is termed fibrillogenesis and is tightly regulated by molecules such as transforming growth factor (TGFβ1) which upregulates FN expression, or MMP2/9 which degrades FN (Wierzbicka-Patynowski & Schwarzbauer, 2003; Galante & Schwarzbauer, 2007).

1.3.4 Fibronectin turnover

Fibronectin is produced as a soluble protein which is polymerized into insoluble fibrillar structures that form the bulk of the ECM. It is this fibrillar form that plays the biggest functional role in the cell (Mosher *et al.,* 1991). The deposition of ECM molecules including

collagen and thrombospondin have been shown to be dependent upon the presence of fibronectin fibrils (Sottile & Hocking, 2002). Treatment of cells with a polyclonal antibody to fibronectin inhibited polymerization of fibronectin into matrix, and FN was found to be endocytosed and localized with lysosomes (Villiger *et al.,* 1981; McKeown-Longo & Mosher, 1983; Sottile & Hocking, 2002). This highlighted a major role for fibronectin in the stability and organization of the ECM although, the exact processes that regulate FN catabolism and turnover are not yet well understood. Since FN binds integrins, particularly the $\alpha_5\beta_1$ integrin, during fibril formation, it is possible that FN becomes internalised with the constitutive endocytosis-recycling pathway of certain integrins (Bretscher, 1989; Shi & Sottile, 2008; Sottile & Chandler, 2005). ECM fibronectin consists of large fibrils of high molecular weight multimers which require initial proteolysis into differentially sized FN fragments (120 kDa, 70 kDa and 40 kDa) before endocytosis (Figure 2B) (Kenny *et al., 2*008; To & Midwood, 2011). Studies by Salicioni *et al.,* (2002) have shown that FN accumulates in the extracellular space in LRP1-deficient CHO/MEF cells. Thus, an alternative or additional pathway to the integrin-mediated pathway, may involve LRP1. Also, LRP1 mediates catabolism of FN thus LRP1 serves as a potential regulator of FN turnover (Salicioni *et al.,* 2002). However, LRP1 may not be the only receptor for FN uptake, as Gaultier *et al.,* (2010) showed that in LRP1-deficient fibroblasts the increased remodelling of FN was dependent on presence of uPA and the urokinase type plasminogen activator receptor (uPAR). Actin cytoskeleton rearrangements have also been shown to play a role in FN assembly (Daley et al., 2008). Activation of Rho GTPases induces changes in actin organization and enhances FN assembly; the inhibition of actin organisation has been shown to promote endocytosis of FN and its subsequent degradation (Wierzbicka-Patynowski & Schwarzbauer, 2003).

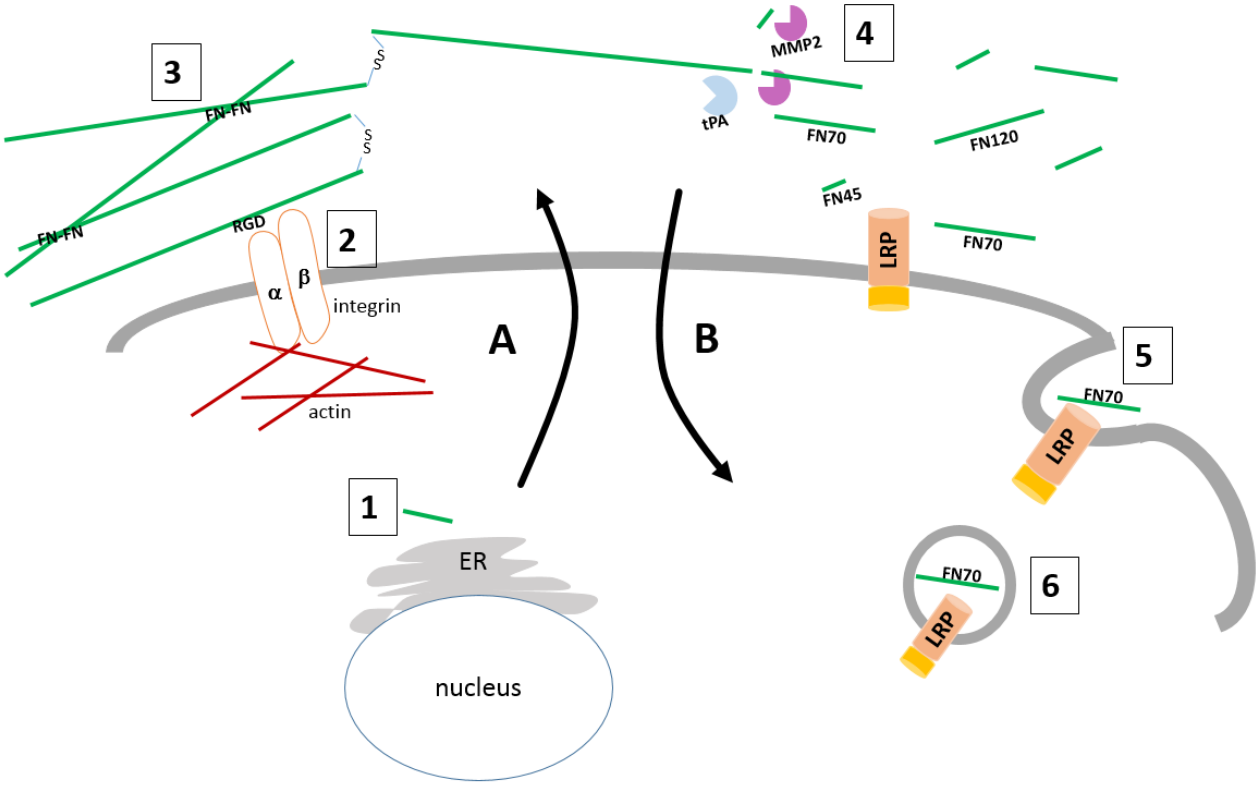

Figure 2: Proposed role of integrins and LRP1 in fibronectin turnover.

A) Fibrillogenesis: (1) Soluble FN is exported to the cell surface, (2) Integrins bind the RGD and synergy motifs on FN and together with actin filaments cause the stretching of fibronectin, 3) which exposes its self-association sites to allow for addition of FN dimers to form an insoluble matrix. **B)** Matrix Degradation: (4) Proteolytic enzymes (MMP2 and uPA amongst others) cleaves fibronectin into smaller fragments (120, 70, 40 kDa). (5) Upon binding LRP1, FN is endocytosed and (6) delivered to lysosomes for degradation whilst LRP1 is recycled to the cell surface.

1.3.5 FN and cancer progression

FN has been described to have tumour suppressor characteristics due to decreased adhesiveness and a reduced ability of tumour cells to deposit a FN matrix (Ryu *et al.,* 1999). FN expression has interestingly been shown to correlate with a poor prognosis in breast cancer and enhance cancer cell proliferation (Ioachim *et al.,* 2002). Conversely, other studies have shown FN expression to be inversely associated with the clinical outcome of breast cancer patients and inhibit cell proliferation and growth (Bae *et al.,* 2013; Swiatoniowski *et al.,* 2005). Previous studies have shown that FN promotes cell invasion and migration via upregulating MMP2 and MMP9 levels in cancer (Lu *et al.,* 2011). FN fragments generated from MMP cleavage have also been shown to have pro-migratory functions and stimulate FN matrix remodelling by activating the p38 MAPK pathway (Bourdoulous *et al.,* 1998; Forsyth *et al.,* 2002).

1.4 LOW DENSITY LIPOPROTEIN RECEPTOR RELATED PROTEIN (LRP1)

The low density lipoprotein (LDL) receptor family consists of more than more than 7 receptors including the LDL receptor, very low density lipoprotein (VLDL) receptor, LRP1, LRP1B, LRP2 (megalin/gp330), LRP5, LRP6, and LR11 (Strickland *et al.,* 1990; Kounnas *et al.,* 1995; Ranganathan *et al.,* 2011). LRP1, also termed CD91, is a multi-ligand transmembrane receptor, mediating the internalisation of proteinases, proteinase-inhibitor complexes (PAIs), lipoproteins, ECM proteins and bacterial toxins and viruses (Herz & Strickland, 2001; Strickland *et al.,* 1995). A list of some of these LRP1 ligands is provided in Table 1. Not only has LRP1 been shown to serve as an endocytic receptor, but also as a signalling receptor in modulating various cellular processes such as cell migration and invasion (Geer, 1999; Boucher & Herz, 2011). LRP1 plays diverse roles in various pathological diseases including inflammation, atherosclerosis, neurodegeneration and cancer (Lillis *et al., 2*008). Studies by Herz *et al.,* (1991) have shown that targeted disruption of the LRP1 gene in mice led to lethality, thereby suggesting the biologically important role for this receptor in early development.

Table 1: LRP1 interacting proteins

Protein	Function	Reference
ApoE	Lipoprotein metabolism	Kowal *et al.,* 1989
α_2M^*	Proteinase inhibitor	Strickland *et al.,* 1990
tPA	Fibrinolysis	Bu *et al.,* 1992
uPA	Cell migration, wound healing	Nykjaer *et al.,* 1992
MMP 9	ECM degradation, metastasis	Hahn-Dantona *et al.,* 2001
PAI-1	Regulates tPA/uPA activity	Nykjaer *et al.,* 1992
APP (β-amyloid precursor protein)	Alzheimer's disease pathogenesis	Kounnas *et al.,* 1995
Thrombospondin 1/2	Collagen assembly	Mikhailenko *et al.,* 1995
RAP	Chaperone	Herz *et al.,* 1991
Hsp90	Chaperone	Basu *et al.,* 2001
Gp96	Chaperone	Binder *et al.,* 2000
Fibronectin	ECM scaffold, adhesion, migration	Salicioni *et al.,* 2002
Lactoferrin	Antibacterial	Vash *et al.,* 1998
Pseudomonas endotoxin A	Bacterial toxin, infection	Kounnas *et al.,* 1992
HIV Tat protein	Transactivator of viral genes	Liu *et al.,* 2000

LRP1 is a large transmembrane receptor, synthesised as a 600 kDa precursor protein and processed in the trans-Golgi to form its 515 kDa extracellular and 85 kDa cytoplasmic domains which associate non-covalently (Herz *et al.,* 1988). The LRP1 structure illustrated in Figure 3 displays its five composing units. The N-terminal 515 kDa α-subunit contains the four ligand binding domains (I-IV) and is solely extracellular. The C-terminal 85 kDa β-subunit contains an extracellular part, a transmembrane spanning domain and a cytoplasmic intracellular domain containing 1 to 3 NPxY motifs that serve as endocytosis signals which target the receptor to clathrin coated pits (Strickland *et al.,* 1995). Ligand binding is regulated, primarily during export of LRP1 to the cell surface, by the receptor-associated protein (RAP) which has a high binding affinity (K_d = 1-10 nM) for LRP1 (Iadonato *et al*., 1993; Bu & Marzolo, 2001). RAP was identified when co-purified with LRP1 in human placenta (Herz *et al., 1*991). The major function of RAP is to serve as a chaperone by transiently binding newly synthesized LRP1 to assist in its transport from the ER to the Golgi without interference from other ligands binding, thereby enabling LRP1 to be successfully delivered to the plasma membrane (Lillis *et al., 2*008). Tissue transglutaminase (tTG) interacts directly with LRP1 and promotes association with β1 integrins and the ECM (Zemskov *et al., 2*007).

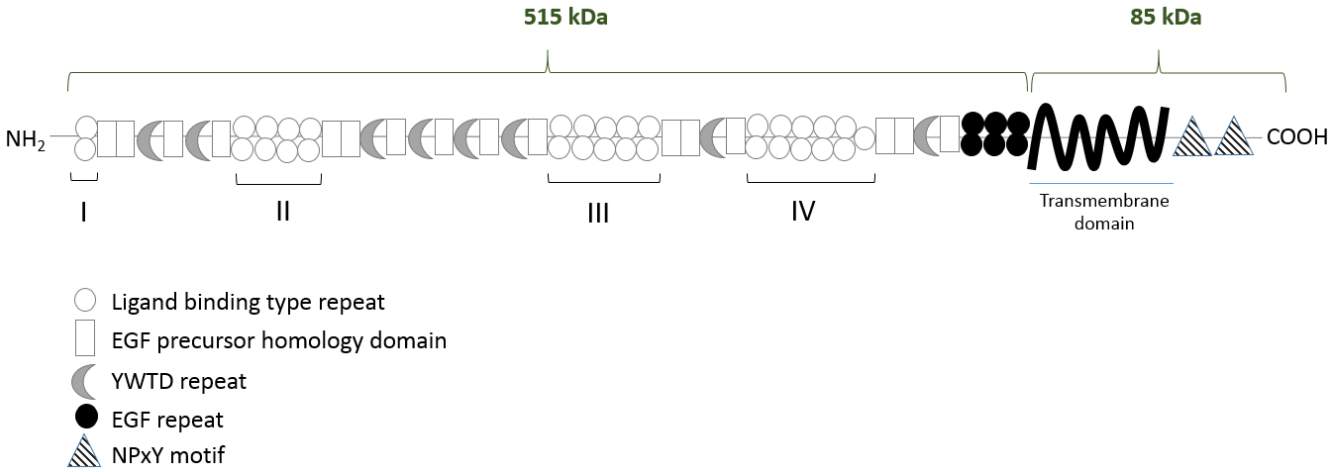

Figure 3: Structure of the 600 kDa low density lipoprotein receptor related protein (LRP1).

Cysteine rich ligand-binding type repeats (white circles) are arranged in four clusters (I-IV) along the extracellular 515 kDa domain. Each cluster is followed by 1-4 EGF homology domains (white rectangle and black circles) and an YWTD repeat (grey half-moon). The transmembrane domain spans the membrane bilayer and is followed by the 85 kDa intracellular domain containing the NPxY motifs (striped triangles). [Adapted from Herz and Strickland, 2001].

The extracellular α-chain contains four ligand-binding domains (clusters I-IV on Figure 3). Most ligands bind clusters II and IV, which are flanked by epidermal growth factor homology domains (Obermoeller-McCormick *et al.,* 2000). Interestingly, the cytoplasmic β-chain has been shown to bind adaptor and scaffold proteins via its NPxY motifs and serine/tyrosine residues which links the receptor to other membrane proteins or initiates signalling cascades within the cell (Boucher & Herz, 2011; Guttman *et al.,* 2009). Phosphorylation of the serine and/or tyrosine residues, in particular Tyr 4507, allows for interaction of the cytoplasmic domain with adaptor proteins such as FE65 for cell signalling (van der Geer, 1999; Li & Bu, 2001). Thus, LRP1 is implicated in two major physiological processes- endocytosis and regulation of signalling pathways. Willnow and colleagues (1994) were one of the first groups to develop LRP1 "mini-receptors" whereby various clusters of ligand-binding repeats were fused to the intracellular domain and tested for their ability to bind and internalize various ligands following their expression in cells. They showed that some ligands occupied distinct binding sites on LRP1 whilst others competed for binding at a particular site. The ability of LRP1 to recognize over 40 structurally distinct ligands and bind them with high affinity lies in the unique contour surface and charge density of each of the repeats as identified by crystallographic and NMR studies (Huang *et al., 2*000). LRP1 cell-surface levelsare regulated by receptor-intermembrane proteolysis (RIP) involving shedding, which is a proteolytic cleavage that releases their extracellular/ectodomain (Quinn *et al.,* 1999). LRP1 also undergoes this shedding process yielding its 515 kDa α-chain by cleavage with MMPs, tPA, BACE-1 (β-site of amyloid precursor protein (APP) cleavage enzyme 1) and ADAMs (a disintegrin and metalloproteinase). Subsequent cleavage of the β-chain by further proteolysis yields additional smaller fragments termed LRP1 intracellular domain (LRP1-ICD) (Spuch *et al.,* 2012). The fate of the shed LRP1 515 kDa fragment of the ectodomain is not known but is thought to be able to still bind ligands, thereby reducing their interaction with the cell and regulating their endocytosis (Gaultier *et al.,* 2008; Gorovoy *et al.,* 2010). The shed LRP1-ICD has been shown to translocate to the nucleus where it interacts with various proteins and transcriptional modulators to regulate cell signalling and gene transcription (Kinoshita *et al.,* 2003; Zurhove *et al.,* 2008).

1.4.1 LRP1 in cell migration

Cell migration involves a series of events which involves cell surface receptors attaching and detaching to the ECM and is central to many biological and pathological processes including embryogenesis, tissue development, growth, wound healing, cancer metastasis, atherosclerosis, angiogenesis and invasion (Ridley *et al.,* 2003). Thus understanding the fundamental mechanisms that regulate migration is of great importance. Cell migration is a multi-step process involving the coordinated action of signalling networks and cytoskeleton dynamics (Friedl & Wolf, 2010). One of the first steps required in the migration process is acquisition of cell polarity whereby a leading edge and rear end of the cell is established (Ridley *et al.,* 2003). For migration to occur a protrusion must extend from the leading edge and adhere to its surroundings. These protrusions can be in the form of broad lamellipodia or spindle-like filopodia and are dependent on the organization of actin filaments (Ponti et al., 2004). Polymerization of the actin network at the leading edge drives the initial extension of the cell (Ponti *et al.,* 2004) Integrins are the major receptor family mediating migration by supporting adhesion to the ECM or other cells and creating a link with the intracellular actin filaments (Labrousse *et al.,* 2003; Webb *et al.,* 2002). Integrins are often recruited to the leading edge of migrating cells and have been shown to recruit proteases to enhance ECM turnover (Webb *et al.,* 2002). Tension is created in the cell causing cell contraction which allows for the rear end of the cell to detach and the cell moves forward over these protrusions. The migration is dependent on a variety of factors, most importantly are cell type and its surrounding environment (Ridley *et al.,* 2003). Weaver and colleagues were among the first to identify a role for LRP1 in cell migration, where they found that LRP1-deficient MEFs migrated faster than LRP1-expressing MEFs. They found this to be true only when migration took place on certain ECM substrates, including FN and vitronectin (Weaver *et al.,* 1997). The exact contribution of LRP1 in this process is not well understood but one of the ways it is thought to stimulate migration is via binding of ligands to LRP1 thereby inducing cell signalling cascades. One such example of this demonstrated by Orr and colleagues was the increased cell migration observed in MEF by thrombospondin signalling which was further blocked by the addition of RAP (Orr *et al.,* 2003). Another study similarly reported that abrogation of LRP1 expression inhibited cell migration in thyroid carcinoma cells, despite increased MMP2 and uPA levels (Dedieu *et al.,* 2008). In contrast to these studies, abrogation of LRP1 expression in U87 glioblastoma cells increased MMP2 and MMP9 levels and increased

cell migration (Song *et al.,* 2009). Additionally, Weaver and colleagues (1997) reported LRP1-deficient MEF cells to migrate faster than wild-type MEF cells, thereby suggesting an anti-migratory role for LRP1. They attribute this finding to a larger proportion of uPAR in LRP1-deficient MEFs. LRP1 has also been reported to modulate cell migration by directly associating with integrins and mediating their internalisation (Lillis *et al.,* 2005). Due to LRP1's role in regulating cell migration, an additional role in cell invasion was investigated which revealed LRP1 to promote breast cancer cell invasiveness (Li *et al.,* 2003). LRP1 localized to the leading edge of breast cancer cells to regulate cell-matrix interactions thereby enhancing cell migration (Chazaud *et al.,* 2002). In apparent contradiction to this, other studies have demonstrated that low LRP1 expression is related to aggressive and invasive carcinomas (Desrosiers *et al.,* 2006; Huang & Greenspan, 2012). Interesting studies by Montel *et al.,* (2007) demonstrated that LRP1 selectively facilitates the growth of tumor cells in metastases but not in the primary tumor. They also proposed the specificity of LRP1 function to be dependent on cell type, LRP1 expression, co-receptor expression, availability of ligands, amongst others.

1.5 WORK LEADING UP TO THIS STUDY AND MOTIVATION

Hsp90 is abundantly expressed in cancer cells and correlates with poor prognosis (Eustace *et al.,* 2004). Fibronectin is secreted as a soluble dimer which is assembled into an insoluble extracellular matrix via integrins and subsequently degraded by an endocytosis-lysosomal pathway (Sottile & Chandler, 2005; Hunter *et al.,* 2014). The dynamics of FN matrix assembly and degradation play a large role in cell migration and invasion contributing to the metastatic potential of cancer cells. LRP1 has a well-defined role as a scavenger receptor, mediating internalisation of over 40 structurally diverse ligands. Studies within our group have shown the presence of surface associated Hsp90 and extracellular soluble Hsp90β in various cancers and that extracellular Hsp90 isoforms or inhibition of Hsp90 with NOV regulates FN dynamics, leading to an increase or decrease in the FN ECM, respectively. Hsp90 is known to bind LRP1 (Basu *et al., 2*001) and LRP1 binds FN (Salicioni *et al.,* 2002). We also showed the direct binding of Hsp90 and FN *in vitro* (Hunter *et al., 2*014), which suggests the possibility of a trimeric complex containing Hsp90, FN and LRP1. It is possible that LRP1 is responsible for mediating this turnover of FN and that Hsp90 is in some way involved in this process. Whether Hsp90 is responsible for binding FN and chaperoning it to LRP1 for internalisation is unknown.

Moreover, the functional consequences of FN turnover related to Hsp90 inhibition in the presence or absence of LRP1 has not been investigated.

1.6 HYPOTHESIS

LRP1 is involved in the NOV mediated endocytosis and turnover of FN

1.7 OBJECTIVES

The broad aim of the project was to elucidate a role for LRP1 in regulating Hsp90-mediated FN matrix dynamics. We addressed the following objectives:

1. To test the effect of Hsp90 inhibition on FN in mouse embryo LRP1-expressing and -deficient fibroblasts;
2. To analyse the components of LRP1 complexes in NOV treated cells;
3. To determine the consequences related to Hsp90 inhibition in LRP1-expressing and LRP1-deficient cells.

Chapter 2. MATERIALS & METHODS

2.1 MATERIALS

Hs578T (ATCC: HTB-126) breast cancer cell line and mouse embryonic fibroblasts (MEF) (i.e. LRP1 wild type MEF-1 [ATCC: CRL-2214], LRP1 deficient PEA-13 [ATCC: CRL-2216] and PEA-10 [ATCC: CRL-2215] heterozygous for LRP1) were purchased from American Type Culture Collection (ATCC). General reagents were from Sigma-Aldrich (Germany) or Saarchem (Merck, South Africa). Tissue culture reagents (Dulbecco's Modified Eagle Medium [DMEM] with GlutaMAX™-I, fetal calf serum [FCS], 10 x Trypsin-Ethylenediaminetetraacetic acid [EDTA] and Penicillin/Streptomycin/Amphotericin [PSA] were from Gibco, Invitrogen [UK] and Biowhittaker [UK]). Tissue culture plasticware was from Corning Incorporated (USA). Hybond nitrocellulose membrane, western blotting power pack and Chemidoc™ XRS were from Bio-Rad (UK). Zeba spin desalting columns (89882), Pierce high capacity endotoxin removal spin columns (88273), 3,3'-dithiobis[sulfosuccinimidyl] propionate [DTSSP] (cat no.: 21578) were from Thermo Scientific (USA). MagReSyn™ Protein A and MagReSyn™ NTA were from ReSyn Biosciences (South Africa). Chelating Sepharose™ fast flow beads were from GE Healthcare (Sweden). Mouse monoclonal anti-human Hsp90α/β (cat no.: sc-13119), goat polyclonal anti-human Hsp90α/β (cat no: sc-1055), rabbit polyclonal anti-human His-probe (sc-804) primary antibodies were from Santa Cruz Biotechnology (USA). Mouse anti-human fibronectin (cat no.: F0916), rabbit anti-human fibronectin (cat no.: F3648), rabbit anti-human actin (cat no.: A2103) primary antibodies and goat anti-mouse IgG-HRP (cat no.: A2304) secondary antibody were from Sigma Aldrich (Germany). Rabbit monoclonal anti-human LRP1 (ab92544), mouse monoclonal [TV.1] anti-human fibronectin (ab194395), rabbit polyclonal anti-human histone H3 (ab1791) primary antibodies and donkey anti-rabbit IgG-HRP (ab16284) secondary antibody were from Abcam (UK). Mouse monoclonal anti-human LRP1 (515 kDa) (GTX79843) was from GeneTex (USA). Alexa Fluor-488 conjugated donkey anti-mouse IgG (cat no.: A21202), Alexa Fluor-546 conjugated donkey anti-rabbit IgG (cat no.: A10040), Alexa Fluor-633 conjugated donkey anti-goat IgG (cat no.: A21082) were from Invitrogen (UK). Suppliers of other specialized reagents are referenced in text.

2.2 METHODS

2.2.1 Routine maintenance of cell lines

Hs578T breast cancer cells were maintained in DMEM supplemented with 10% [v/v] FCS, 2 mM GlutaMAX™, 100 U/ml PSA and 2 mM human insulin (Novarapid). Murine embryonic fibroblast lines (MEF-1, PEA-10 and PEA-13) were maintained in DMEM supplemented with 10% [v/v] FCS, 2 mM GlutaMAX™ and 100 U/ml PSA. All cell lines were maintained at 37 °C in a humidified atmosphere with 5% CO_2.

2.2.2 Sodium Dodecyl Sulfate-Polyacrylamide Gel Electrophoresis (SDS-PAGE)

Proteins were separated by discontinuous SDS-PAGE according to the method described by Laemmli (1970). Proteins were resolved using a 4% [v/v] stacking gel (0.5 M Tris-Cl, pH 6.8) and 10% [v/v] resolving gel (1.5 M Tris-Cl, pH 8.8) at 120 V for 90 minutes in SDS-PAGE running buffer (0.25 mM Tris, 192 mM glycine, 1% [w/v] SDS). Samples were mixed with 5x SDS sample buffer (0.05 M Tris-Cl, 10% [v/v] glycerol, 2% SDS, 1% [w/v] bromophenol blue, 5% [v/v] β-mercaptoethanol) and boiled for 5 minutes before being loaded onto the gel. Blue prestained protein standard (New England BioLabs) or prestained protein marker (Thermo Scientific) was used for estimating molecular weights of proteins.

2.2.3 Immunoblotting and chemiluminescence detection

Resolved proteins were transferred from the gel onto nitrocellulose membrane in western transfer buffer (25 mM Tris-Cl, 192 mM glycine, 20% [v/v] methanol) using a semi-dry blotting system SD20 Semi Dry Blotter Maxi for 50 minutes at 0.4 A. Membranes were blocked for at least 1 hour at room temperature in 5% BLOTTO (5% [w/v] non-fat milk powder in Tris buffered saline [TBS: 50 mM Tris, 150 mM NaCl pH 7.5]). Membranes were incubated with primary antibody in 1% [w/v] BLOTTO at the recommended dilution overnight at 4˚C with gentle shaking. Membranes were washed thrice in TBST (TBS with 0.1% [v/v] Tween-20) for 5 minutes each time. Species matched secondary antibody conjugated to HRP was incubated with the membrane in 1% [w/v] BLOTTO for 45 minutes at room temperature. Membranes were washed in TBST four times for 5 minutes each time. Detection of proteins was carried out using ECL Advanced western blotting detection kit in the Chemidoc™ XRS system (BioRad).

2.2.4 Indirect Immunofluorescence and Fluorescence microscopy

Cells were seeded (1.5 x 10^5 cells/ml) into a 15-well ibidi plate and incubated overnight to allow cells to adhere. Cells were washed in phosphate buffered saline (PBS: pH 7.4; 137 mM NaCl, 27 mM KCl, 4.3 mM Na_2HPO_4, 4 mM KH_2PO_4), flash-treated (<1 min) with ice-cold ethanol and allowed to air dry. Cells were blocked with 1 % [w/v] BSA/TBS for 45 minutes and incubated with appropriate primary antibodies in 1 % [w/v] BSA/TBS overnight at 4 °C. Cells were washed twice with 0.1 % [w/v] BSA/TBS followed by 1 hour incubation with species specific fluorophore conjugated secondary antibodies at room temperature in the dark. Cells were washed twice with 0.1 % [w/v] BSA/TBS and rinsed briefly with Hoechst-33342 dye (Invitrogen) (1 µg/ml in distilled water) to stain nuclei blue. Immunofluorescence was detected using the Zeiss LSM 510 or LSM780 Meta laser scanning confocal microscopes and images analysed using Zen Blue Software.

2.2.5 WST-1 cytotoxicity assay

The toxicity of NOV was assessed in the Hs578T, MEF-1, PEA-10 aqnd PEA-13 cell lines using a WST-1 cell proliferation kit (Roche) carried out according to manufacturer's instructions. Cells of equal density (4 x 10^4 cells/ml) were seeded in a 96 well plate and treated the following day with a range of NOV concentrations (0-1000 µM). After 3 days, 10 µl of a 5 mg/ml WST-1 reagent was added to each of the wells and incubated for 4 hours prior to reading absorbance at 450 nm. The cell viability was determined by cleavage of the tetrazolium salt, WST-1, to formazan by metabolically active cells to produce a coloured product (Roche). This viability assay was carried out quintuplicate and the dose response and half maximal effective concentrations (EC50) determined using GraphPad Prism 4.

2.2.6 Biochemical fractionation of insoluble and soluble fibronectin using a deoxycholate (DOC) assay

This assay was adapted from that published by Brenner and colleagues (Brenner, Corbett, & Schwarzbauer, 2000). MEF-1 and PEA-13 cells were seeded in a 6-well plate (3 x 10^5 cells/ml) and allowed to adhere overnight. Cells were treated with increasing concentrations of NOV for 16 hours and scraped into DOC buffer (2% [w/v] deoxycholate, 20 mM Tris-HCl, pH 8.8, 2 mM phenylmethanesulfonylflouride [PMSF], 2 mM EDTA and 0.05% [v/v] protease inhibitor cocktail). Samples were vortexed for 2 minutes and centrifuged at 13000 rpm in a microfuge for 20 minutes at 4 ˚C. A volume of 200 µl of the supernatant containing soluble fibronectin

was mixed with 80 µl of SDS sample buffer (1% [w/v] SDS, 25 mM Tris-HCl, pH 8.0, 2 mM PMSF, 2 mM EDTA and 0.05% [v/v] protease inhibitor cocktail) and the pellet containing insoluble fibronectin was resuspended in 80 µl SDS sample buffer and resolved on SDS-PAGE.

2.2.7 Cell surface biotinylation and streptavidin affinity purification

Adherent MEF-1 and PEA-13 cells were treated for 16 hours with or without 200 µM NOV at 37 ˚C. Cell surface proteins were incubated with 1 mg/ml EZ-Link™ Sulfo-NHS-SS-Biotin in PBS (pH 8) for 1 hour at 4 ˚C with gentle shaking. This biotinylation reagent contains a cell-impermeable NHS ester group which reacts with amines on lysines residues of nearby proteins (Hunter *et al.,* 2014). Tris-Cl (1 M, pH 7.5) was added to quench the biotinylation reagent and cells were subsequently washed twice in PBS and lysed in 500 µl radio-immunoprecipitation assay (RIPA) buffer (50 mM Tris-Cl, pH 7.4, 150 mM NaCl, 1 mM EDTA, 1 mM Na_3VO_4, 1% [v/v] Nonidet P-40 [NP40], 1 mM sodium deoxycholate, 1 mM PMSF, 0.05% [v/v] protease inhibitor cocktail) with gentle scraping. A second biotinylated flask (negative control) was lifted with trypsin/EDTA (to cleave surface protein interactions) followed by centrifugation at 2000 rpm for 2 minutes in a microfuge. Pelleted cells were resuspended in 500 µl RIPA buffer. Biotinylated scraped or trypsinised cells were lysed for 30 minutes at 4 ˚C with gentle shaking. Lysates were cleared by centrifugation in a microfuge at 13000 rpm for 5 minutes at 4 ˚C and incubated with a volume of 100 µl pre-equilibrated streptavidin conjugated agarose beads (Thermo Scientific, USA) for 1 hour at 4 ˚C. After centrifugation, the supernatant was discarded and proteins were released from the beads by boiling in 5x SDS sample buffer. Samples were resolved by SDS-PAGE and analysed by immunoblotting as described previously.

2.2.8 DTSSP cell surface crosslinking and immunoprecipitation of LRP1 containing complexes

Adherent cells were left untreated or treated with NOV as indicated in figure legends. Cells were washed twice in PBS and incubated with DTSSP (3 mg/ml) at 4˚C for 2 hours to allow for crosslinking of protein interactions. The DTSSP crosslinker contains NHS moeities on both ends which are able to interact with lysine residues on proteins that are within interacting range (12Å) (Thermo Scientific). DTSSP was quenched with 1 M Tris-Cl (pH 7.5) at 4˚C for 15 minutes. Cells were lysed in ice cold non-denaturing buffer (20 mM Tris-Cl, pH 8, 137 mM NaCl, 1% [v/v] NP40, 2 mM EDTA, 0.05% [v/v] protease inhibitor cocktail) with gentle scraping.

Cell lysates were transferred to a chilled epp and centrifuged at 13000 rpm in a microfuge for 20 minutes at 4 ˚C. A volume of 10 µl of magnetic MagReSyn™ Protein A, which had been pre-equilibrated according to manufacturer's instructions and bound to rabbit LRP1 or isotype control capture antibodies at room temperature for 30 minutes, were incubated with cleared lysates overnight at 4 ˚C. Beads in suspension were collected using a magnet and washed three times in wash buffer (50 mM Tris, pH 7, 150 mM NaCl, 1% [v/v] Tween 20) followed by a final wash in dH_2O. Flow through and wash samples were retained for analysis by SDS-PAGE. LRP1 complexes were eluted from the beads by boiling in 5x SDS sample buffer containing β-mercaptoethanol to cleave DTSSP bound proteins from the LRP1 complex. Samples were resolved by SDS-PAGE and anlysed by SDS-PAGE and immunoblotting as described previously.

2.2.9 Quantitative reverse transcriptase-polymerase chain reaction (qRT-PCR) for detection of FN mRNA

MEF-1 and PEA-13 cells were seeded into 6 well plates (3 x 10^5 cells/ml) and allowed to adhere overnight before being treated with increasing concentrations of NOV in duplicate for 16 hours. Total RNA was extracted from treated cells in an RNase-free environment using Direct-zol™ RNA miniprep kit (Zymo, USA) and quantified using absorbance at 260 nm on the NanoDrop 2000 (Thermo Scientific, USA). Equal amounts of RNA (1 µg) were converted into cDNA using the RevertAid H Minus First Strand cDNA Synthesis Kit (Thermo) with oligo (dT) primers according to manufacturer's instructions. To quantify the mRNA levels of FN in each of the treatments, qRT-PCR was carried out with a CFX96 Real Time PCR Detection System (BioRAD) using KAPA SYBR® FAST qPCR master mix (KAPA Biosystems, USA) according to the manufucturer's instructions. The cDNA generated from 1 µg of RNA and mouse FN1 specific primers (forward primer 1: 5'-GAGCTATCCATTTCACCTTCAGA-3'; reverse primer 2: 5'-TTGTTCGTAGACACTGGAGAC-3') were used in each of the qRT-PCR reactions for FN1 gene specific amplification. A 3-step cycling protocol was used with the following parameters: enzyme activation at 95 ˚C (3 minutes), 1) denaturation at 95 ˚C (3 seconds), 2) annealing at 55.2 ˚C (20 seconds), and 3) extension at 72 ˚C (20 seconds), which were repeated for 40 cycles. Melt curves were incorporated to show whether multiple amplicons were present. Melt curves displayed single peaks indicating specific FN1 gene amplification. FN DNA standards were constructed as described in 2.2.10 to serve as a comparison for absolute quantification of mRNA levels. Test samples and standards were run in triplicate on the same

plate and the data analysed in BioRAD CFX Manager 3.1 Software. Statistical analysis was performed in GraphPad Prism 4.

2.2.10 Cloning of mouse FN DNA into pTZ57R vector to generate a FN standard for absolute quantification of FN mRNA levels in MEFs by qRT-PCR

In order to quantify the total murine FN mRNA levels we required a murine FN standard of known concentration to allow for the generation of standard curves with which we could quantify measured mRNA in our treatments. Total RNA was extracted and purified from untreated MEF-1 cells using the Direct-zol™ kit and was reverse transcribed into cDNA with RevertAid H Minus First Strand cDNA synthesis kit. The cDNA was amplified by standard PCR using mouse FN1 specific primers as described in 2.2.9. The PCR amplified cDNA was concentrated using a Zymo DNA Clean and Concentrate kit and cloned into the pTZ57R vector by TA cloning (#K1213, Thermo Scientific) (Figure 4A). A total of 1 µg of the ligated product (pTZ-FN) was transformed into *Escherichia coli* JM109 competent cells by incubation on ice for 2 minutes, followed by heat shock for 45 seconds at 42 ˚C and a further 10 minutes on ice. Cells were incubated with 2 x YT broth (16 g/l tryptone, 10 g/l yeast extract, 5 g/l NaCl) for 1 hour at 37 ˚C and a volume of 100 µl plated on 2 x YT agar plates with 100 µg/ml ampicillin overnight at 37 ˚C. Single positive transformants were inoculated into 5 ml 2 x YT broth and incubated overnight at 37 ˚C with shaking. The plasmid was extracted using a Miniprep kit according to manufacturer's instructions (Zymo) and a restriction digest was performed to confirm the successful cloning of the pTZ-FN construct using *Eco*RI and *Hin*dIII to yield a FN insert of ~100 bp. The plasmid was incubated without restriction enzymes (U), with *Eco*RI alone (SD) and a combination of *Eco*RI and *Hind*III (DD) for 90 minutes at 37 ˚C. Restriction digest reactions were analysed on a 1.2% [w/v] agarose gel in Tris acetate EDTA buffer (TAE: 40 mM Tris, 20 mM acetic acid, 1 mM EDTA) containing 1 µg/ml ethidium bromide. DNA was visualized using UV illumination with the Chemidoc XRS (BioRAD) (Figure 4B).

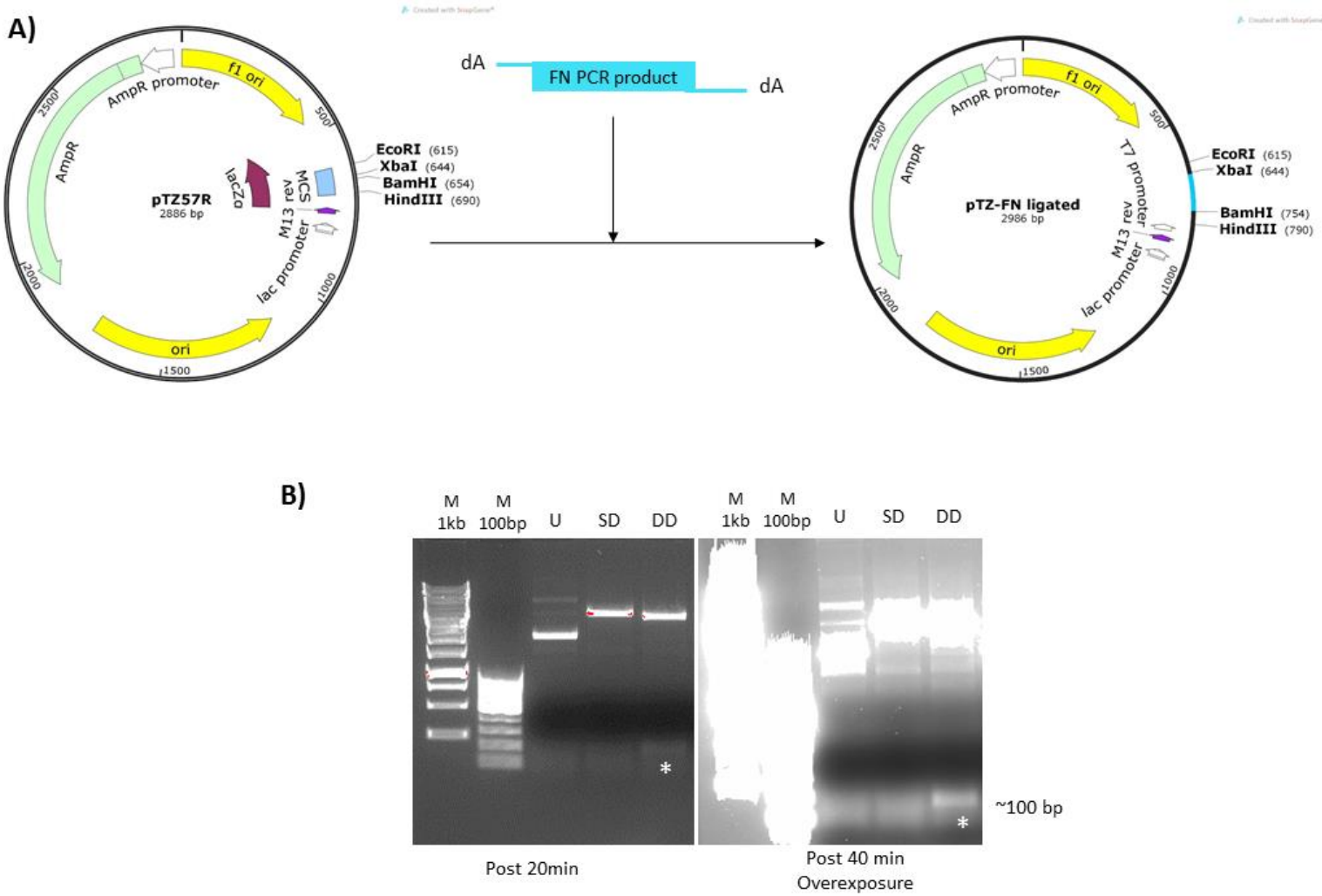

Figure 4: Cloning strategy of mouse FN DNA into pTZ57R vector.

A) FN PCR product with 'A' overhangs was ligated into the MCS of a pTZ57R vector backbone to produce the pTZ-FN clone. Plasmid maps were generated using SnapGene® Software. **B)** To confirm successful cloning, the pTZ-FN construct was left uncut (U), digested with *Eco*RI (SD) and *Eco*RI and *Hin*dIII (DD). These digests were run in the presence of ethidium bromide on a 1.2% [w/v] agarose gel at 120V and visualised after 20 minutes (left) and 40 minutes (right). Two markers (M) were run alongside (1 kb and 100 bp). The single digest (SD) linearized the plasmid to produce a product which resolved at ~3000 bp. The double digest (DD) confirmed the presence of the FN insert (indicated *) at approximately 100 bp.

2.2.11 Wound Healing assay

To test for the contribution of FN and/or LRP1 on migration of Hs578T, MEF-1 and PEA-13 cells, cells were plated in a 24 well culture dish and grown until confluent. To create wounds, a scratch was made down the centre of the well using a toothpick. Cells were washed with spent media and returned to incubate at 37 ˚C in fresh media containing NOV at concentrations indicated in Figure legends for 12 hours to observe migration. Photographs were taken immediately after wound initiation (t=0 hrs) and again 12 hours later using a Zeiss Primovert inverted light microscope. Marks were made on the bottom surface of wells to ensure identical fields of view were captured each time. Wound images were taken at 0 hrs and 12 hrs. For each image, distances between the two opposing lead edges were measured at least three times at different points across the length of the wound. Distances migrated were calculated by subtracting distance measured at 12 hrs from distance at 0 hrs.

2.2.12 Induction and purification of His-RAP1

The pQTEV-LRPAP1 plasmid encoding N-terminally His-tagged RAP1 was a gift from Konrad Buessow (Addgene plasmid # 31327) . pQTEV-LRPAP1 was transformed in *E.coli* BL21 competent cells and grown on ampicillin (100 µg/ml) containing 2x YT agar plates overnight at 37 ˚C. Single transformed colonies were inoculated into 25 ml 2x YT broth containing ampicillin (100 µg/ml) overnight at 37 ˚C with shaking. The overnight culture was inoculated into 225 ml YT broth and incubated at 37 ˚C shaking until an OD_{600} of 0.4-0.6 was reached to ensure cells were in the exponential growth phase upon induction. The culture was induced with 1 mM isopropyl β-D-1-thiogalactopyranoside (IPTG) at 37 ˚C with shaking, to allow for protein expression, and samples were taken at various time intervals (0 hrs- overnight) and OD_{600} of each was measured. Pelleted samples were resuspended according to equation below, boiled and resolved by SDS-PAGE and immunoblotting.

$$\text{Resuspension volume (ml)} = \frac{OD600}{6}$$

2.2.13 Solubility study of His-RAP1

Following induction of His-RAP1, cells were harvested by centrifugation at 6000 x*g* for 30 minutes at 4 ˚C and resuspended in wash buffer containing either 0.2 % [v/v] Triton-X-100, 0.4 % [v/v] Tween-20, a combination of 0.2 % [v/v] Triton-X-100 and 0.4 % [v/v] Tween-20, 1 % [v/v] NP40, 6% [v/v] sarcosyl, 0.1 % [v/v] TBST or 4 % [v/v] Triton-X-100. Cell lysates were

sonicated and centrifuged at 16 000 x*g* for 30 minutes at 4 ˚C. Pellets and supernatants from each of the detergent treatments were boiled in 5x SDS sample buffer and resolved by SDS-PAGE and immunoblotting with rabbit polyclonal anti-human His-probe (sc-804) primary antibody to detect the His-tag.

2.2.14 Optimisation of purification of His-RAP1

The expression of His-RAP1 was induced with 1 mM IPTG for 4 hours as described previously. Cells were pelleted at 6000 x*g* for 30 minutes at 4 ˚C and resuspended in wash buffer (10 mM Tris-Cl, 300 mM NaCl pH 7.5, 50 mM imidazole) with lysozyme (1 mg/ml) and 0.05% [v/v] protease inhibitor cocktail. After incubation on ice for 30 minutes, the cell lysate was sonicated at 50 Hz alternating 30 seconds on and 30 seconds off for five repeats, followed by centrifugation at 16 000 x*g* for 30 minutes at 4 ˚C. A volume of 50 µl of MagReSyn™-NTA magnetic beads were pre-equilibrated according to the user manual and incubated with cleared lysate overnight at 4 ˚C with gentle shaking. Beads were collected using a magnet, washed three times with wash buffer and proteins eluted from the beads in elution buffer (10 mM Tris-Cl, 300 mM NaCl pH 7.5, 500 mM imidazole) for 2 minutes at room temperature. Purified protein was buffer exchanged using a Zeba Spin desalting column into buffer F (10 mM Tris-Cl, 300 mM NaCl pH 7.5) and endotoxin was removal using Pierce High Capacity Endotoxin Removal Resin according to manufacturer's instructions. Protein concentrations were determined by absorbance at 280 nm using the NanoDrop 2000 spectophotometer.

Chapter 3. RESULTS

3.1 Determining the cytotoxicity of the Hsp90 inhibitor NOV in Hs578T breast cancer cells and mouse embryonic fibroblasts

Previous studies from our group have shown the direct binding of Hsp90 and FN *in vitro* and that inhibition of Hsp90 with NOV caused internalisation of the FN matrix by receptor mediated endocytosis (Hunter *et al.,* 2014). However, the receptor mediating this internalisation is currently unknown. LRP1 is a likely candidate as it is a ubiquitous receptor responsible for regulating internalisation of numerous diverse ligands and is known to bind both Hsp90 (Basu *et al.,* 2001) and FN (Salicioni *et al.,* 2002). We decided to investigate the mechanisms associated with FN turnover in mouse embryonic fibroblasts (MEFs) upon Hsp90 inhibition and how this may regulate cancer progression. We used the MEFs/PEA-10/PEA-13 lines as they are an isogenic model system for LRP1 knockout and are known to have high levels of ECM (T E Willnow & Herz, 1994). To determine whether LRP1 and FN levels were sensitive to Hsp90 inhibition, we first determined the cytotoxicity of NOV to each of the three MEF cell lines (MEF-1 [$LRP^{+/+}$], PEA-13 [$LRP^{-/-}$] and PEA-10 [$LRP^{+/-}$]), as well as the Hs578T breast cancer cells using a WST-1 assay (Figure 5). Each of the cell lines were incubated for 72 hours with increasing concentrations of the inhibitor before addition of WST-1 reagent and the absorbance read at 450 nm after 4 hours. The half maximal effective concentration (EC50) was determined using a non-linear regression equation in GraphPad Prism 4. In each of the graphs (Figure 5A-D), a dose dependent decrease in percentage viability was observed as the concentration of NOV increased. Cell viabilty was maintained upon no addition of NOV but at its highest concentration (1000 µM) it is shown to cause almost complete death of cells (0% viability). Wild type MEF-1 cells (Figure 5A), with an EC50 of 45.6 µM, were nearly three-fold more sensitive to NOV than the LRP1-deficient counterpart (PEA-13 EC50: 130.4 µM) (Figure 5B). PEA-10 cells (Figure 5C) had the highest EC50 value of the murine cells at 157.2 µM. Each of these MEFs had lower EC50 values in comparison to the Hs578T cells (EC50: 214.9 µM) (Figure 5D). The reason for the difference in sensitivity to NOV between each of these cell lines is unclear. NOV is an antibiotic administered to humans at drug concentrations equivalent to 300-500 µM (Marcu *et al.,* 2000). This confirms that, for the purpose of our study, the use of concentrations within this range and less than the EC50 recorded for each of the cell lines would maintain cell viability.

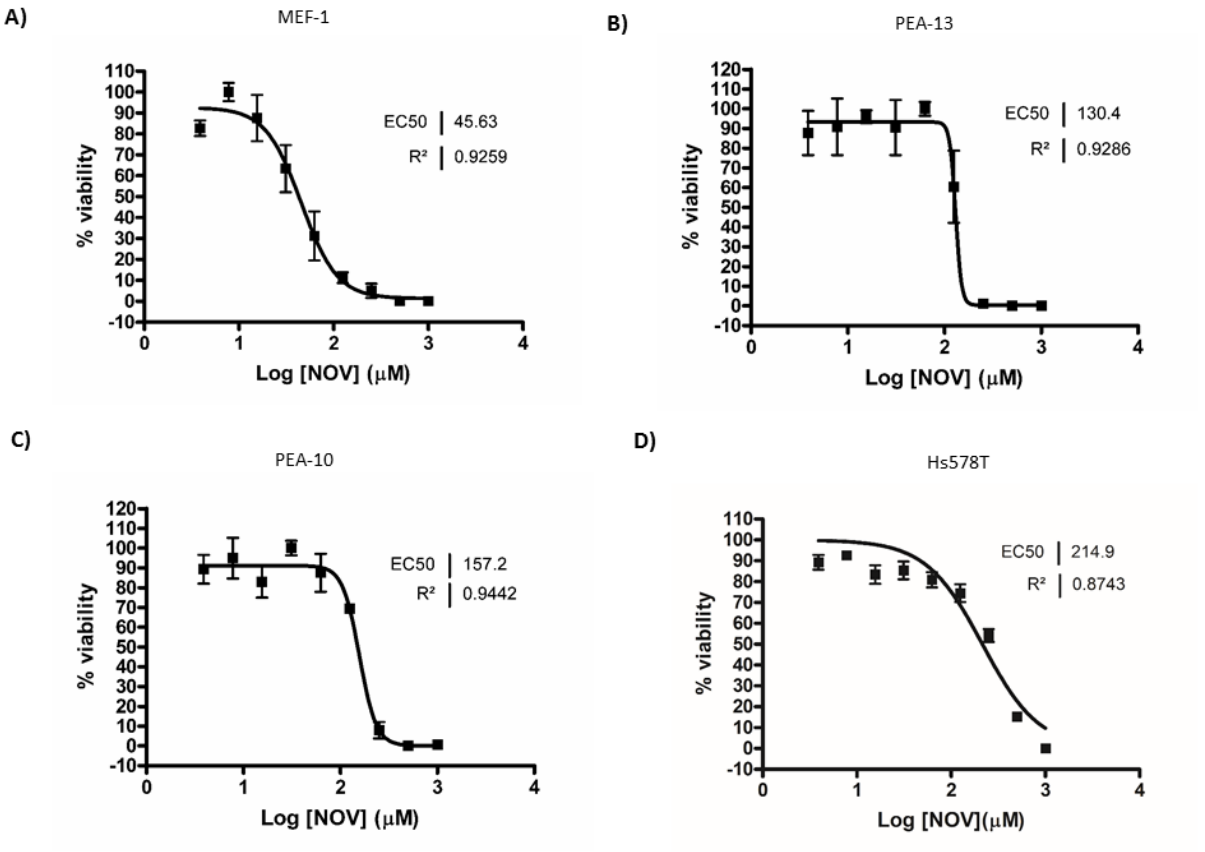

Figure 5: Analysis of the toxicity of NOV.

The cytotoxicity of Hsp90 small molecule inhibitor NOV was determined for **A)** MEF-1, **B)** PEA-13, **C)** PEA-10 and **D)** Hs578T breast cancer cells using a WST-1 assay. Cells were seeded in a 96 well plate and treated with increasing doses of NOV (0-1000 μM) for 72 hours. Cells were incubated with WST-1 reagent for 4 hours and absorbance at 450 nm recorded. Percentage viability is represented here against the log of the inhibitor concentration. Half maximal inhibitory concentrations (EC50) was determined using GraphPad Prism 4. Data represent the average of 6 independent experiments.

3.2 Effect of NOV on total FN and LRP1 levels

Western analysis was carried out on each of the MEF cell lines to compare their respective levels of FN (190+ kDa) and LRP1 (85 kDa) (Figure 6A). Levels of FN relative to Histone H3 were quantified in ImageJ and the densitometric ratios are indicated below the immunoblot. Equal amounts of protein from untreated cell lysates revealed that PEA-13 cells constitutively expressed greater levels of FN relative to the PEA-10 and MEF-1 cells. Cells treated with an LRP1 blocking antibody (mLRPab) recognising the 515 kDa extracellular fragment of LRP1 caused an accumulation of FN in LRP1-expressing cells (PEA-10 and MEF-1). The absence of LRP1 (85 kDa) was confirmed in PEA-13 cells and its presence in MEF-1 and PEA-10 cells increased slightly in the mLRPab treatments. These data suggest that loss or blocking of LRP1 causes accumulation of FN.

MEF-1, PEA-13 and Hs578T cell lines were then treated with increasing doses of NOV from 0-1000 μM to observe the changes in protein levels at both low and high concentrations of the Hsp90 inhibitor (Figures 6B-D). Cell lysates were probed for FN and LRP1 and the densitometry for each was determined using ImageJ, shown alongside western analyses (Figure 6B-D, right), relative to a loading control. Western analysis of MEF-1 cells revealed significantly increased total FN (tFN) levels upon NOV treatment at the lowest concentration (50 μM) and then a dose-dependent decrease at higher concentrations (Figure 6B). Comparatively, LRP1-deficient PEA-13 cells showed no significant changes in tFN levels at equivalent concentrations. Interestingly, in MEF-1 cells, lower molecular weight FN bands (85 kDa) were observed in the lower NOV treatments (50 μM, 100 μM and to a lesser extent in 200 μM). These were not observed in any of the NOV treatments of PEA-13 lysates. A gradual dose dependent increase in FN levels in Hs578T cells was observed in 0-500 μM NOV treatments, with a decrease in FN levels at 1000 μM (Figure 6D). Treatment at 200 μM and 500 μM were statistically higher than untreated cells. These results suggest that, in response to NOV treatment at concentrations at or near the EC50 value, in LRP1-expressing cells (i.e. MEF-1 and Hs578T) tFN levels increase, while in LRP1-deficient cells, tFN levels do not change.

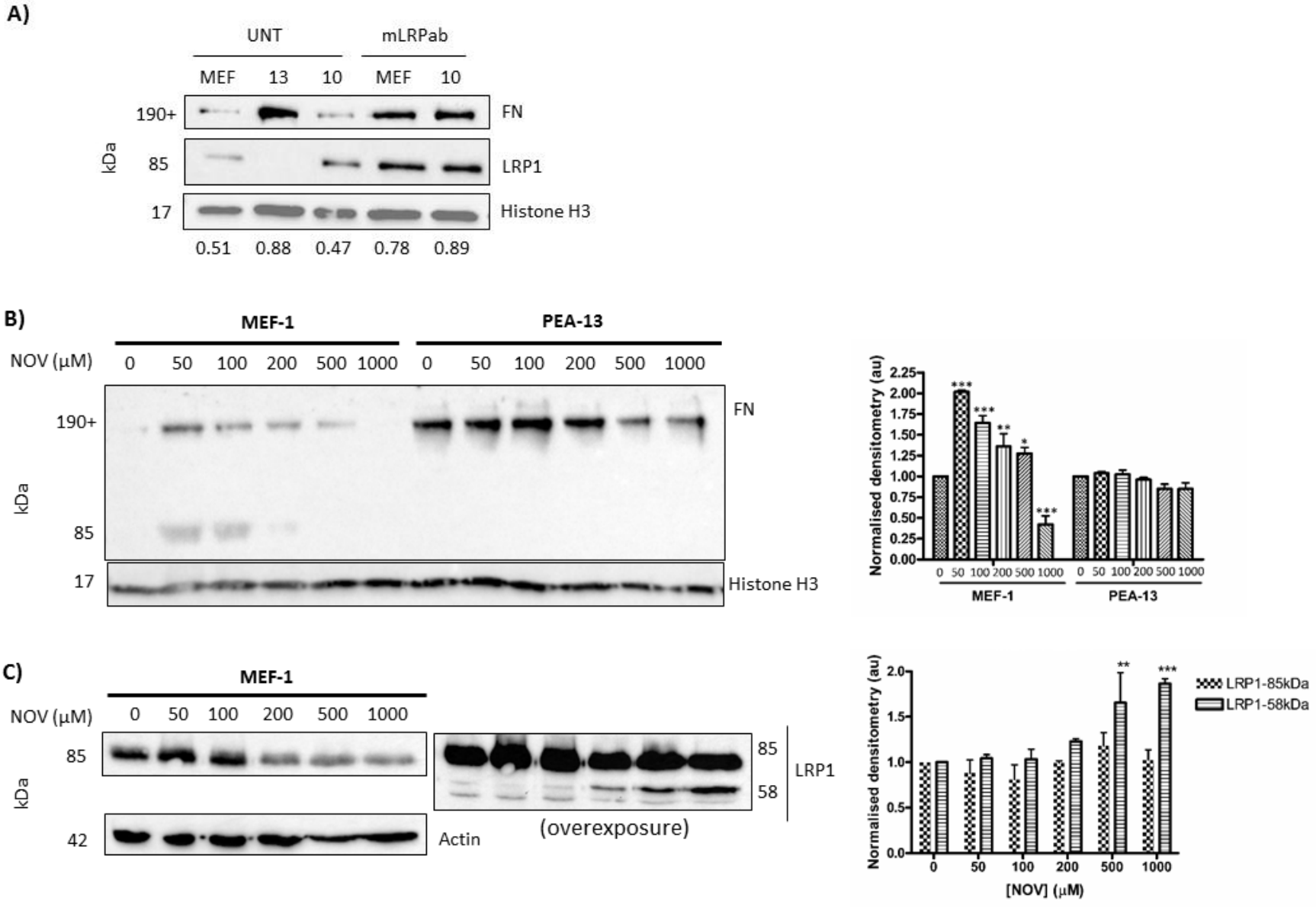
A)
UNT
mLRPab
MEF
13
10
MEF
10
190+
85
17
kDa
FN
LRP1
Histone H3
0.51
0.88
0.47
0.78
0.89
B)
MEF-1
PEA-13
NOV (μM)
0
50
100
200
500
1000
0
50
100
200
500
1000
190+
85
17
kDa
FN
Histone H3
Normalised densitometry (au)
MEF-1
PEA-13
C)
MEF-1
NOV (μM)
0
50
100
200
500
1000
85
42
kDa
Actin
85
58
LRP1
(overexposure)
LRP1-85kDa
LRP1-58kDa
Normalised densitometry (au)
[NOV] (μM)

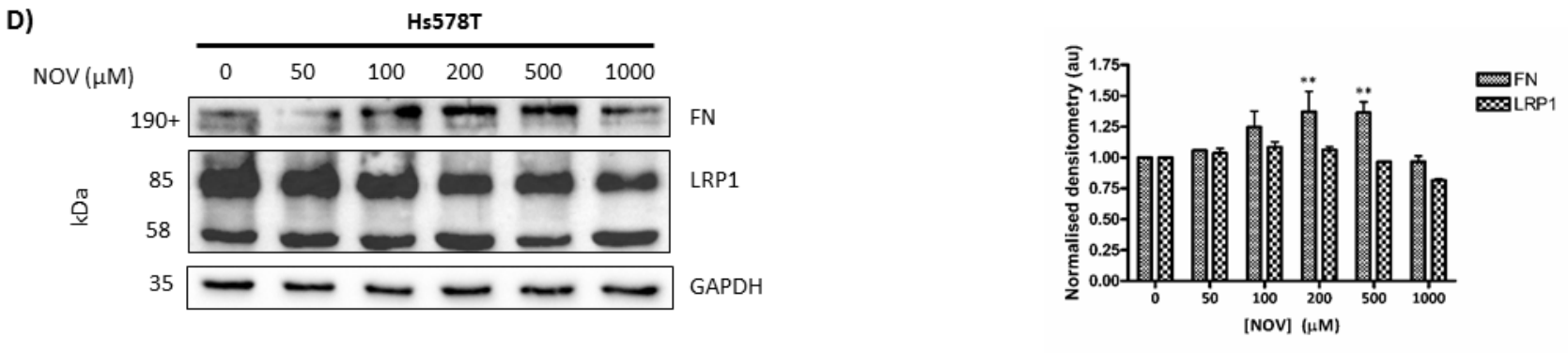

Figure 6: Expression of tFN in LRP1-expressing cells is significantly increased upon Hsp90 inhibition compared to LRP1-deficient cells.

Adherent cells were treated with increasing concentrations of NOV for 16 hours at 37˚C. Cells were lysed and equal amounts of total protein (50 μg) were loaded. **A)** MEF-1 (MEF), PEA-13 (13) and PEA-10 (10) cell lines were left untreated or treated with a mouse monoclonal LRP1 blocking antibody for 16 hours before lysis. Equal amounts of total protein (50 μg) were probed for FN and LRP1 using rabbit anti-FN and rabbit anti-LRP1 antibodies respectively. Values below represent the densitometry values calculated in ImageJ of FN relative to Histone H3. **(B)** MEF-1 and PEA-13 cells were treated with increasing concentrations of NOV for 16 hours and cell lysates were probed for levels of FN using rabbit anti-FN primary antibodies and **(C)** Analysis of LRP1 levels in MEF-1 lysates using rabbit anti-LRP1 antibodies. **(D)** Hs578T lysates were treated with NOV and probed for FN and LRP1 as described previously. Actin, Histone H3 or GAPDH were used as loading controls. The densitometry represented alongside each of the immunoblots A)-C) was determined using ImageJ. Statistical significance was determined using a two-way ANOVA in GraphPad Prism 4 (*= $p<0.05$, **= $p<0.01$, ***= $p<0.001$). A) was performed in duplicate and B)-D) are representative of triplicate experiments.

We then probed for levels of LRP1 (using an antibody directed against the LRP1 intracellular domain [LRP-ICD]) in MEF-1 and Hs578T cell lysates (Figure 6C and D respectively) and identified two LRP1 bands in both cell lines. In MEF-1 cells, one band was observed at 85 kDa (the predicted molecular weight of the LRP1-ICD) and upon overexposure, a second band at approximately 58 kDa (henceforth referred to as LRP1-85 and LRP1-58 (Figure 6C). The relative expression of each of these LRP1 isoforms was quantified using ImageJ, with actin used as a loading control, and revealed that LRP1-85 had similar levels across the range of NOV concentrations although this did not correlate with the WB which shows an obvious reduction of LRP1-85. LRP1-58 levels increased in a dose-dependent manner with 500 µM and 1000 µM NOV treatments being significantly higher compared to the untreated and lower NOV concentration MEF-1 lysates. These results suggest that NOV treatment may induce the processing of the LRP1 receptor. In the Hs578T cell lysates (Figure 6D), LRP1 bands were observed at 85 kDa and 58 kDa, similar to those in MEF-1 cells however, levels of both 85 kDa and 58 kDa LRP1 fragments were much higher than in MEF-1 cells. Additionally, the levels of LRP-58 did not appear to increase and were present even in the absence of NOV treatment. This might suggest a constitutive processing of LRP1 present in this cell line compared to an activated LRP1 processing response in MEF-1 cells.

Taken together, LRP1-expressing cells (i.e. MEF-1 and Hs578T) had increased levels of tFN upon NOV treatment at concentrations close to the EC50 values and demonstrated processing of LRP1-ICD. LRP1-deficient PEA-13 cells showed no significant changes in FN levels with NOV treatment.

3.3 Influence of NOV on the degradation of FN proteins and mRNA expression in MEF-1 and PEA-13 cells

The changes in tFN observed in the MEF-1 cells (Figure 6B) could be due to changes in rates of FN synthesis or degradation. In order to assess the effect of Hsp90 inhibition on the levels of FN protein turnover, we performed a time course measurement of FN levels in MEF-1 cells when translation was blocked with cycloheximide (CHX) (Zhang *et al.,* 2012). MEF-1 cells were treated in fresh media supplemented with CHX in the presence (+NOV) and absence (-NOV) of NOV for the indicated time periods, and lysates probed for FN by western analysis (Figure 7A). The loss of FN over time normalised to relative histone levels was quantified in Image J

(Figure 7B). When translation of FN was blocked, a loss in tFN protein levels occurred earlier in NOV treated cells (+NOV) over 12 hours compared to the untreated control (-NOV). When compared with the control (-NOV) where FN levels appear stable with a noticeable loss observed only after 12 hours with CHX alone, levels of FN in NOV and CHX treated lysates were reduced after as little as 0.5 hrs and continued to reduce over the time period (Figure 7B). This suggested that the dose dependent decrease in tFN levels of MEF-1 cells above 50 μM NOV (Figure 6B) was most likely due to enhanced degradation.

To further assess whether tFN in NOV treated MEF-1 and PEA-13 cells was indeed being degraded, we tested what effect blocking of the proteasomal and lysosomal degradation pathways would have on levels of FN in these cell lines. The main proteolytic pathway for intracellular proteins is the proteasome, while extracellular proteins are predominantly processed by the lysosome (reviewed in Ciechanover, 2005). Cells were treated with the highly specific proteosomal inhibitor, MG132, in the presence and absence of NOV for 16 hours before being lysed and analysed by western analysis (Figure 7C). In PEA-13 cells, addition of MG132 in the presence of NOV caused accumulation of FN relative to NOV or MG132 treatments alone, as indicated by densitometry values relative to the loading control shown below the western blot. This result would suggest that NOV treatment led to degradation of FN via the proteosome in PEA-13 cells. In MEF-1 cells, treatment with the proteosomal inhibitor did not cause an increase in FN in NOV treated cells. On the other hand, treatment of MEF-1 cells with the lysosomal inhibitor (+CLQ) (Figure 7D) increased levels of FN compared to control cells (-CLQ). Interestingly, NOV treated cells in the presence of CLQ had increased FN levels relative to untreated cells or cells treated with NOV alone. Thus, given that intracellular proteins are processed by the proteasome and extracellular proteins are processed by the lysosome, taken together these data could be interpreted to suggest that the observed loss of FN in PEA-13 cells is primarily loss of intracellular FN (inFN), while the loss of FN in NOV treated MEF1 is due to internalization and degradation of extracellular FN (exFN). However, this experiment needs to be repeated to confirm these data.

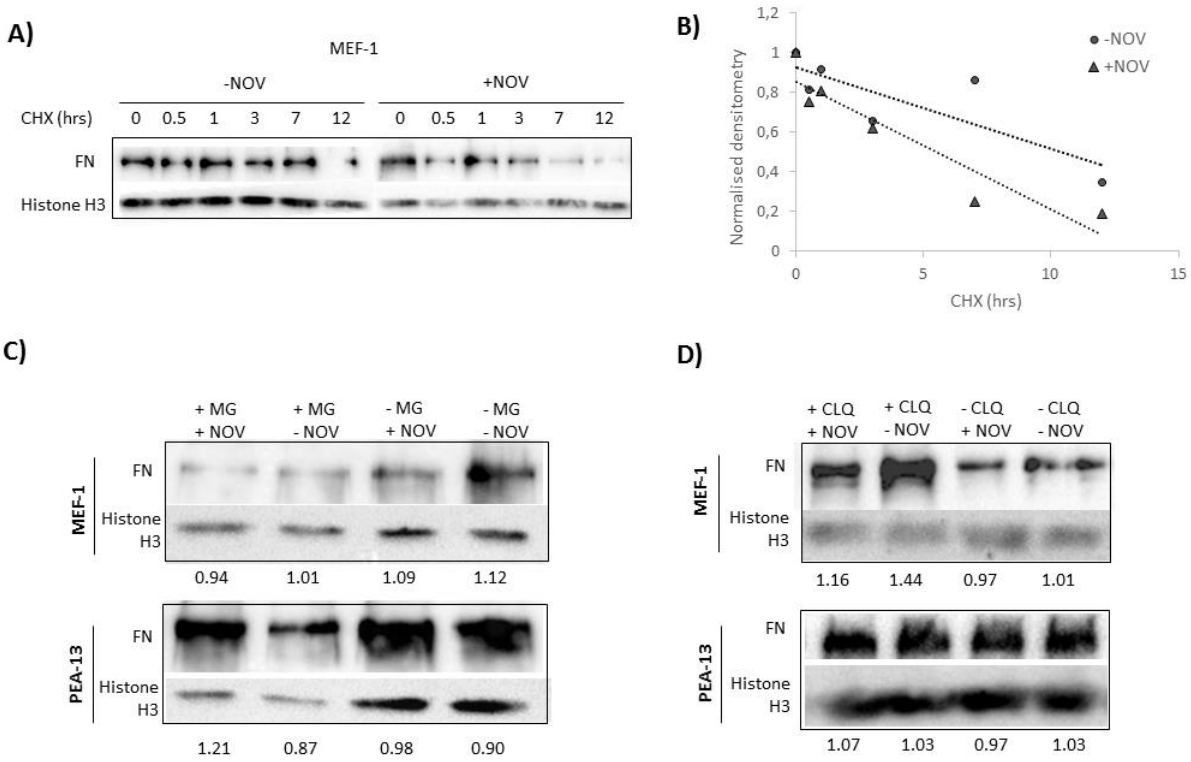

Figure 7: Effects of Hsp90 inhibition on the degradation of FN proteins in MEF-1 and PEA-13 cells

A) MEF-1 cells were treated with 100 µg/ml cycloheximide (CHX) in the presence or absence of 200 µM NOV and lysates prepared at the indicated time points. Equal amounts of total protein were probed for FN on a western blot with rabbit anti-FN antibody. Histone H3 was used as a loading control. **B)** The associated densitometry was determined using ImageJ software. Adherent MEF-1 and PEA-13 cells were treated **C)** with (+) or without (-) MG132 (MG) (5 µM) and **D)** with or without chloroquine (CLQ) (100 µM) in the presence or absence of 200 µM NOV for 16 hours before lysing. Equal amounts of total protein (50 µg) were loaded and probed for FN by western analysis. Densitometry values were calculated in ImageJ and are indicated below western blots. Results in A) and C) are representative of duplicate experiments with similar results. Results in D) were representative of a single experiment.

We next investigated the effects of Hsp90 inhibition at the mRNA level to determine whether changes in FN mRNA transcripts may be contributing to the changes observed in levels of tFN. Adherent MEF-1 and PEA-13 cells were treated for 16 hours with increasing concentrations of NOV (0-1000 μM) and lysed in Trizol reagent. RNA extracted from NOV treated lysates was reverse transcribed into cDNA and the relative mRNA levels of FN assessed using q-RT-PCR with mouse FN specific primers. Absolute quantification of FN mRNA levels in each of the treatments was assessed by comparison to a FN standard curve generated from known amounts of FN cDNA. See the Appendix for FN standard curves (Figure 17). MEF-1 cells had 100-fold lower FN mRNA levels compared to PEA-13 cells (Figure 8) which may account for the increased total FN observed in the LRP1-deficient cell line. MEF-1 cells showed no statistically significant changes in levels of FN mRNA with NOV treatment. In PEA-13 cells (Figure 8B), a statistically significant decrease ($p<0.01$) in FN mRNA at 50 μM and 100 μM NOV and 200 μM NOV ($p<0.05$) was observed relative to untreated. Due to the large error bars at 500 μM and 1000 μM, we can assume that mRNA levels returned to levels that were not statistically different to the untreated. In addition, from these data it would appear that NOV treatment in the PEA-13 cells reduced levels of FN mRNA to levels equivalent to those seen in MEF-1 cells.

These data suggest that the loss of FN observed in MEF-1 cells as a result of Hsp90 inhibition with NOV was not due to reduced FN mRNA levels.

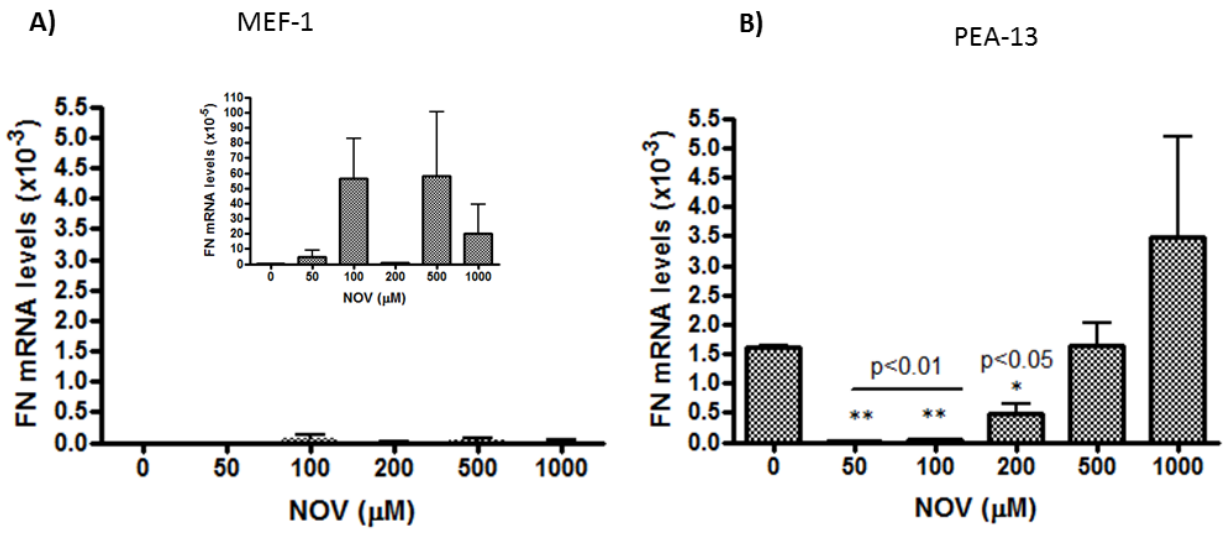

Figure 8: Hsp90 inhibition has no significant changes at the FN mRNA level in MEF-1 cells.

Measurement of FN mRNA levels in NOV treated **A)** MEF-1 and **B)** PEA-13 cells. Cells were treated with increasing concentrations of NOV for 16 hours and total RNA was extracted using Trizol. RNA was reverse transcribed using a RevertAid cDNA synthesis kit with oligo dT primers. Quantitative RT-PCR was performed using SYBR® FAST and mRNA transcript levels were quantified from a FN cDNA standard curve. This experiment is representative of three biological replicates performed in triplicate.Statistical analyses were performed in GraphPad Prism 4 using a two-way ANOVA (*= $p<0.05$, **= $p<0.01$).

3.4 Immunofluorescence reveals a loss in extracellular FN matrix in LRP1-expressing Hs578T and MEF-1 cells upon NOV treatment

Fluorescence microscopy was used to evaluate the subcellular localisation of FN in NOV treated Hs578T and MEF cells. Adherent cells were left untreated (UNT) or treated for 16 hours with varying concentrations of NOV as indicated in the figure legend before being fixed and stained for FN using a mouse anti-fibronectin antibody (Figure 9). In all cell lines (i.e. Hs578T, MEF-1 and PEA-13), untreated cells had a distinct fibrillar network in the extracellular space between neighbouring cells indicated by white arrows. In particular, untreated PEA-13 cells had a comparatively higher proportion of FN matrix to MEF-1 cells. In Hs578T cells (Figure 9A), upon higher NOV treatments (200 µM and 500 µM), the matrix is almost entirely lost appearing more intracellular (red arrows), with a concomittant appearance of vesicle-like structures within these cells (Figure 9A). A magnified image of this NOV induced phenotype is shown alongside. MEF-1 cells followed a similar trend, in that at low NOV concentrations the FN matrix (white arrows) is maintained but at 100 µM NOV, MEF-1 cells had very little to no noticeable exFN matrix remaining (Figure 9B, upper panel), which further decreases in a dose-dependent manner at higher concentrations. At concentrations above 100 µM NOV, FN appears solely intracellular. PEA-13 cells did not lose their exFN matrix as readily as the MEF-1 cells in response to NOV and a large proportion of exFN is seen to be retained in even the highest NOV concentration (1000 µM) (Figure 9B, lower panel). The vesicle-like morphology observed in the Hs578T NOV treatments was however not detected in either of the MEF cell lines. Taken together, these data suggested that LRP1 expressing cells (Hs578T and MEF-1) showed a dose-dependent loss in exFN in response to NOV treatment, while the LRP1-null PEA-13 cells did not.

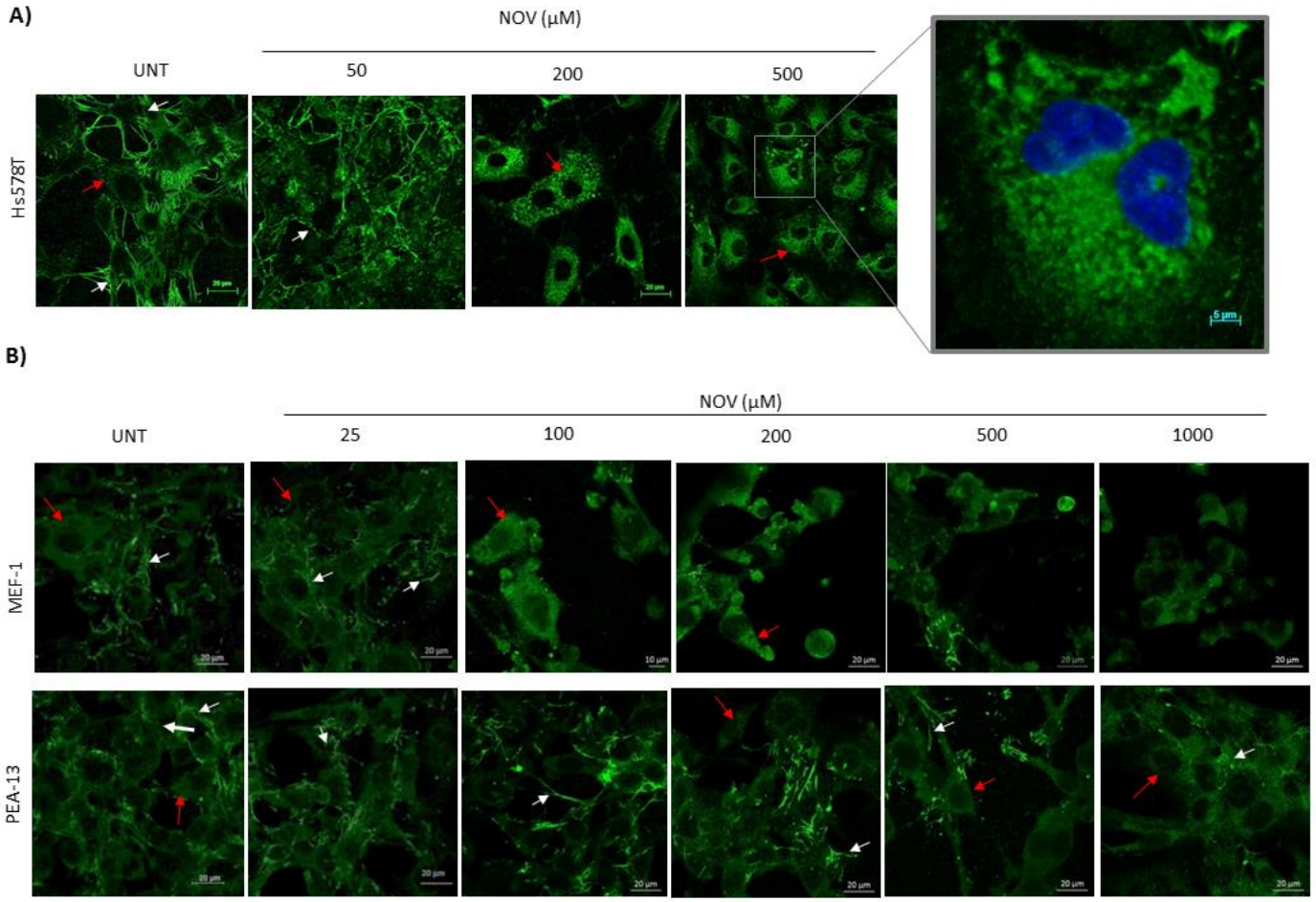

Figure 9: NOV induces a greater loss of extracellular fibronectin matrix in Hs578T and MEF-1 cells compared to PEA-13 cells.

Cells were allowed to adhere overnight in a glass bottomed 15 well ibidi microdish and were treated with increasing concentrations of NOV in **A)** Hs578T cells (0-500 µM) and **B)** MEF-1 and PEA-13 cells (0-1000 µM) for 16 hours at 37 ˚C. Cells were fixed with ethanol and incubated with mouse primary antibody against fibronectin (ab194395) followed by donkey anti-mouse Alexa Fluor-488. Images were captured using the Zeiss LSM 780 Meta laser scanning confocal microscope with the 63x oil objective and analysed using Zen Blue software. White arrows indicate extracellular FN matrix or FN fibrils and red arrows indicate intracellular FN. Data are representative of images obtained from triplicate experiments. Scale bars represent 20 µm.

3.5 Analysis of extracellular FN levels by a DOC assay and biotin-streptavidin affinity chromatography

At the cell surface, integrins bind and mediate the assembly of soluble FN (derived from intracellular FN) which induces the formation of short detergent soluble fibrils. These fibrils propogate to form a dense matrix of detergent insoluble fibrils, which are largely extracellular (Schwarzbauer & Sechler, 1999). To determine the location of FN detected in LRP1-deficient and -expressing cells (Figure 6B) we employed two different protocols. The first was an adapted DOC assay protocol from Brenner and colleagues (2000) for separating soluble and insoluble pools of FN, which putatively represent intracellular and extracellular FN, respectively. These two pools of fibronectin are separated based on their difference in solubility. The deoxycholate (DOC) soluble pool represents fibronectin binding to cell surface receptors, which remains in solution after centrifigation, whilst the DOC insoluble pool represents fibronectin incorporated into the extracellular matrix separated as a pellet (McKeown-Longo & Mosher, 1985). Since PEA-13 cells experienced an increased tolerance for NOV compared to MEF-1 cells (as determined by WST1 assay; Figure 5) we treated PEA-13 cells here with double the concentrations of those used in MEF-1 cells. DOC-soluble and insoluble fractions from cell lysates were probed for FN in western analysis. In agreement with earlier results, PEA-13 cells expressed increased levels of FN in both forms of soluble and insoluble FN relative to MEF-1 cells (Figure 10). The insoluble FN in MEF-1 cells (Figure 10, upper panel) dose dependently decreased to levels below that of the untreated control. The soluble levels of FN in this cell line also decreased in a dose dependent manner from 0-1000 µM. Insoluble FN levels of PEA-13 cells (Figure 10, lower panel) appeared to be constant across the range of NOV concentrations and were only lost entirely at the highest concentration (2000 µM NOV). Soluble FN levels were stable until concentrations above 200 µM, after which there was a dose dependent decrease. If we compare the proportion of insoluble:soluble FN ratio in each of the cell lines, it is observed that insoluble FN levels in MEF-1 cells are reduced at lower concentrations of NOV compared to its soluble FN counterpart and relative to the change in the insoluble FN levels in PEA-13. PEA-13 cells however, have noticeably more insoluble FN to soluble FN, and this insoluble exFN was more resistant to NOV treatment. These data suggest that NOV treatment induces loss of insoluble exFN in the LRP1 expressing MEF1 but not in the LRP1 deficient PEA-13 cells.

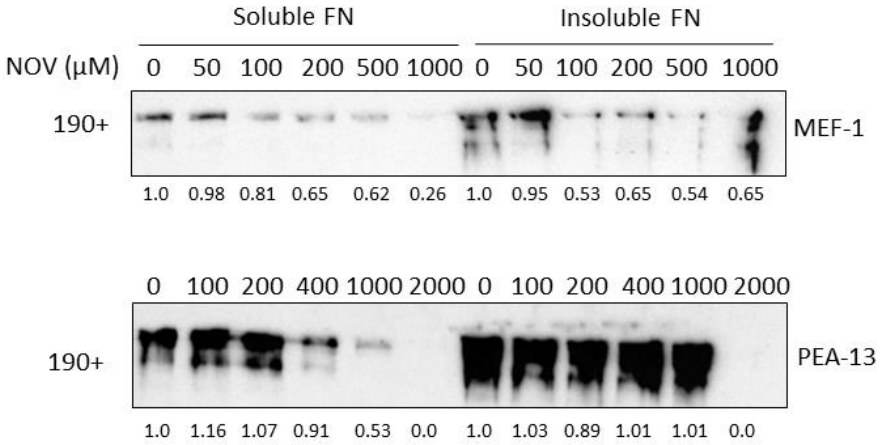

Figure 10: NOV causes a greater loss of extracellular FN levels in MEF-1 cells compared to PEA-13 cells.

To test the effect of Hsp90 inhibition on soluble and insoluble levels of fibronectin, MEF-1 (wild type) and PEA-13 (LRP1-deficient) cells were treated with increasing doses of NOV for 16 hours at 37˚C. Equivalent numbers of cells were harvested and the soluble and insoluble FN fractions separated using the DOC assay. Levels of FN were detected by immunoblotting with rabbit anti-human FN antibody. Densitometry values of the band intensities as determined in ImageJ are indicated below each lane.

The second protocol for analysing exFN levels included a biotin-streptavidin affinity purification previously optimized by members of our group (Hunter *et al.,* 2014). Adherent MEF-1 and PEA-13 cells were treated for 16 hours with or without 200 µM NOV at 37 ˚C before cell surface proteins were biotinylated with EZ-Link™ Sulfo-NHS-SS-Biotin. This biotinylation reagent contains a cell-impermeable NHS ester group which reacts with ε-amines on lysines residues of nearby proteins (ThermoScientific). Biotin-labelled extracellular proteins could then be isolated using a biotin-streptavidin affinity column. NHS-biotin reagent was incubated with the cell monolayer strictly for 1 hour at 4 ˚C to ensure that only exFN species would be labelled with biotin and that biotin would not be internalised. The reaction was terminated upon addition of 1 M Tris-Cl and cells lysed in RIPA buffer with gentle scraping. Lysates were incubated with streptavidin agarose beads overnight at 4 ˚C and affinity purified proteins were released from the beads by boiling with SDS sample buffer. In order to confirm that the isolated biotin fraction represented surface bound extracellular FN we included an additional flask each of treated and untreated cells which were biotinylated and trypsinized before streptavidin affinity purification. Trypsin, a serine protease, digests proteins at the carboxyl end of lysine and arginine residues and should thus theoretically cleave any surface bound biotin-protein interactions and reduce the amount of FN in affinity purified fractions (Hunter *et al.,* 2014).

Figure 11 shows the western analysis of the affinity purified fractions with (+) and without (-) NOV and/or trypsin treatment. The biotinylated MEF-1 fractions revealed reduced levels of FN (190+ kDa) in (+NOV) samples compared to (-NOV) samples. Equivalent control fractions which had been trypsin treated resulted in an almost complete loss of biotinylated FN. Biotinylated PEA-13 fractions revealed an opposite trend to the MEF-1 in western analysis. Increased surface FN was observed in NOV treated samples compared to (-NOV). Interestingly, affinity purified FN in PEA-13 cells appeared to be more resistant to trypsin treatment (+trypsin) in comparison to MEF-1 cells and in fact displayed higher levels of FN than the (-trypsin) fractions. This could be attributed to the protein being more protease resistant. We also probed for total Hsp90 on the same western blot (Figure 11, middle panel) and observed similar levels of Hsp90 in both the untreated and NOV treated fractions (-trypsin) in MEF-1 and PEA-13 cells. Hsp90 levels were not reduced in (+trypsin) fractions. It is unclear why Hsp90 was more resistant to trypsin cleavage in these samples. The presence of

LRP1 (Figure 11, lower panel) in MEF-1 cells appeared higher in the NOV treated fraction and were reduced in trypsinized samples. Since the controls (+trypsin) did not appear to cause a consistent reduction in protein levels, and in the case of PEA-13 cells appeared to cause increased FN levels, we must interpret the results with caution.

Collectively these data demonstrate that LRP1-deficient cells have high levels of exFN which do not decrease upon Hsp90 inhibition as observed by confocal microscopy (Figure 9) and DOC assay (Figure 10). LRP1-expressing cells have comparatively less exFN, the levels of which decrease dose dependently upon Hsp90 inhibition.

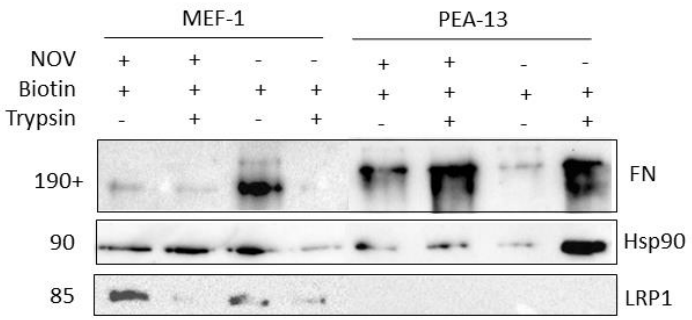

Figure 11: Cell-surface associated FN is reduced upon NOV treatment in MEF-1 cells but not PEA-13 cells

Cells were allowed to adhere overnight in a T-75 flask and treated for 16 hours with 200 µM NOV (NOV) or left untreated. Cells were then incubated with the cell impermeable EZ-Link™Sulfo-NHS-SS-Biotin for 1 hour at 4 ˚C. NHS-biotin was quenched with 1 M Tris-Cl. Cells were scraped in RIPA buffer and surface biotinylated proteins were purified by streptavidin affinity chromatography. Biotinylated fractions from equal numbers of cells of each sample were probed for the presence of FN and Hsp90 by western analysis.

3.6 LRP1 partially colocalises with FN in NOV treated MEF-1 cells

Next we investigated whether LRP1 colocalised with FN (Figure 12) and/or Hsp90 (Figure 13) in NOV treated MEF-1 cells by confocal microscopy. Adherent MEF-1 cells were treated with increasing NOV concentrations for 16 hours before being stained for LRP1 and either FN or Hsp90α/β using relevant fluorescently conjugated antibodies. The colocalisation was measured in ImageJ using the Intensity Correlation Analysis plugin (Li *et al.,* 2004). The degree of colocalisation is represented using colour scatter plots alongside, where the intensity of one signal along the x-axis is plotted against the intensity of a second signal along the y-axis. Under conditions of perfect colocalisation, each of the signals of the scatterplot cluster around a straight line indicating a linear relationship. In contrast, under conditions of no colocalisation, each of the signals are distributed in two distinct separate groups along each axis (Dunn *et al.,* 2011). The degree of colocalisation between the red and green channels representing (LRP1 and FN respectively) (Figure 12) showed little to no colocalisation in untreated cells as represented by the scatter plot where the red and green channels have distinct populations along each axis. The colocalisation increased in a dose dependent manner as seen by the yellow overlap in merged images, as well as increased clustering of red and green signals around a straight line with an overlap indicated in yellow in scatter plots. PEA-13 cells are represented below showing no colocalisation, as expected in this LRP1-deficient cell line.

MEF-1 cells were treated with increasing concentrations of NOV as described previously and incubated with rabbit anti-LRP1 and goat anti-Hsp90 primary antibodies followed by donkey anti-rabbit Alexa Fluor-546 and donkey anti-goat Alexa Fluor-660 (Figure 13). A diffuse staining pattern of Hsp90 was observed in all NOV treatments and there appears to be colocalisation in both untreated and NOV treated MEF-1 cells as observed by yellow pixels in merged images. The colour scatter plots indicated alongside show that there is no change in overlap of signals between the different treatments, although there does appear to be an increase in the number of individual cells showing colocalisation between Hsp90 and LRP1.

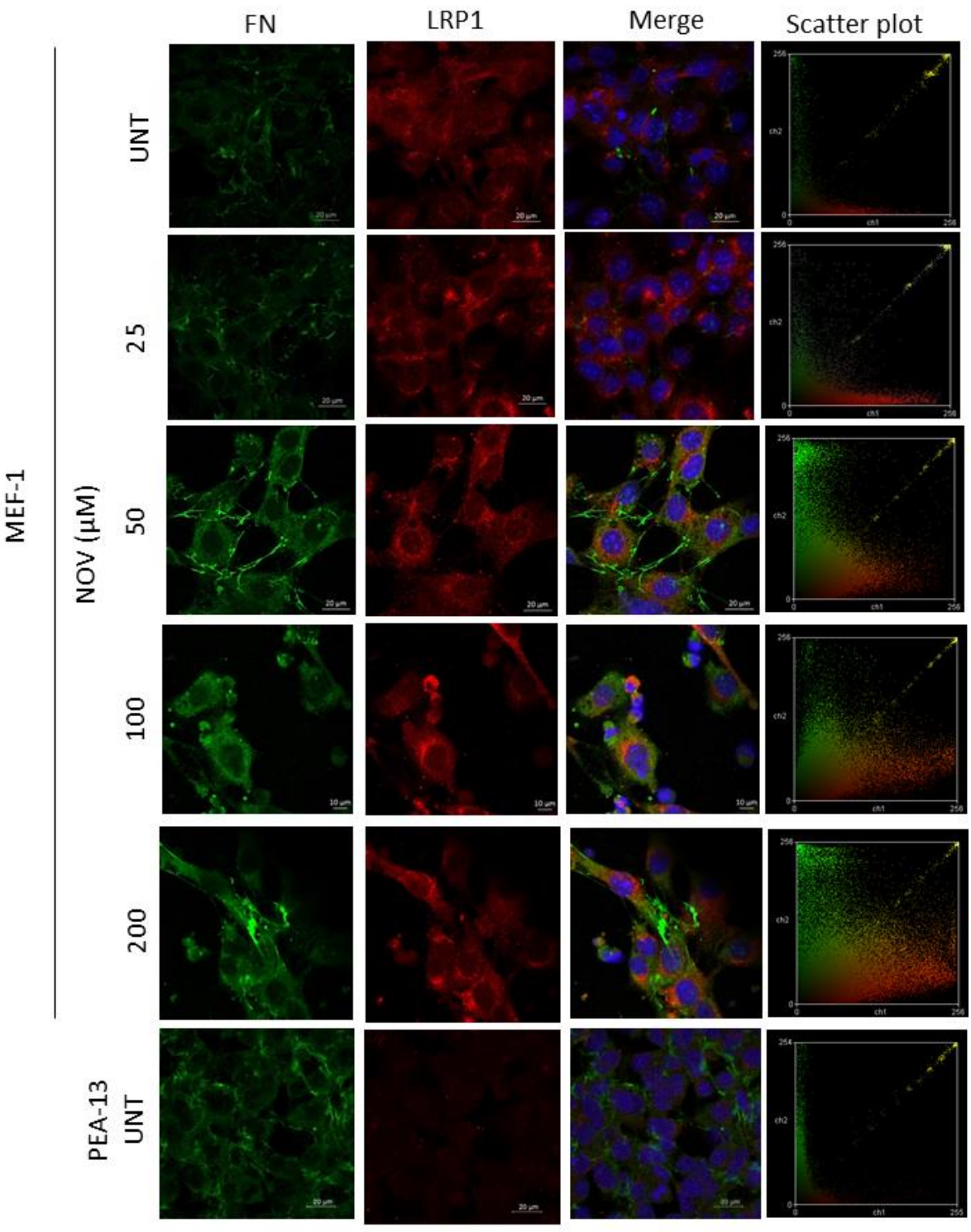

Figure 12: Legend over page

Figure 12: FN and LRP1 partially colocalize upon NOV treatment in MEF-1 cells.

Cells were allowed to adhere overnight in a glass bottom 15 well ibidi microdish and were treated with increasing concentrations of NOV (0-200 μM) for 16 hours. Cells were fixed with ethanol and incubated with mouse anti-fibronectin (green) and rabbit anti-LRP1 (red) primary antibodies followed by donkey anti-mouse Alexa Fluor-488 and donkey anti-rabbit Alexa Fluor-546 respectively. Nuclei were stained with 1 μg/ml Hoechst 33342 (blue). Images were captured using the 63x objective of the Zeiss LSM 780 Meta laser scanning confocal microscope and analyzed using Zen Blue software (Zeiss, Germany). Data are representative of images obtained from duplicate experiments with similar results. Scale bars represent 20 μm. Colocalisation analysis and scatter plots were generated using ImageJ.

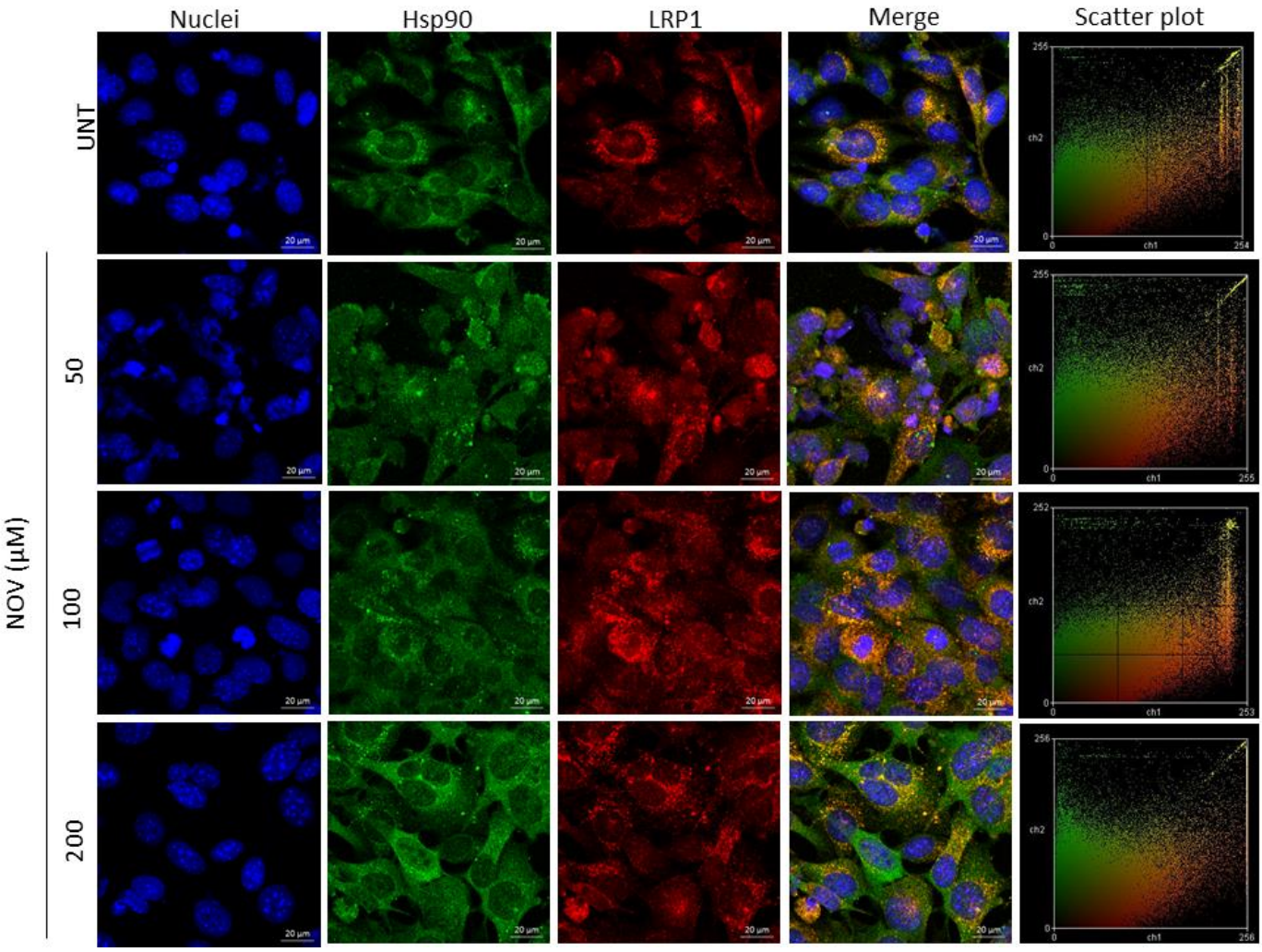

Figure 13: LRP1 and Hsp90 localize in NOV treated and untreated MEF-1 cells.

MEF-1 cells were allowed to adhere overnight in a 15 well ibidi microdish and treated with increasing concentrations of NOV (0-200 µM) for 16 hours. Cells were fixed with ethanol and incubated with goat anti-human Hsp90α/β and rabbit anti-human LRP1 followed by donkey anti-goat Alexa Fluor-660 and donkey anti-rabbit Alexa Fluor-546 respectively. Nuclei were stained with Hoechst-33342 (1 µg/ml). Images were captured using the 63x objective on the Zeiss LSM 780 Meta laser scanning confocal microscope and analyzed using Zen Blue software (Zeiss, Germany). Co-localisation analysis and scatter plots were generated using Intensity Correlation Analysis plugin in ImageJ. Data are representative of images obtained from triplicate experiments with similar results. Scale bars represent 20 µm.

3.7 LRP1 is in a common complex with FN and Hsp90 in Hs578T breast cancer cells and MEF-1 cells

Here, we demonstrate that a putative complex exists between Hsp90, FN and LRP1. LRP1 coimmunoprecipitation was carried out using an adapted protocol from Muratoglu and colleagues (Muratoglu *et al.,* 2010). Confluent Hs578T and MEF-1 cells were left untreated or treated with 200 µM NOV or 50 µM NOV respectively for 16 hours. The cell-impermeable DTSSP crosslinker was incubated with cell monolayers for 2 hours at 4 ˚C to covalently crosslink cell surface proteins. The DTSSP crosslinker contains NHS moeities on both ends which are able to interact with lysine residues on proteins that are within interacting range (12Å) (Thermo Scientific). Crosslinked LRP1 containing complexes were selected for by immunoprecipitation using a rabbit LRP1 antibody coupled to MagReSyn™ Protein A. An isotype control IgG antibody coupled to MagReSyn™ Protein A was used as a control. Lysates of untreated (U) and NOV (N) treated samples were prepared from equal cell numbers and split equally between the LRP1 coupled beads and IgG coupled beads. Following overnight incubation of lysates with beads at 4 ˚C, protein complexes were eluted from the beads. Samples were collected throughout the immunoprecipitation procedure for downstream analysis. Protein fractions were resolved on SDS-PAGE in the presence of β-mercaptoethanol to ensure cleavage of the crosslinker.

Figure 14A shows the immunblot of flow through (FT), wash and elution fractions of the LRP1 and IgG antibody coupled MagReSyn complexes from Hs578T cells. The presence of LRP1 (85 kDa) (Figure 14A, middle panel) in the elution samples which had been immunoprecipitated with LRP1 antibody confirmed that the isolation and enrichment for LRP1 containing complexes was successful. The absence of LRP1 in elution fractions of IgG immunoprecipitated samples confirmed there was no non-specific binding to the beads. In the immunoblot for FN (upper left panel), there were low levels of FN in the elution fractions; overexposure revealed the presence of two different molecular weight FN bands (190+ kDa and 100 kDa) (upper right panel). There appeared to be a slightly higher intensity of both the 190+ kDa and 100 kDa bands in the untreated sample (U) compared to NOV (N), although this may be due to slightly higher levels of LRP1 in the NOV treated IP. A small degree of non-specific binding of FN to the IgG antibody IP fractions was also observed but these are lower in comparison to the LRP1 antibody IP. The western blot for Hsp90 (lower panel) in the elution

fractions confirmed the presence of an Hsp90:LRP1:FN complex at the cell surface. A slight decrease in Hsp90 was observed in the NOV treated LRP1 IP fraction, which again may be due to the slightly lower levels of LRP1 in this IP.

Figure 14B shows the immunoblot analysis of LRP1 immunoprecipitates from MEF-1 cells treated with 50 µM NOV. In the elution fractions of the LRP1 IP, treatment with NOV appeared to increase FN (190+ kDa) slightly in comparison to untreated. An enriched fraction of FN (100 kDa) was immunoprecipitated in comparison to the 190+ kDa FN fragments as observed by the intensity of bands. Similar levels of LRP1 (85 kDa) were isolated in the untreated and NOV treated samples of LRP1 IP (Figure 10B, middle panel). The absence of proteins detected in the IgG IP elution fractions confirmed there were no non-specific binding of proteins to the MagReSyn™ Protein A beads. Upon overexposure, similar levels of Hsp90 were detected in the NOV (N) and untreated (U) fractions (lower right panel). The bands below Hsp90 likely represent non-specific binding. In both Figures 10A and B, bands detected at 50 kDa are likely the detection of heavy chains (~55 kDa) of the capture antibody used (MagReSyn™, South Africa). In all cases, flow through (FT) and wash lanes show unbound proteins that had not been immunoprecipitated. These data support the presence of a complex containing Hsp90, LRP1 and FN in both Hs578T and MEF-1 cells in both the absence and presence of NOV.

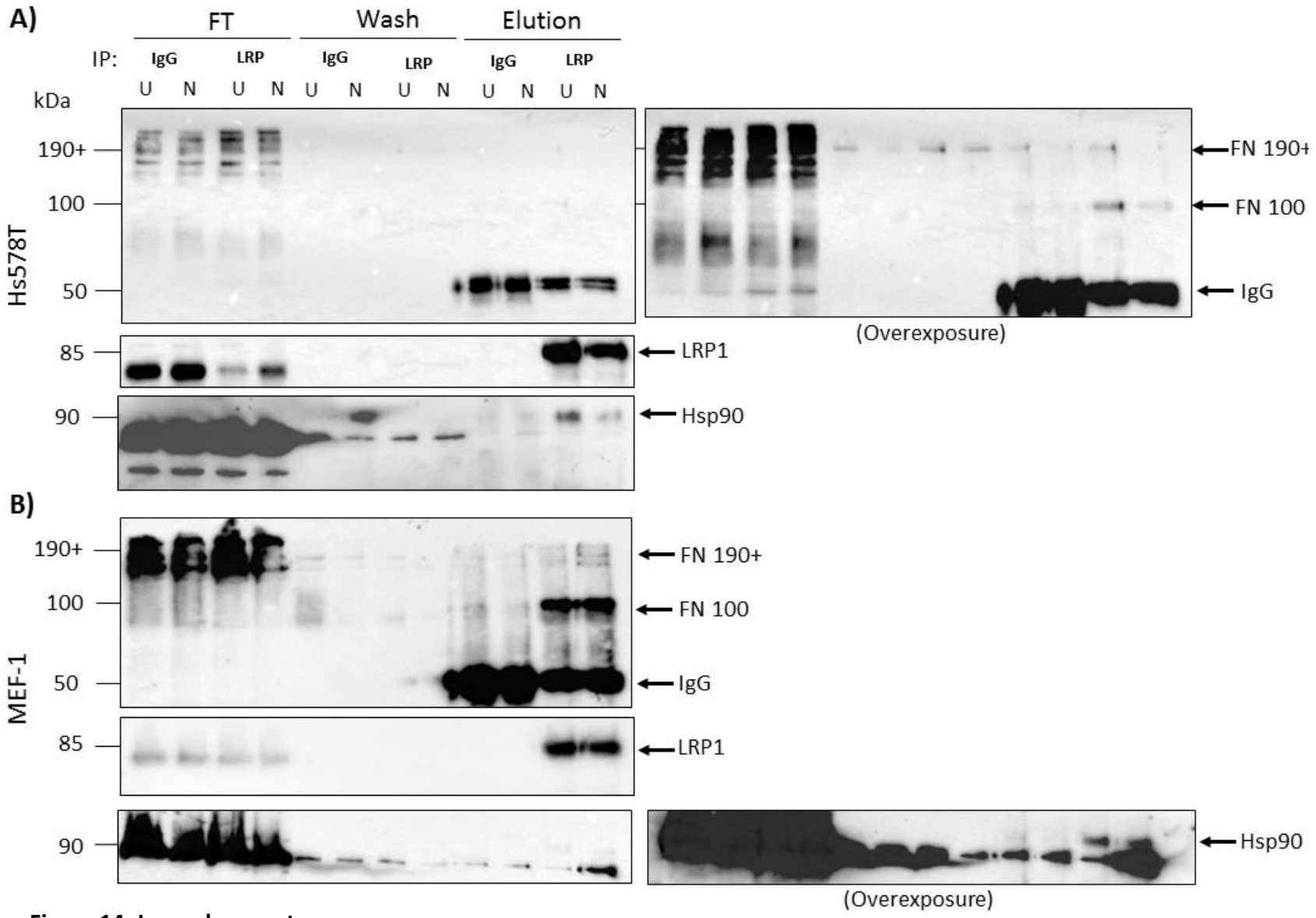

Figure 14: Legend on next page

Figure 14: Confirming the presence of Hsp90 and FN in an extracellular complex with LRP1 by immunoprecipitation.

A) Hs578T cells were seeded into a T-75 culture dish until 90% confluency was observed and treated with or without NOV at 200 µM for 16 hours. Extracellular proteins were crosslinked with the cell-impermeable crosslinker, DTSSP (3 mg/ml), for 2 hours at 4 ˚C. The reaction was terminated by quenching in 1 M Tris-Cl (pH 7.5). Cells were scraped in non-denaturing lysis buffer and centrifuged at 12000 rpm in a microfuge for 20min at 4 ˚C. LRP1-containing complexes were isolated by immunoprecipitation (IP) with MagReSyn™ Protein A coupled to either LRP1 or isotype control IgG antibodies. Flow through (FT) and elution fractions were resolved and probed (WB) for FN, LRP1 and Hsp90. **B)** MEF-1 cells were seeded into a T-150 dish until 90% confluency was observed and treated with or without NOV at 50 µM for 16 hours and harvested as described in A). FT, wash and elution fractions were probed for levels of FN, LRP1 and Hsp90. Data shown are representative of duplicate experiments with similar results.

3.8 Analysis of Hsp90 inhibition on cell migration in LRP1-deficient and -expressing cell lines

FN is a major cell adhesion molecule of the ECM and plays a role in cell migration. Remodelling of the extracellular matrix is an integral process in wound healing and is regulated by various growth factors, proteases and receptors amongst others (Hynes, 2009). By performing wound healing assays we hoped to determine what role LRP1 (or a lack thereof) would have on cell migration upon Hsp90 inhibition, given that a substantial loss of FN matrix was observed previously in LRP1-expressing cells but not LRP1-deficient cells (Figure 9).

Adherent cells were grown to confluency in a 24 well culture dish to ensure that upon wound denudation only cell migration and not growth would be observed. Wounds of cell monolayers were created with a single stroke of a toothpick down the middle of each well. Cells were treated in fresh media containing NOV for 12 hours at the time of wound denudation and images captured at time 0 and 12 hours post treatment. Control cells were treated in fresh media without NOV and images taken at the same time points. Marks on the bottom of the culture dish were made with a pen to ensure that identical positions were imaged at each time point. Figure 15A shows a representative study of MEF-1, PEA-13 and Hs578T migration into "wounds" upon treatment with a range of NOV concentrations. The wound size in each of the treatments were captured by microscopy and measured immediately after wounds were made at 0 hrs, and after incubation for 12 hrs as described in Methods.

Quantification of distances migrated (Figure 15B and C) were calculated in ImageJ and statistical significance of different responses for each cell line to Hsp90 inhibition were determined using an unpaired two-tailed t-test in GraphPad Prism 4. In MEF-1 cells, cells treated with 50 µM NOV migrated significantly more ($p= 0.018$), with a mean distance (MD) of 561 µm ± 29.98, compared to the control (UNT) of 459.7 µm ± 20.33 (Figure 15B). MEF-1 cells treated with 100 µM NOV were less migratory than the 50 µM NOV (MD= 488.8 µm ± 45.98) but were still more migratory than its untreated counterpart (MD= 430 µm ± 43.02), although this difference was not significant. From these data, it would appear that NOV was promoting migration of MEF-1 cells. This trend however, did not extend to the 200 µM NOV treatment, as untreated MEF-1 cells were found to be more migratory (MD= 384.7 µm ± 7.1) compared to NOV treated cells (269 µm ± 21.52).

PEA-13 cells treated with 50 μM NOV were found to migrate less (MD= 268 μm ± 8.0) than untreated PEA-13 cells (MD= 310.7 μm ± 38.4) (Figure 15B). The same was true for PEA-13 cells treated with 100 μM NOV, which migrated a MD of 261.4 μm ± 21.7 versus the untreated control (MD= 301.8 μm ± 17.6). The 200 μM NOV treated PEA-13 cells were the least migratory (MD= 156 μm ± 9.2) and this was found to be significant with a p value of 0.0007 compared to untreated cells (MD= 297 μm ± 11.5).

A slight increase in migration of Hs578T cells was observed for 100 μM NOV treatment (MD= 227 μm ± 7.2) compared to its untreated counterpart (MD= 198 μm ± 12.7) (Figure 15C) although this change in distance migrated was found to be non-significant. The 200 μM NOV treatment increased the distance migrated after 12 hours following treatment (MD= 584 μm ± 19.3) as compared to the distance migrated in untreated Hs578T cells after 12 hours (MD= 295 μm ± 37.6). This result however was not statistically significant.

Additionally when comparing the average migration of untreated MEF-1 and PEA-13 cells directly with each other, it was noted that MEF-1 cells were significantly more migratory (where # denotes the statistical significance between cell lines, Figure 15B) (MD= 424 μm ± 15.8) than PEA-13 cells (MD= 302 ± 22.4 μm). NOV treated MEF-1 cells at either concentration were also significantly more migratory than NOV treated PEA-13 cells. Collectively, these data suggest that there was an increase in migration in LRP1-expressing cells (Hs578T and MEF-1) which had been treated with concentrations of NOV for 12 hours that had previously been shown to lead to the loss of exFN and an increase in inFN.

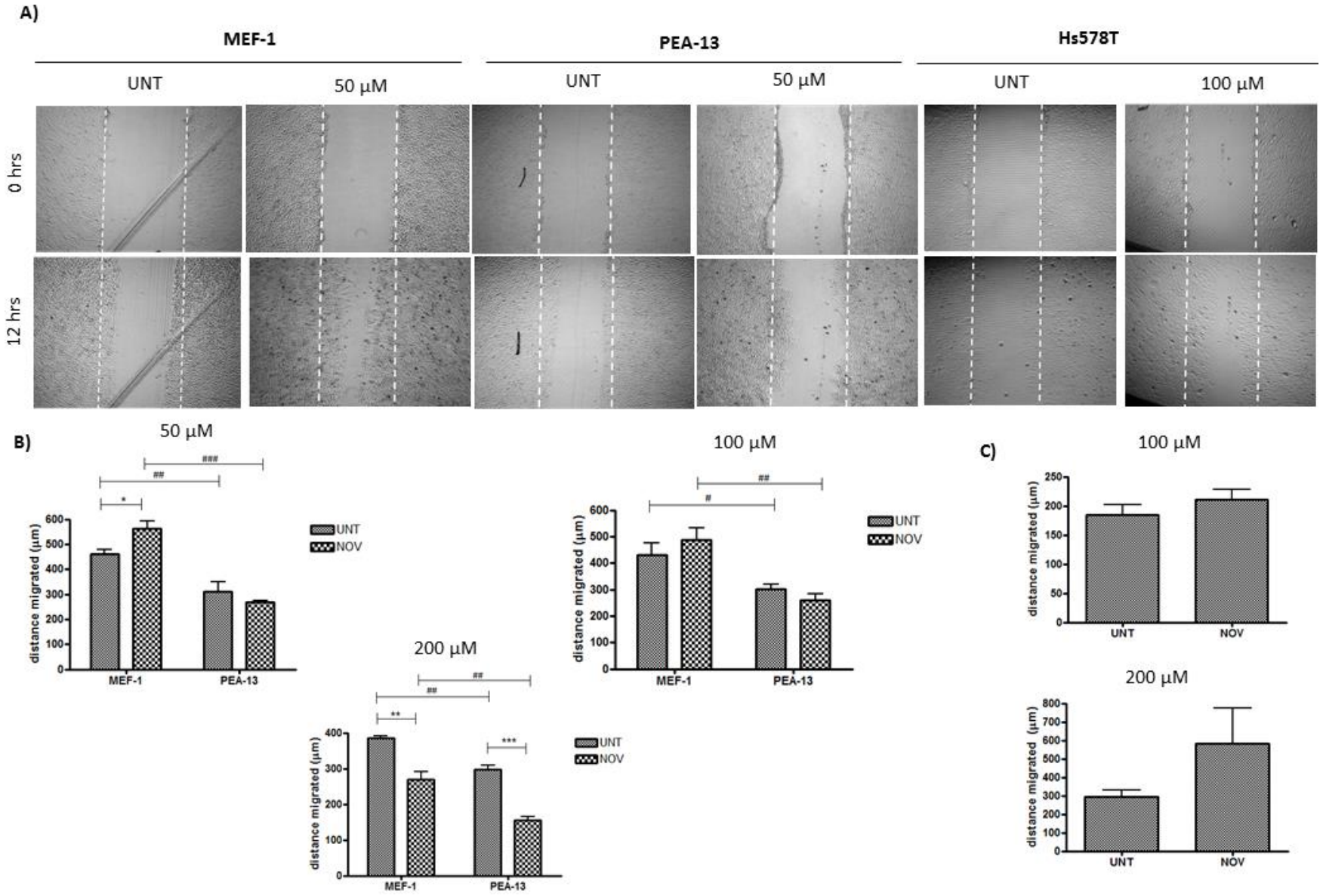

Figure 15: Legend on next page

Figure 15: Wound healing assay comparing migratory capacity of MEF-1, PEA-13 and Hs578T cells with or without NOV treatment.

A) MEF-1, PEA-13 and Hs578T cells were grown to confluency in a 24 well plate. Wounds were made by scraping the cell monolayer down the middle of the well with a sterile toothpick. Cells were treated in media with or without NOV at varying concentrations and incubated at 37 ˚C, 9% CO_2. Images were captured at time 0 hrs and 12 hrs post NOV treatment with a Zeiss Primovert inverted light microscope with camera using the 5x objective lens and analysed in ImageJ. White dotted lines denote the edges of wounds at time 0 in each image. Images are representative of triplicate experiments. **B)** Average distances migrated for MEF-1, PEA-13 and **C)** Hs578T cells were measured using ImageJ. Three measurements along the length of the wounds at time 12 hrs were subtracted from lengths measured at time 0 hrs. Statistical analysis was performed using unpaired two-tailed t-tests in GraphPad Prism 4. Statistics are indicated on the graph as such: *= $p<0.05$, **= $p<0.01$, ***= $p< 0.001$ for comparison within a cell line for different treatments; #= $p<0.05$, ##= $p<0.01$, ###= $p<0.001$ comparing between cell lines.

Chapter 4. DISCUSSION

4.1 A ROLE FOR LRP1 IN NOV-INDUCED FN TURNOVER

Studies within our group (BioBRU) have shown the presence of surface associated Hsp90 and extracellular soluble Hsp90β in various cancer cell lines and that extracellular Hsp90 isoforms may be responsible for regulating the turnover of FN (Hunter *et al.,* 2014). A study from our group reported FN as a novel interacting protein of eHsp90 and suggested a direct role for Hsp90 in FN matrix remodelling (Hunter *et al.,* 2014). Upon inhibition of Hsp90 by NOV, we observed the FN matrix to become unstable and degrade by a receptor-mediated endocytosis mechanism (Hunter *et al.,* 2014). However, the receptor mediating this NOV-induced internalisation of FN is currently unknown. LRP1 was a likely candidate as it is a ubiquitous receptor responsible for regulating internalisation of numerous diverse ligands, and is known be a receptor for both Hsp90 (Basu *et al.,* 2001) and FN (Salicioni *et al.,* 2002). To better understand the mechanism of Hsp90-mediated FN internalisation, we focused on the role of LRP1 as the putative endocytic receptor responsible for the uptake of FN. We used genetically modified murine embryonic fibroblasts (MEFs) for LRP1 knockout as they are an isogenic model system and are known to have high levels of ECM, making this an ideal system to test whether the FN response to NOV is affected by the presence or absence of LRP1. To the best of our knowledge, this is the first report to investigate Hsp90 inhibition on FN turnover in MEFs and to link a dual role for Hsp90 and LRP1 in the turnover of FN.

4.1.1 Loss of extracellular FN in response to NOV is dependent on the presence of LRP1

Hsp90 inhibition with NOV appeared to have similar effects in Hs578T breast cancer and MEF-1 cells (both of which contain LRP1) which differs to the response observed in an LRP1-deficient cell line. In Hs578T breast cancer cells, levels of tFN increased upon Hsp90 inhibition at concentrations below its EC50 value (214.9 μM) and dose dependently decreased at the higher NOV concentrations. These data support previous findings within our group having shown that NOV treatment above the EC50 caused a loss of tFN in Hs578T cells (Hunter *et al.,* 2014). Our data extend this study by showing that at the lower range of NOV, an initial increase in FN is observed. A similar response was observed in MEF-1 cells where tFN increased at concentrations below its EC50 (45.6 μM) but subsequently decreased dose dependently at higher concentrations. In LRP1-deficient PEA-13 cells, no increase in FN was observed across the range of NOV concentrations, as such, the increase in tFN seemed to be

dependent on the presence of LRP1. We suspect that the increase in tFN observed in both Hs578T and MEF-1 cells (but not PEA-13 cells) upon Hsp90 inhibition at the lower range of NOV might be as a result of internalisation of extracellular FN (exFN) and increased levels of intracellular FN (inFN). This hypothesis was supported by the results of our deoxycholate fractionation study, which showed higher stability of insoluble exFN in NOV treated PEA-13 compared with the MEF-1 cells. Studies by Sotille and Chandler (2005) also showed that loss of extracellular FN matrix was accompanied with an increase in endocytosed FN which was subsequently degraded.

Salicioni and colleagues were one of the first groups to identify that FN interacted with LRP1 and regulated FN levels. They proposed LRP1 to be a catabolic receptor for exFN (Salicioni *et al.,* 2002). In an attempt to analyze the dynamics of exFN upon Hsp90 inhibition in an LRP1-expressing and deficient cell line, we processed cells by extraction in DOC buffer and separated DOC-insoluble (matrix-associated) FN from DOC soluble (cell-associated) FN as described (McKeown-Longo & Mosher, 1985). In both untreated and NOV treated conditions, greater exFN (insoluble) levels were detected in PEA-13 cells compared to MEF-1 cells. This was found to be true for inFN (soluble) too. A dose-dependent loss of both exFN and inFN in MEF-1 cells was observed in our DOC assay. No loss in exFN was observed in PEA-13 cells, but inFN levels decreased dose-dependently. This demonstrates that exFN in LRP1-deficient PEA-13 cells was more stable than exFN in MEF-1 cells with NOV and suggests a dependency on LRP1 for the internalisation of exFN. In surface biotinylation assays a similar response (i.e. a loss in surface associated FN upon NOV treatment) in MEF-1 cells supported the loss observed previously for tFN and exFN. These data were less convincing due to the inability of trypsin to cleave surface bound protein interactions particularly in PEA-13 cells. Perhaps this could be explained by a requirement for proteases in FN turnover. Also, Dedieu *et al.,* (2008) reported that LRP1-deficient carcinoma cells were twice more resistant to trypsin cleavage. Our findings are in agreement with studies by Salicioni and colleagues, who showed that both LRP1-deficient MEFs and LRP1-deficient 13-5-1 Chinese hamster ovary (CHO) cells accumulated greatly increased levels of surface FN in comparison to LRP1-wild type cells (Salicioni *et al.,* 2002; Gaultier *et al.,* 2010). In addition they also showed that LRP1-deficient cells dissociated from monolayer culture had increased FN levels which remained associated with the cells. We extended this study by demonstrating a link with NOV and the loss of

surface FN. This is the first report of a NOV-induced loss of surface FN selective to LRP1-expressing cells.

One could argue that the reduction in exFN be attributed to reduced FN synthesis or export from the cell. We therefore decided to conduct quantitative q-RT-PCR experiments to evaluate whether NOV was reducing FN mRNA levels. We found that NOV was not inducing any significant changes in the FN transcript levels in MEF-1 cells and concluded that the loss of FN matrix was due to its increased internalisation and degradation by the cells intracellularly. Moreover, levels of FN mRNA were significantly reduced in PEA-13 cells at low NOV concentrations, however these reductions were not detected at a protein level. Additionally, reports from our group have shown NOV to have no effect on FN mRNA levels in Hs578T cells (Dhanani, 2015). It is not uncommon for changes in protein abundance to be disproportional to mRNA levels; a landmark study by Gygi *et al.,* (1999) examined the relationship between proteins and mRNA levels in yeast and revealed that transcript levels, in fact, provide little predictive value of protein expression. Similarly, cancer cells treated with Hsp90 inhibitors demonstrated an upregulation in total mitochondrial proteins without a corresponding increase in mRNA (Margineantu *et al.,* 2007). Treatments with cycloheximide (CHX) which blocks translation served to determine whether the dose dependent loss of tFN and exFN levels observed following the initial increase in MEF-1 cells were as a result of degradation of FN. A loss of tFN was accelerated by NOV in the presence of CHX over the same time period compared to the control (-NOV). This supports earlier data showing that the loss of tFN is due to degradation of FN. Together, these data suggest a likely mechanism for the loss of NOV-induced FN is via protein turnover which is dependent on the presence of LRP1 highlighting a role for this receptor in regulating FN matrix dynamics in response to Hsp90 inhibition.

4.1.2 NOV-induced loss of exFN is degraded by lysosomes in LRP1-expressing cells

To better understand the role for LRP1 as a putative catabolic receptor in mediating NOV-induced degradation of FN, we treated cells with proteosomal and lysosomal degradation inhibitors. Chloroquine, a drug typically used to treat malaria is known to inhibit clathrin-mediated endocytosis by affecting the function of clathrin in the membrane (Schlesinger *et*

al., 1988) and also serves to prevent lysosomal enzyme activity (Gonzalez-Noriega *et al.,* 1980). FN accumulated in PEA-13 cells upon proteosomal inhibition in the presence of NOV, whereas FN accumulated in MEF-1 cells upon lysosomal inhibition. These data would support the fact that NOV-induced increase of tFN in MEF-1 cells may be due to internalisation and degradation of exFN by lysosomes. The ubiquitin-proteasomal pathway is a key regulator of intracellular proteins involving their ubiquitination and targeted delivery to the proteasome for its degradation (Amazit *et al.,* 2011). Conversely, extracellular or membrane-associated proteins tend to be degraded via the lysosomal pathway following its internalisation (Sotille and Chandler, 2005). Thus, in LRP1-expressing cells we observed internalisation of exFN which is degraded by the lysosomes, however, in LRP1-deficient cells, exFN cannot be internalised and thus upon Hsp90 inhibition we see degradation of soluble intracellular FN. From these data we could speculate that the type of FN being degraded may influence the degradation pathway. Sotille and Chandler (2005) also importantly note that FN degradation via certain pathways may be dependent on cell type. In smooth muscle cells (SMCs), treatment with the LRP1 inhibitor, RAP, was not able to prevent degradation of FN (Godyna *et al.,* 1995), whereas studies by Salicioni *et al.,* (2002) demonstrate in MEF-1 cells that RAP effectively blocks degradation of FN. Given that in most cases, intracellular proteins are processed by the proteasome and extracellular proteins are processed by the lysosome, taken together these data could be interpreted to suggest that the observed loss of FN in PEA-13 is primarily loss of intracellular FN, while the loss of FN in NOV treated MEF1 is due to internalization and degradation of extracellular FN. Considering the majority of FN available for degradation in PEA-13 cells is intracellular and in a soluble form, the proteosomal degradation pathway may be highly active in these cells. It would have been interesting to test whether Hsp90 inhibition leads to increased FN ubiquitination in this cell line. In additional experiments, we attempted to fractionate lysosomes from Hs578T and MEF-1 cells to compare levels of FN being degraded upon NOV treatment. Although unsuccessful, further optimizations of this may prove to be useful in demonstrating a dependency for exFN degradation by lysosomes. Also, analysis of LRP1 levels in lysosomal compartments would allow us to determine whether LRP1 was directly involved in delivering FN to lysosomes in response to NOV, or whether its role was more indirect- involving bridging to other receptors or integrins (Salicioni *et al.,* 2002).

In support of a role for LRP1 as a catabolic receptor for exFN uptake upon Hsp90 inhibition we observed a substantial loss of FN matrix in confocal analyses in NOV treated MEF-1 cells. Conversely, the Hsp90 inhibitor had only a modest effect on exFN matrix stability in PEA-13 cells. We also showed that treatment with NOV in Hs578T cells caused the extracellular fibronectin matrix to be internalised forming vesicle-like structures intracellularly. This phenotype has been reported in several other studies including Lobert *et al.,* (2010) who showed early endosomes of FN endocytosed in complex with $\alpha_5\beta_1$ receptor which they predicted to be targeted for lysosomal degradation. Our group has shown that NOV induces the internalisation of FN via receptor-mediated endocytosis (RME) which colocalised with endocytic markers (Rab5 and Lamp1) and that endocytosis inhibitors were able to block the effect of NOV treatment on FN (Hunter *et al.,* 2014). Considering this, and the ability of LRP1 to bind both Hsp90 (Basu *et al.,* 2001; Cheng *et al.,* 2008) and FN (Salicioni *et al.,* 2002) we proposed a RME pathway involving LRP1 to be responsible for mediating the loss of exFN in response to NOV. Whilst Salicioni and colleagues demonstrated binding of FN to LRP1, to date, the specific binding site of FN on LRP1 not known. Using soluble recombinant LRP1 fragments (see Appendix- Figure 20), kindly provided by Dr Dudley Strickland (University of Maryland, USA), we hope to determine which of the four ligand-binding domains on LRP1 FN preferentially binds, using SPR and solid-phase binding assays.

4.2 A REGULATORY MECHANISM FOR NOV-INDUCED FN TURNOVER IN LRP1-EXPRESSING CELLS

Having provided evidence to support that LRP1 is required for the NOV-induced turnover of FN, we aimed to investigate the mechanism by which NOV is able to modulate the response of FN. Western analyses revealed an interesting response of LRP1 levels to NOV treatments in MEF-1 and Hs578T cells. Several membrane spanning proteins (including LRP6, Erb4 and NOTCH) are known to undergo regulated intramembrane proteolysis (RIP), a process which allows for cells to respond to extracellular signals or regulate their surface levels (Gaultier *et al.,* 2008). Evidence of RIP has also been shown for LRP1 which involves two cleavage events and has been shown to also be a mechanism of cell signalling (Quinn *et al.,* 1999). In the first step of LRP1 RIP, furin cleavage of the ectodomain releases the 515 kDa α subunit of LRP1 followed by membrane proteolysis of the 85 kDa β subunit involving γ-secretase to yield a smaller LRP1 intracellular domain (LRP1-ICD) fragment of ~55 kDa and ~25 kDa (Derocq *et al.,*

2012; May *et al.,* 2002). The shed LRP1-ICD has been shown to translocate to the nucleus where it interacts with various transcription modulators (Kinoshita *et al.,* 2003; Zurhove *et al.,* 2008). The function of this LRP1-ICD, however, has not yet been fully elucidated and the exact mechanism of how LRP1-ICD modulates cellular signalling is not known. It is thought to involve the binding of various scaffold and adaptor proteins such as FE65, which constitutively or under specific conditions, recruits other proteins such as kinases to form a complex. This complex is proposed to translocate to other locations in the cell, even the nucleus, where it may deregulate gene transcription (May *et al.,* 2002). A study by Zurhove and colleagues (2008) indicated that a subset of LPS-inducible genes (p65, NFkB and IRF-3) are repressed by LRP1-ICD, thereby limiting the inflammatory response. They demonstrate that LRP1-ICD interacts with these transcription factors and limits their activity by facilitating their export from the nucleus. Other studies have revealed a functional role for LRP1-ICD in ischemic cell death (Polavarapu *et al.,* 2008), however a recent review revealed that the genes modulated by LRP1-ICD are not yet fully elucidated (Etique *et al.,* 2013).

We predict the 85 kDa LRP1 band represents the β-chain of LRP1 and the bands observed at 58 kDa to represent membrane cleavage fragments of the β-chain in response to RIP. These two fragments were observed to have different responses to Hsp90 inhibition; LRP1-85 levels noticeably appeared to decrease in a dose-dependent manner whilst LRP1-58 increased significantly with an increase in NOV concentration. Upon immunofluorescent staining with anti-FN and anti-LRP1 (recognizing the β-chain) antibodies we further showed that NOV was associated with an increased colocalisation of inFN with the LRP1-ICD. Perhaps this increased colocalisation is possible by the increase in LRP1-58 in MEF-1 cells made available by NOV-induced RIP of LRP1. Furthermore, although there was no apparent change in colocalisation of Hsp90 and LRP1-ICD, there was an increase in the number of cells showing colocalisation which appeared perinuclear in support of a possible nuclear transport mechanism for altered signalling/gene expression.

Moreover, FN, LRP1 and eHsp90 were found to occur in a common complex on the surface of Hs578T and MEF-1 cells in both untreated and NOV-treated immunoprecipitates. Immunoprecipitated LRP1 complexes containing FN and Hsp90 were not substantially perturbed by NOV treatments. By forming heterocomplexes with its substrates, Hsp90 has been shown to play a key role in signalling events (Pratt, 1998). The biological function of

eHsp90 remains relatively uncharacterized compared to its intracellular counterpart but various studies have shown eHsp90α to be primarily involved in cell migration and wound healing (Cheng *et al.,* 2008; Li *et al.,* 2011). Tsen and colleagues (2013) reported a role for eHsp90-LRP1 cross-membrane signalling, whereby binding of eHsp90 to LRP1 induced the activation of downstream signalling pathways involving Akt and mTOR to promote migration. Several other groups have also suggested a role for eHsp90 in LRP1-mediated signalling by activation of various pathways including ERK, MMP2/9 (Hance *et al.,* 2014; Song *et al.,* 2009). It is evident that eHsp90 binding to LRP1 has multiple downstream targets, several of which we identified to converge in regulating FN matrix dynamics. Chen and colleagues reported that the activation of NFkB pathway by eHsp90-LRP1 signalling induces FN expression (Chen *et al.,* 2013) and that activation of the Akt pathway is also important for the expression of FN (Qin *et al.,* 2015). Also, Somanath and colleagues showed that Akt was involved in regulating integrin activation and FN matrix assembly (Somanath *et al.*, 2007). We might then expect a scenario where Hsp90 inhibition disrupts the eHsp90-LRP1 induced signalling pathways to reduce FN expression, however, this was not observed in our study as FN mRNA levels did not substantially change upon novobiocin treatment in wild type MEFs. We showed too that the inhibition of Hsp90 with novobiocin did not hugely affect the Hsp90:LRP1:FN complex, suggesting that the regulation of FN turnover is probably not due to a direct interaction. Thus, if we consider these eHsp90-LRP1 mediated signalling pathways in light of our own data we could speculate that the mechanism responsible for modulating FN dynamics is unlikely to occur via disruption of eHsp90 binding to LRP1, or deactivation of Akt and NFkB pathways. We could suggest a role for the NOV induced LRP1-58 fragments in regulating FN turnover, however, in NOV treated Hs578T cells we still observed similar effects on FN although levels of LRP1-58 appeared to be unaffected by NOV treatment. This may suggest RIP is not induced by NOV and that a constitutively active system exists in these cells. A role for eHsp90 in stabilizing MMPs and protecting them from degradation was demonstrated by Song *et al.,* (2010). Perhaps a role may be extended for eHsp90 in stabilizing LRP1 and/or FN and that inhibition of Hsp90 causes instability of the FN matrix coupled with increased proteolytic processing of LRP1.

The downstream signalling pathways of eHsp90:LRP1:FN (if any) which may regulate FN matrix dynamics in response to NOV still needs to be identified, as well as the influence of

NOV-induced FN turnover in various cancer types and origin. Thus, at this point we are not able to fully elucidate by what signalling mechanism LRP1 regulates novobiocin-induced FN turnover. As an initial step, we might consider developing a non-cleavable LRP1 mutant to demonstrate that the LRP1-ICD is indeed involved in this process. Further, we might then identify which genes are implicated in the control of NOV-mediated FN turnover by LRP1-ICD.

4.3 THE PHYSIOLOGICAL SIGNIFICANCE OF LRP1-MEDIATED FN TURNOVER BY NOV

Having provided evidence for a role for LRP1 in FN turnover in response to NOV, we further investigated the consequences that may be associated with this ECM remodelling. We demonstrated that NOV treatment at low concentrations decreased exFN and increased inFN levels in LRP1-expressing cells and that this could be associated with an increased migratory capacity. Whilst localized, controlled proteolysis has been shown to be essential for migration and tumour invasiveness, the uncontrolled degradation of FN may hinder migration through loss of cell adhesiveness, tissue polarity and organization and disruption of homeostasis due to loss of function (Ryu *et al.,* 1999; Lu *et al.,* 2011). This might explain why higher concentrations of NOV reduced the ability of LRP1-expressing cells to migrate.

High levels of FN matrix and increased expression of FN has been associated with increased cell migration and poor prognosis in breast carcinomas (Chen *et al.,* 2010b; Ioachim *et al.,* 2002). Despite generally higher FN protein and mRNA levels in PEA-13 cells compared to MEF-1 cells, this did not translate into an increased ability to migrate as we found MEF-1 cells to be significantly more migratory in comparison to PEA-13 cells. On the other hand, downregulation of FN was shown to increase the number and size of lung metastases in an orthotopic mouse model of thyroid cancer (Liu *et al.,* 2008). Also, studies by Inoue and colleagues (2001) showed migrating epithelial cells to have reduced FN mRNA expression compared to non-migrating cells which they explained to be due to a reduction in the amount of FN but the presence of a highly active variant of FN (i.e. EDA-containing FN). EDA-containing FN are variants of FN produced by the alternative splicing of its primary transcripts and have been shown to be upregulated in migrating cells (Inoue *et al.,* 2001). Our data were in contrast to wound-healing studies by Weaver *et al.,* (1997) who showed that LRP1-deficient MEFs migrated more rapidly into an area of denudation, compared to LRP1-expressing cells on a fibronectin coated surface. They observed no difference in migration on Matrigel-coated

surfaces however. Our wound healing assays showed an increase in average distance migrated after 12 hours following NOV treatment in MEF-1 and Hs578T cells at concentrations below the EC50. When comparing migration in the PEA-13 cells, no increase in distance migrated was observed relative to its untreated control. Although MEF-1 cells are the more NOV sensitive cell line, this did not correspond with a reduced ability to migrate; which makes our data even more convincing in that increased cell migration was not observed in the cell line with a greater resistance to NOV. NOV-induced migration results were consistent in both a tumour and non-tumour cell model, taken as such, these findings would suggest that Hsp90 inhibition by NOV (at low concentrations) may have implications in cancer development and progression as well as normal cell physiological functions. Recent studies by Ghosh and colleagues (2015) revealed decreased cell migration in PUC33 cancer cells treated with various Hsp90 inhibitors, including NOV, however they used concentrations of 1000 µM which is almost 10 fold higher than ours. Indeed we too observed decreased migration in MEF-1 cells at higher NOV concentrations (200 µM NOV), but we predict these to occur due to reduced cell fitness at these concentrations of the inhibitor.

Cell migration is a complex process regulated by a large number of molecules. Fibronectin, LRP1 and Hsp90 have each been shown to play a role in regulating the mechanisms involved in this process (Salicioni *et al.,* 2002; Sidera *et al.,* 2008; Weaver *et al.,* 1997). Notwithstanding the endocytic and cell signalling functions of LRP1, its role in cell migration remains to date largely controversial. Increased cell migration in cells with low LRP1 expression (Kancha *et al.,* 1994) or RAP treated LRP1-expressing cells (Ma *et al.,* 2002; Weaver *et al.,* 1997; Webb *et al.,* 2000) have previously been reported. In contradiction, highly expressing LRP1 cells have been found to be more migratory (Li *et al.,* 1998) and that neutralized/RAP treated LRP1-expressing cells decreased or abolished cell migration (Chazaud *et al.,* 2002; Dedieu & Langlois, 2008; Li *et al.,* 2003). A link with cell migration in Hsp90 inhibited LRP1-expressing/deficient cells has not yet been identified. This is the first study to report that increased cell migration in LRP1-expressing cells may correlate with an enhanced capacity for these cells to turnover FN in response to NOV.

Moreover, proteolysis of the ECM may also regulate cell migration by producing fragments or exposing hidden regulatory sites of ECM proteins which have functions distinct to that of the native protein (Xu *et al.,* 2001). Cleavage of lamin V and collagen by extracellular proteases

have been reported to generate proteolytic fragments which promote cell migration (Giannelli *et al.,* 1997; Stringa *et al.,* 2000). MMPs are known to regulate ECM remodelling by cleavage of ECM proteins, including FN, into smaller fragments to assist in the initial degradation prior to endocytosis (Etique *et al.,* 2013; Hynes & Naba, 2012). We propose then that the presence of 85 kDa FN fragments observed in NOV treated MEF-1 lysates, at the lower concentrations, may represent degradation fragments of FN caused by extracellular proteolysis. These putative 85 kDa FN degradation fragments were not present in NOV treated PEA-13 lysates. Proteolytically cleaved FN fragments have been reported to activate NFkB pathways and increase expression of MMP2 to promote ECM turnover (Hwang *et al.,* 2015; Schedin *et al.,* 2000). Perhaps the presence of 85 kDa FN fragments in the NOV treated (50 µM and 100 µM) MEF-1 lysates increased MMP2 levels and could explain the increased migratory capacity at these concentrations by enhanced FN turnover. Additionally, FN has itself been shown to increase cell migration by increasing levels of MMP (Chen *et al.,* 2010b). Furthermore, FN fragments from MMP degradation can also inhibit FN-matrix assembly by competing for FN assembly sites and in this way may regulate cell surface levels of FN (Bourdoulous *et al.,* 1998). These fragments were not observed in Hs578T cells (although these also increased in migration) which may suggest that MMP2 degradation of FN into smaller fragments is not an essential requirement for internalisation of FN by LRP1. The inability of PEA-13 cells to experience a NOV-induced increase in migration could be explained by the lack of LRP1, as well as these potential pro-migratory FN fragments, and consequent inability to turnover FN. LRP1 and eHsp90α have also been shown to increase expression of certain MMPs and consequently increase migration (Song *et al.,* 2009; Sims *et al.,* 2011). We might then anticipate that inhibition of Hsp90 would reduce MMP levels and prevent cell migration by deregulating the downstream pathways which are dependent on functional Hsp90 and/or LRP1. However, we know from the high level of LRP1 fragments generated by RIP that MMPs are still active and may in fact be enhanced in the presence of NOV (Sims *et al.,* 2011; Song *et al.,* 2010) and this, coupled with the pro-migratory FN fragments, may explain why Hsp90 inhibition at low concentrations increases migration. Further, direct binding of ligands to LRP1 such as Hsp90 and PN1 (protease nexin 1) have been observed to directly induce cell signalling in cancer cells and non-transformed cells (Fayard *et al.,* 2009; Gopal *et al.,* 2011) by activating ERK and JNK pathways downstream of LRP1 which supports migration and promotes cancer progression (Langlois *et al.,* 2010; Song *et al.,* 2009). Our IP

data showed that the binding of Hsp90 and FN to LRP1 was not perturbed by NOV which we could interpret to represent that the increased cell migration observed in LRP1 containing cells is probably not due to a direct interaction of these three proteins or disruption of this complex but instead is related to consequences associated with this interaction.

From these migration data it is unclear whether increased migratory capacity observed in NOV treated MEF-1 and Hs578T cells was due to loss of exFN levels, Hsp90 inhibition or a combination of these. It seems most likely that the response observed be explained by a collective effect but to address the possibility of reduced exFN, treatment of cells with pUR4 which binds to and blocks polymerization of FN (Tomasini-Johansson *et al.,* 2001) would allow for us to determine the contribution of FN levels to the increased migratory induced by NOV. To support a contributing role of LRP1 we would need to neutralize LRP1 with either an LRP1 blocking antibody or RAP (purification attempts shown in Appendix) in LRP1-expressing cells or reintroduce LRP1 into LRP1-deficient cells in the presence and absence of NOV.

From these data we can speculate that remodelling of FN via NOV may culminate in cell migration in LRP1-expressing cells, however, the functional relevance of ECM turnover is an unresolved controversy. Some studies have demonstrated that the matrix provides a scaffold by which cells are able to migrate and regulate cell growth and that removal of this matrix renders cells immobile (McCarthy and Furcht, 1984; Daley *et al.,* 2008). Contradictory studies have argued that degradation of the ECM allows for cells to detach and migrate to other sites consequently promoting metastases (Egeblad *et al.,* 2010; Friedl & Wolf, 2010). Our findings presented here would err on supporting the latter. Whilst we acknowledge that FN is a major component of the ECM, there are other matrix proteins, such as, collagen, laminin and vitronectin which may allow for migration when FN is lost. Also, we observed an increased migratory phenotype for both normal and tumorigenic cells thus highlighting that the role of the ECM is more complex than originally thought and it remains inconclusive as to whether Hsp90 inhibition, particularly with NOV, may be beneficial or detrimental to metastases of tumors. Moreover, a greater understanding of the NOV-induced changes in both tumorigenic and non-tumorigenic cells may have therapeutic importance in determining whether interventions should be done through inhibiting FN/eHsp90 itself, LRP1 or intracellular signaling in response to ECM turnover. In addition, considering NOV is also used to treat bacterial infections (Marcu *et al.,* 2000) an important consideration will be to assess the side

effects induced by regular treatment with NOV and how this may impact on FN turnover and consequent cancer progression in the long term. Also, an interesting study by Riebold and colleagues (2015) demonstrated in contrast to other studies, that C-terminal Hsp90 inhibition with NOV (0-150 μM) increased the number and stability of GR receptors in mouse AtT-20 corticotroph cells but degraded Cdc2 at equivalent concentrations. They also noted that NOV in high concentrations (1-10 mM) may behave more like an N-terminal Hsp90 inhibitor (Kanelakis *et al.*, 2002). From our data, it is unclear whether the effects on FN are as a result of Hsp90 inhibition or another effect related to treatment with NOV. Therefore, it may be worthwhile investigating the effects on FN turnover by alternative C-terminal Hsp90 inhibitors, as well as an N-terminal inhibitor.

4.4 CONCLUSIONS

We have presented evidence to demonstrate that LRP1 may be required for NOV induced FN turnover by showing that loss of LRP1 renders cells less sensitive to exFN turnover and degradation in response to NOV. Together with previous studies showing that NOV causes instability of the FN matrix and its subsequent internalisation (Hunter *et al.,* 2014), we further showed that this internalisation was dependent on LRP1 and that increased proteolytic processing of this receptor by NOV may be involved in the process. The NOV induced loss of exFN in LRP1-expressing cells was associated with an increased migratory capacity, potentially highlighting an important consequence related to Hsp90 inhibition and loss of ECM. Taken together, we suggest that NOV may mediate its effects on FN by the direct LRP1-mediated endocytic clearance of exFN and targeted lysosomal degradation, an indirect eHsp90-LRP1 dependent signalling pathway activated in response to NOV induced proteolytic processing of LRP1 or indeed a combination of both mechanisms.

The major objective of this present study was to demonstrate the significance of Hsp90 and LRP1 involvement in maintenance of ECM stability and turnover of FN. We successfully showed that LRP1 is involved in the novobiocin-mediated endocytosis and turnover of fibronectin which has functional migratory consequences for both normal and cancer cells.

Chapter 5. REFERENCES

Akerfelt, M., Morimoto, I.R., Sistonen, L. (2010). Heat shock factors: integrators of cell stress, development and lifespan. *Nat Rev Mol Cell Bio*, 11(8), 545-555.

Alexander, L. D., Sellers, R. P., Davis, M. R., Ardi, V. C., Victoria, A., Vasko, R. C., & McAlpine, S. R. (2009). Evaluation of Di-Sansalvamide A derivatives: Synthesis, structure-activity relationship, and mechanism of action. *Journal of Medicinal Chemistry*, *52*(24), 7927–7930.

Allan, R. K., Mok, D., Ward, B. K., & Ratajczak, T. (2006). Modulation of Chaperone Function and Cochaperone Interaction by Novobiocin in the C-terminal Domain of Hsp90. *Journal of Biological Chemistry*, *281*(11), 7161–7171.

Althoff, K., Müllberg, J., Aasland, D., Voltz, N., Kallen, K., Grötzinger, J., & Rose-John, S. (2001). Recognition sequences and structural elements contribute to shedding susceptibility of membrane proteins. *The Biochemical Journal*, *353*(Pt 3), 663–72.

Altieri, D. C. (2006). Targeted therapy by disabling crossroad signaling networks: the survivin paradigm. *Molecular Cancer Therapeutics*, *5*(3), 478–82.

Amazit, L., Roseau, A., Khan, J. a, Chauchereau, A., Tyagi, R. K., Loosfelt, H., & Guiochon-Mantel, A. (2011). Ligand-dependent degradation of SRC-1 is pivotal for progesterone receptor transcriptional activity. *Molecular Endocrinology (Baltimore, Md.)*, *25*(3), 394–408.

Anckar, J., & Sistonen, L. (2011). Regulation of HSF1 Function in the Heat Stress Response : Implications in Aging and Disease. *Annual Review of Biochemistry*, *80*, 1089–1115.

Bae, Y. K., Kim, A., Kim, M. K., Choi, J. E., Kang, S. H., & Lee, S. J. (2013). Fibronectin expression in carcinoma cells correlates with tumor aggressiveness and poor clinical outcome in patients with invasive breast cancer. *Human Pathology*, *44*(10), 2028–37.

Bagatell, R., & Whitesell, L. (2004). Altered Hsp90 function in cancer : A unique therapeutic opportunity. *Molecular Cancer Therapeutics*, *3*, 1021–1030.

Basu, S., Binder, R. J., Ramalingam, T., & Srivastava, P. K. (2001). CD91 is a common receptor for heat shock proteins gp96, hsp90, hsp70, and calreticulin. *Immunity*, *14*(3), 303–13.

Binder, R., Han, D.K., & Srivastava, P.K. (2000). CD91: a receptor for heat shock protein gp96. *Nature Immunology,* 2, 151–155.

Bonnans, C., Chou, J., & Werb, Z. (2014). Remodelling the extracellular matrix in development and disease. *Nature Reviews Molecular Cell Biology*, *15*(12), 786–801.

Bornstein, P., & Sage, E. H. (2002). Matricellular proteins: extracellular modulators of cell function. *Current Opinion in Cell Biology*, *14*(5), 608–16.

Boucher, P., & Herz, J. (2011). Signaling through LRP1: Protection from atherosclerosis and beyond. *Biochemical Pharmacology*, *81*(1), 1–5.

Bourdoulous, S., Orend, G., Mackenna, D. A., & Pasqualini, R. (1998). Fibronectin Matrix Regulates Activation of RHO and CDC42 GTPases and Cell Cycle Progression. *Journal of Cell Biology*, *143*(1), 267–276.

Brenner, K. A., Corbett, S. A., & Schwarzbauer, J. E. (2000). Regulation of fibronectin matrix assembly by activated Ras in transformed cells. *Oncogene*, *19*, 3156–3163.

Bretscher, M. S. (1989). Endocytosis and recycling of the fibronectin receptor in CHO cells. *EMBO Journal*, *8*(5), 1341–8.

Bridgewater, R. E., Norman, J. C., & Caswell, P. T. (2012). Integrin trafficking at a glance. *Journal of Cell Science*, *125*(Pt 16), 3695–701.

Bu, G., Williams, S., Strickland, D.K. (1992). Low density lipoprotein receptor-related protein/alpha 2-macroglobulin receptor is an hepatic receptor for tissue-type plasminogen activator. *Proc Natl Acad Sci*, 89:7427–7431.

Bu, G., & Marzolo, M. P. (2001). Role of RAP in the Biogenesis of Lipoprotein Receptors. *Trends Cardiovascular Medicine*, *10*(4), 148–155.

Burlison, J. A., Neckers, L., Smith, A. B., Maxwell, A., & Blagg, B. S. J. (2006). Novobiocin : Redesigning a DNA Gyrase Inhibitor for Selective Inhibition of Hsp90. *Journal of American Chemical Society*, *128*(7), 15529–15536.

Calderwood, S. K. (2006). Heat shock proteins in cancer: chaperones of tumorigenesis. *Trends in biochemical sciences,* 31(3): 164-172.

Chang, H. C., Nathan, D. F., & Lindquist, S. (1997). In vivo analysis of the Hsp90 cochaperone Sti1 (p60). *Molecular and Cellular Biology*, *17*(1), 318–325.

Chaudhuri, T. K., & Paul, S. (2006). Protein-misfolding diseases and chaperone-based therapeutic approaches. *The FEBS Journal*, *273*(7), 1331–49.

Chazaud, B., Ricoux, R., Christov, C., Plonquet, A., Gherardi, R. K., & Barlovatz-Meimon, G. (2002). Promigratory effect of plasminogen activator inhibitor-1 on invasive breast cancer cell populations. *The American Journal of Pathology*, *160*(1), 237–46.

Chen, C., Chen, Y., Dai, K., Chen, P., Riley, D. J., & Lee, W. (1996). A New Member of the hsp90 Family of Molecular Chaperones Interacts with the Retinoblastoma Protein during Mitosis and after Heat Shock. *Molecular and Cell Biology*, *16*(9), 4691–4699.

Chen, J.-S., Hsu, Y.-M., Chen, C.-C., Chen, L.-L., Lee, C.-C., & Huang, T.-S. (2010a). Secreted heat shock protein 90alpha induces colorectal cancer cell invasion through CD91/LRP-1 and NF-kappaB-mediated integrin alphaV expression. *The Journal of Biological Chemistry*, *285*(33), 25458–66.

Chen, S., Lin, C., Lee, L., Chang, G., Lee, P., Hung, C., & Lee, M. (2010b). Up-regulation of Fibronectin and Tissue Transglutaminase Promotes Cell Invasion Involving Increased Association with Integrin and MMP Expression in A431 Cells. *Anticancer Research*, *30*, 4177–4186.

Chen, W., Chen, C., Chen, L., Lee, C., & Huang, T. (2013). Secreted Heat Shock Protein 90alpha (HSP90α) Induces Nuclear Factor-k B-mediated TCF12 Protein Expression to Down-regulate E-cadherin and to Enhance Colorectal Cancer Cell Migration and Invasion. *Journal of Biological Chemistry*, *288*(13), 9001–9010.

Cheng, C.-F., Fan, J., Fedesco, M., Guan, S., Li, Y., Bandyopadhyay, B., & Li, W. (2008).

Transforming growth factor alpha (TGFalpha)-stimulated secretion of HSP90alpha: using the receptor LRP-1/CD91 to promote human skin cell migration against a TGFbeta-rich environment during wound healing. *Molecular and Cellular Biology*, *28*(10), 3344–58.

Chiosis, G., Lucas, B., Shtil, A., Huezo, H., & Rosen, N. (2002). Development of a purine-scaffold novel class of Hsp90 binders that inhibit the proliferation of cancer cells and induce the degradation of Her2 tyrosine kinase. *Bioorganic & Medicinal Chemistry*, *10*(11), 3555–64.

Ciechanover, A. (2005). Intracellular protein degradation : from a vague idea thru the lysosome and the ubiquitin – proteasome system and onto human diseases and drug targeting. *Cell Death and Differentiation*, *12*, 1178–1190.

Csermely, P., Schnaider, T., Soti, C., Prohászka, Z., & Nardai, G. (1998). The 90-kDa Molecular Chaperone Family: Structure, function, and clinical applications. A comprehensive review. *Pharmacology & Therapeutics*, *79*(2), 129–168.

Daley, W. P., Peters, S. B., & Larsen, M. (2008). Extracellular matrix dynamics in development and regenerative medicine. *Journal of Cell Science*, *121*(Pt 3), 255–264.

Deboer, C., Meulman, P., Wnuk, R., & Peterson, D. (1970). Geldanamycin, a new antibiotic. *The Journal of Antibiotics*, (9), 442–447.

Dedieu, S., & Langlois, B. (2008). LRP-1: a new modulator of cytoskeleton dynamics and adhesive complex turnover in cancer cells. *Cell Adhesion & Migration*, *2*(2), 77–80.

Derocq, D., Prébois, C., Beaujouin, M., Laurent-Matha, V., Pattingre, S., Smith, G. K., & Liaudet-Coopman, E. (2012). Cathepsin D is partly endocytosed by the LRP1 receptor and inhibits LRP1-regulated intramembrane proteolysis. *Oncogene*, *31*(26), 3202–12.

Desrosiers, R. R., Rivard, M. E., Grundy, P. E., & Annabi, B. (2006). Decrease in LDL receptor-related protein expression and function correlates with advanced stages of Wilms tumors. *Pediatric Blood and Cancer*, *46*, 40–49.

Dhanani, K. (2014). Human FN1 is regulated by the heat-shock response.

Donnelly, A., & Blagg, B. S. J. (2008). Novobiocin and Additional Inhibitors of the Hsp90 C-Terminal Nucleotide-binding Pocket. *Curr Med Chem*, *15*(26), 2702–2717.

Dunn, W. K., Kamocka, M. M., & McDonald, H. J. (2011). A practical guide to evaluating colocalization in biological microscopy. *American Journal of Physiology Cell Physiology*, *300*(4).

Edkins, A.L. & Boshoff, A. (2014). General structural and functional features of molecular chaperones. Chapter in: Heat shock proteins of malaris. Springer, ISBN 978-94-007-7437-7, 5-45.

Egeblad, M., Rasch, M. G., & Weaver, V. M. (2010). Dynamic interplay between the collagen scaffold and tumor evolution. *Current Opinion in Cell Biology*, *22*(5), 697–706.

Egeblad, M., & Werb, Z. (2002). New functions for the matrix metalloproteinases in cancer progression. *Nature Reviews Cancer*, *2*(3), 161–174.

Erickson, H. P. (2002). Stretching fibronectin. *Journal of Muscle Research and Cell Motility*,

23(5-6), 575–80.

Eskew, J. D., Sadikot, T., Morales, P., Duren, A., Dunwiddie, I., Swink, M., & Vielhauer, G. A. (2011). Development and characterization of a novel C-terminal inhibitor of Hsp90 in androgen dependent and independent prostate cancer cells. *BMC Cancer*, *11*(1), 468.

Etique, N., Verzeaux, L., Dedieu, S., & Emonard, H. (2013). LRP-1 : A Checkpoint for the Extracellular Matrix Proteolysis. *BioMed Research International*, 1–7.

Eustace, B. K., Sakurai, T., Stewart, J. K., Yimlamai, D., Unger, C., Zehetmeier, C., & Jay, D. G. (2004). Functional proteomic screens reveal an essential extracellular role for hsp90 alpha in cancer cell invasiveness. *Nature Cell Biology*, *6*(6), 507–14.

Fayard, B., Bianchi, F., Dey, J., Moreno, E., Djaffer, S., Hynes, N. E., & Monard, D. (2009). The serine protease inhibitor protease nexin-1 controls mammary cancer metastasis through LRP-1-mediated MMP-9 expression. *Cancer Research*, *69*(14), 5690–5698.

Felts, S. J., Owen, B. A. L., Trepel, J., Donner, D. B., Toft, D. O., & Nguyen, P. (2000). PROTEIN STRUCTURE AND FOLDING : The hsp90-related Protein TRAP1 Is a Mitochondrial Protein with Distinct Functional Properties. *The Journal of Biological Chemistry*, *275*, 3305–3312.

Forsyth, C. B., Pulai, J., & Loeser, R. F. (2002). Fibronectin fragments and blocking antibodies to alpha2beta1 and alpha5beta1 integrins stimulate mitogen-activated protein kinase signaling and increase collagenase 3 (matrix metalloproteinase 13) production by human articular chondrocytes. *Arthritis and Rheumatism*, *46*(9), 2368–2376.

Frantz, C., Stewart, K. M., & Weaver, V. M. (2010). The extracellular matrix at a glance The Extracellular Matrix at a Glance. *Journal of Cell Science*, *2010*, 4195–4200.

Friedl, P., & Gilmour, D. (2009). Collective cell migration in morphogenesis, regeneration and cancer. *Nature Reviews. Molecular Cell Biology*, *10*(7), 445–57.

Friedl, P., & Wolf, K. (2010). Plasticity of cell migration: a multiscale tuning model. *The Journal of Cell Biology*, *188*(1), 11–19.

Fulda, S., Gorman, A. M., Hori, O., & Samali, A. (2010). Cellular stress responses: cell survival and cell death. *International Journal of Cell Biology*, *2010*, 214-224.

Galante, L. L., & Schwarzbauer, J. E. (2007). Requirements for sulfate transport and the diastrophic dysplasia sulfate transporter in fibronectin matrix assembly. *The Journal of Cell Biology*, *179*(5), 999–1009.

Garrido, C., Gurbuxani, S., Ravagnan, L. (2001). Heat shock proteins: endogenous modulators of apoptotic cell death. *Biochem Biophys Res Commun,* 286:433–442.

Gaultier, A., Arandjelovic, S., Li, X., Janes, J., Dragojlovic, N., Zhou, G. P., & Campana, W. M. (2008). A shed form of LDL receptor – related protein – 1 regulates peripheral nerve injury and neuropathic pain in rodents. *Journal of Clinical Investigation*, *118*(1), 161–172.

Gaultier, A., Hollister, M., Reynolds, I., Hsieh, E., & Gonias, S. L. (2010). LRP1 regulates remodeling of the extracellular matrix by fibroblasts. *Matrix Biology : Journal of the International Society for Matrix Biology*, *29*(1), 22–30.

Geer, P. Van Der. (1999). Phosphorylation of LRP1 : Regulation of Transport and Signal

Transduction. *Trends Cardiovascular Medicine*, *12*(4), 160–165.

Ghosh, S., Shinogle, H. E., Garg, G., Vielhauer, G. A., Holzbeierlein, M., Dobrowsky, R. T., & Blagg, B. S. J. (2015). Hsp90 C-Terminal Inhibitors Exhibit Antimigratory Activity by Disrupting the Hsp90 α/Aha1 Complex in PC3-MM2 Cells. *American Chemical Society*, *10*, 577–590.

Giannelli, G., Falk-marzillier, J., Schiraldi, O., Stetler-stevenson, W. G., & Quaranta, V. (1997). Induction of Cell Migration by Matrix Metalloprotease – 2 Cleavage of Laminin-5. *Science*, *277*, 225–227.

Godyna, S., Liau, G., Popa, I., Stefansson, S., Argraves, W. S., Departments, M. B., & Cross, A. R. (1995). Identification of the Low Density Lipoprotein Receptor-related Protein (LRP) as an Endocytic Receptor for Thrombospondin-1 Solid-phase Binding Assays. *Journal of Cell Biology*, *129*(5), 1403–1410.

Gonzalez-Noriega, A., Grubb, J. H., Talkad, V., & Sly, W. S. (1980). Chloroquine inhibits lysosomal enzyme pinocytosis and enhances lysosomal enzyme secretion by impairing receptor recycling. *The Journal of Cell Biology*, *85*(3), 839–52.

Gopal, U., Bohonowych, J. E., Lema-tome, C., Liu, A., Garrett-, E., Wang, B., & Isaacs, J. S. (2011). A Novel Extracellular Hsp90 Mediated Co-Receptor Function for LRP1 Regulates EphA2 Dependent Glioblastoma Cell Invasion. *PLoS ONE*, *6*(3), 1–14.

Gorovoy, M., Gaultier, A., Campana, W. M., & Firestein, G. S. (2010). Inflammatory mediators promote production of shed LRP1 / CD91 , which regulates cell signaling and cytokine expression by macrophages. *Journal of Leukocyte Biology*, *88*(October), 769–778.

Grammatikakis, N., Vultur, A., Ramana, C. V, Siganou, A., Schweinfest, C. W., Watson, D. K., & Raptis, L. (2002). TRANSDUCTION : The Role of Hsp90N , a New Member of the Hsp90 Family , in Signal Transduction and Neoplastic Transformation The Role of Hsp90N , a New Member of the Hsp90 Family , in Signal Transduction and Neoplastic Transformation. *The Journal of Biological Chemistry*, *277*, 8312–8320.

Grenert, J. P., Sullivan, W. P., Fadden, P., Haystead, T. a, Clark, J., Mimnaugh, E., & Toft, D. O. (1997). The amino-terminal domain of heat shock protein 90 (hsp90) that binds geldanamycin is an ATP/ADP switch domain that regulates hsp90 conformation. *The Journal of Biological Chemistry*, *272*(38), 23843–23850.

Gutman, A., Yamada, K. M., & Kornblihtt, A. (1986). Human fibronectin is synthesized as a pre-propolypeptide. *FEBS Letters*, *207*(1), 145–148.

Guttman, M., Betts, G. N., Barnes, H., Ghassemian, M., Geer, P. Van Der, & Komives, E. A. (2009). Interactions of the NPXY microdomains of the LDL Receptor-Related Protein 1. *Proteomics*, *9*(22), 5016–5028.

Gygi, S. P., Rochon, Y., Franza, B. R., & Aebersold, R. (1999). Correlation between Protein and mRNA Abundance in Yeast. *Molecular and Cellular Biology*, *19*(3), 1720–1730.

Haggerty, T. J., Dunn, I. S., Rose, L. B., Newton, E. E., Pandolfi, F., & Kurnick, J. T. (2014). Heat Shock Protein-90 Inhibitors Enhance Antigen Expression on Melanomas and Increase T Cell Recognition of Tumor Cells. *PLoS ONE*, *9*(12), 1–23.

Hahn-Dantona, E., Ruiz, J.F., Bornstein, P., & Strickland, D.K. (2001). The low density lipoprotein receptor-related protein modulates levels of matrix metalloproteinase 9 (MMP-9) by mediating its cellular catabolism. *J. Biol. Chem*, 276, 15498–15503.

Hanahan, D., & Weinberg, R. A. (2000). The hallmarks of cancer. *Cell*, *100*(3), 57–570.

Hance, M. W., Nolan, K. D., & Isaacs, J. S. (2014). The Double-Edged Sword: Conserved Functions of Extracellular Hsp90 in Wound Healing and Cancer. *Cancers*, *6*, 1065–1097.

Hartl, F. U., Bracher, A., & Hayer-Hartl, M. (2011). Molecular chaperones in protein folding and proteostasis. *Nature*, *475*.

Hartl, F. U., & Hayer-Hartl, M. (2002). Molecular Chaperones in the Cytosol: from Nascent Chain to Folded Protein. *Science*, *295*, 1852–1858.

Hegmans, J. P. J. J., Bard, M. P. L., Hemmes, A., Luider, T. M., Kleijmeer, M. J., Prins, J.-B., & Lambrecht, B. N. (2004). Proteomic analysis of exosomes secreted by human mesothelioma cells. *The American Journal of Pathology*, *164*(5), 1807–1815.

Hendrick, J.P., & Hartl, F.U. (1993). Molecular chaperone functions of heat-shock proteins. *Annu Rev Biochem,* 62, 349–384.

Herz, J., Goldstein, L., Stricklandn, K., & Brown, S. (1991). 39-kDa Protein Modulates Binding of Ligands to Low Density Lipoprotein Receptor-related Protein/α2-Macroglobulin Receptor*. *Journal of Biological Chemistry*, *266*(31), 21232–21236.

Herz, J., Hamann, U., Rogne, S., Myklebost, O., Gausepohl, H., & Stanley, K. K. (1988). Surface location and high affinity for calcium of a 500-kd liver membrane protein closely related to the LDL-receptor suggest a physiological role as lipoprotein receptor. *The EMBO Journal*, *7*(13), 4119–4127.

Herz, J., & Strickland, D. K. (2001). Multiligand receptors LRP : a multifunctional scavenger and signaling receptor. *J.Clin.Invest*, *108*(6), 779–784.

Horibe, T., Kohno, M., Haramoto, M., Ohara, K., & Kawakami, K. (2011). Designed hybrid TPR peptide targeting Hsp90 as a novel anticancer agent. *Journal of Translational Medicine*, *9*(1), 8.

Huang, G., & Greenspan, D. S. (2012). ECM roles in the function of metabolic tissues. *Trends in Endocrinology and Metabolism: TEM*, *23*(1), 16–22.

Huang, W., Dolmer, K., Liao, X., & Gettins, P. G. W. (2000). NMR Solution Structure of the Receptor Binding Domain of Human 2-Macroglobulin. *Journal of Biological Chemistry*, *275*(2), 1089–1094.

Hunter, M. C., O'Hagan, K. L., Kenyon, A., Dhanani, K. C. H., Prinsloo, E., & Edkins, A. L. (2014). Hsp90 Binds Directly to Fibronectin (FN) and Inhibition Reduces the Extracellular Fibronectin Matrix in Breast Cancer Cells. *PLoS ONE*, *9*(1), e86842.

Hwang, H. S., Park, S. J., Cheon, E. J., Lee, M. H., & Kim, H. A. (2015). Fibronectin fragment-induced expression of matrix metalloproteinases is mediated by MyD88-dependent TLR-2 signaling pathway in human chondrocytes. *Arthritis Research & Therapy*, 1–12.

Hynes, R. O. (2009). The extracellular matrix: not just pretty fibrils. *Science*, *326*(5957), 1216–

1219.

Hynes, R. O., & Naba, A. (2012). Overview of the matrisome--an inventory of extracellular matrix constituents and functions. *Cold Spring Harbor Perspectives in Biology*, *4*(1), a004903.

Iadonato, S. P., Bu, G., Maksymovitch, E. a, & Schwartz, a L. (1993). Interaction of a 39 kDa protein with the low-density-lipoprotein-receptor-related protein (LRP) on rat hepatoma cells. *The Biochemical Journal*, *296 (Pt 3*, 867–75.

Inoue, T., Nabeshima, K., Shimao, Y., Meng, J. Y., & Koono, M. (2001). Regulation of fibronectin expression and splicing in migrating epithelial cells: migrating MDCK cells produce a lesser amount of, but more active, fibronectin. *Biochemical and Biophysical Research Communications*, *280*(5), 1262–8.

Ioachim, E., Charchanti, a, Briasoulis, E., Karavasilis, V., Tsanou, H., Arvanitis, D. & Pavlidis, N. (2002). Immunohistochemical expression of extracellular matrix components tenascin, fibronectin, collagen type IV and laminin in breast cancer: their prognostic value and role in tumour invasion and progression. *European Journal of Cancer*, *38*(18), 2362–2370.

Jakob, U., Gaestel, M., Engel, K., & Buchner, J. (1993). Small heat shock proteins are molecular chaperones. *The Journal of Biological Chemistry*, *268*(3), 1517–1520.

Kalluri, R., & Zeisberg, M. (2006). Fibroblasts in cancer. *Nature Reviews Cancer*, *6*, 392–401.

Kamal, A., Thao, L., Sensintaffar, J., Zhang, L., Boehm, M. F., Fritz, L. C., & Burrows, F. J. (2003). A high-affinity conformation of Hsp90 confers tumour selectivity on Hsp90 inhibitors. *Nature*, *425*(6956), 407–10.

Kanelakis, K. C., Shewach, D. S., & Pratt, W. B. (2002). Nucleotide binding states of hsp70 and hsp90 during sequential steps in the process of glucocorticoid receptor.hsp90 heterocomplex assembly. *The Journal of Biological Chemistry*, *277*(37), 33698–703.

Kenny, H. A., Kaur, S., Coussens, L. M., & Lengyel, E. (2008). The initial steps of ovarian cancer cell metastasis are mediated by MMP-2 cleavage of vitronectin and fibronectin. *Journal of Clinical Investigation*, *118*(4), 1367–1379.

Khalil, A. a, Kabapy, N. F., Deraz, S. F., & Smith, C. (2011). Heat shock proteins in oncology: diagnostic biomarkers or therapeutic targets? *Biochimica et Biophysica Acta*, *1816*(2), 89–104.

Kinoshita, A., Shah, T., Tangredi, M. M., Strickland, D. K., & Hyman, B. T. (2003). The Intracellular Domain of the Low Density Lipoprotein Receptor-related Protein Modulates Transactivation Mediated by Amyloid Precursor Protein and Fe65 *. *The Journal of Biological Chemistry*, *278*(42), 41182–41188.

Kounnas, M.Z., Morris, R. E., Thompson, M. R., Fitzgerald, D. J., Strickland, D. K., Saelinger, C. B. (1992). The α2-macroglobulin receptor/low density lipoprotein receptor-related protein binds and internalizes Pseudomonas exotoxin A. *J. Biol. Chem,* 267, 12420–12423.

Kounnas, M. Z., Moir, R. D., Rebeck, G. W., Bush, a I., Argraves, W. S., Tanzi, R. E., & Strickland, D. K. (1995). LDL receptor-related protein, a multifunctional ApoE receptor, binds

secreted beta-amyloid precursor protein and mediates its degradation. *Cell*, *82*(2), 331–40.

Kowal, R.C., Herz, J., Goldstein, J.L., Esser, V., Brown, M.S. (1989). Low density lipoprotein receptor-related protein mediates uptake of cholesteryl esters derived from apoprotein E-enriched lipoproteins *Proc Natl Acad Sci*, 86, 5810–5814.

Kumazaki, T., Mitsui, Y., Hamada, K., Sumida, H., & Nishiyama, M. (1999). Detection of alternative splicing of fibronectin mRNA in a single cell. *Journal of Cell Science*, *112 (Pt 1*, 1449–53.

Kusuma, B. R., Duerfeldt, A. S., & Blagg, B. S. J. (2011). Synthesis and biological evaluation of arylated novobiocin analogs as Hsp90 inhibitors. *Bioorganic & Medicinal Chemistry Letters*, *21*(23), 7170–4.

Langlois, B., Perrot, G., Schneider, C., Henriet, P., Emonard, H., Martiny, L., & Dedieu, S. (2010). LRP-1 Promotes Cancer Cell Invasion by Supporting ERK and Inhibiting JNK Signaling Pathways. *PLoS ONE*, *5*(7), e11584.

Lemmon, C. a, Ohashi, T., & Erickson, H. P. (2011). Probing the folded state of fibronectin type III domains in stretched fibrils by measuring buried cysteine accessibility. *The Journal of Biological Chemistry*, *286*(30), 26375–82.

Li, J., & Buchner, J. (2013). Structure, function and regulation of the hsp90 machinery. *Biomedical Journal*, *36*(3), 106–17.

Li, Q., Lau, A., Morris, T. J., Guo, L., Fordyce, C. B., & Stanley, E. F. (2004). A syntaxin 1, Galpha(o), and N-type calcium channel complex at a presynaptic nerve terminal: analysis by quantitative immunocolocalization. *The Journal of Neuroscience : The Official Journal of the Society for Neuroscience*, *24*(16), 4070–81.

Li, W., Li, Y., Guan, S., Fan, J., Cheng, C.-F., Bright, A. M., & Woodley, D. T. (2007). Extracellular heat shock protein-90alpha: linking hypoxia to skin cell motility and wound healing. *The EMBO Journal*, *26*(5), 1221–1233.

Li, W., Sahu, D., & Tsen, F. (2011). Secreted heat shock protein-90 (Hsp90) in wound healing and cancer. *Biochimica et Biophysica Acta (BBA)*, *1823*(3), 730–41.

Li, Y., & Bu, G. (2001). Identification of a Major Cyclic AMP-Dependent Protein Kinase A Phosphorylation Site within the Cytoplasmic Tail of the Low-Density Lipoprotein Receptor-Related Protein : Implication for Receptor-Mediated Endocytosis. *Molecular and Cellular Biology*, *21*(4), 1185–1195.

Li, Y., & C. Reynolds, R. (2012). LRP1: A Tumor and Metastasis Promoter or Suppressor? *Biochemistry & Pharmacology: Open Access*, *01*(05), 1–2.

Li, Y., Lu, W., & Bu, G. (2003). Essential role of the low density lipoprotein receptor-related protein in vascular smooth muscle cell migration. *FEBS Letters*, *555*(2), 346–350.

Lillis, A. P., Mikhailenko, I., & Stricklandg, D. K. (2005). Beyond endocytosis : LRP function in cell migration , proliferation and vascular permeability. *Journal of Thrombosis and Haemostasis*, *3*, 1884–1893.

Lillis, A. P., Duyn, L. B. Van, Murphy-Ullrich, J. E., & Strickland, D. K. (2008). The low density lipoprotain receptor-related protein 1: Unique tissue-specifici functions revealed by selective gene knockout studies. *Physiol Rev*, *88*(3), 887–918.

Lin, Q. C., & Bissell, M. J. (1993). Multi-faceted regulation of of cell differentiation by extracellular matrix. *The FASEB Journal*, *7*, 737–743.

Liu, Y. et al. (2000). Uptake of HIV-1 Tat protein mediated by low-density lipoprotein receptor-related protein disrupts the neuronal metabolic balance of the receptor ligands. *Nature Medicine*, 6, 1380–1387.

Liu, W., Cheng, S., Asa, S. L., & Ezzat, S. (2008). The melanoma-associated antigen A3 mediates fibronectin-controlled cancer progression and metastasis. *Cancer Research*, *68*(19), 8104–12.

Lobert, V. H., Brech, A., Pedersen, N. M., Wesche, J., Oppelt, A., Malerød, L., & Stenmark, H. (2010). Ubiquitination of alpha 5 beta 1 integrin controls fibroblast migration through lysosomal degradation of fibronectin-integrin complexes. *Developmental Cell*, *19*(1), 148–59.

Lu, P., Takai, K., Weaver, V. M., & Werb, Z. (2011). Extracellular Matrix Degradation and Remodeling in Development and Disease. *Cold Spring Harbor Perspectives in Biology*, *3*, 1–21.

Ma, Z., Thomas, K. S., Webb, D. J., Moravec, R., Salicioni, A. M., Mars, W. M., & Gonias, S. L. (2002). Regulation of Rac1 activation by the low density lipoprotein receptor-related protein. *The Journal of Cell Biology*, *159*(6), 1061–1070.

Marcu, M. G., Chadli, A., Bouhouche, I., Catelli, M., & Neckers, L. M. (2000). The Heat Shock Protein 90 Antagonist Novobiocin Interacts with a Previously Unrecognized ATP-binding Domain in the Carboxyl Terminus of the Chaperone *. *Journal of Biological Chemistry*, *275*(47), 37181–37186.

Margineantu, D. H., Emerson, C. B., Diaz, D., & Hockenbery, D. M. (2007). Hsp90 Inhibition Decreases Mitochondrial Protein Turnover. *PLoS ONE*, *2*(10), 1–14.

May, P., Reddy, Y. K., & Herz, J. (2002). Proteolytic processing of low density lipoprotein receptor-related protein mediates regulated release of its intracellular domain. *The Journal of Biological Chemistry*, *277*(21), 18736–43.

Mayer, M. P., & Bukau, B. (2005). Hsp70 chaperones: Cellular functions and molecular mechanism. *Cellular and Molecular Life Sciences*, *62*(6), 670–684.

McCarthy, J. B., & Furcht, L. T. (1984). Laminin and Fibronectin Promote the Haptotactic Migration of B16 Mouse Melanoma Cells In Vitro. *Journal of Cell Biology*, *98*, 1474–1480.

McCready, J., Sims, J. D., Chan, D., & Jay, D. G. (2010). Secretion of extracellular hsp90α via exosomes increases cancer cell motility : a role for plasminogen activation. *BMC Cancer*, *10*.

McKeown-Longo, P. J., & Mosher, D. F. (1985). Interaction of the 70,000-mol-wt amino-terminal fragment of fibronectin with the matrix-assembly receptor of fibroblasts. *The Journal of Cell Biology*, *100*(2), 364–74.

Mikhailenko, I., Kounnas, Z., & Strickland, D. (1995). Low density lipoprotein receptor-related protein/alpha 2-macroglobulin receptor mediates the cellular internalization and degradation of thrombospondin. A process facilitated by cell-surface proteoglycans. *J. Biol. Chem*, 270, 9543–9549.

Mikhailenko, I., Battey, F. D., Migliorini, M., Ruiz, J. F., Argraves, K., Moayeri, M., & Strickland, D. K. (2001). Recognition of alpha 2-macroglobulin by the low density lipoprotein receptor-related protein requires the cooperation of two ligand binding cluster regions. *The Journal of Biological Chemistry*, *276*(42), 39484–91.

Montel, V., Gaultier, a., Lester, R. D., Campana, W. M., & Gonias, S. L. (2007). The Low-Density Lipoprotein Receptor Related Protein Regulates Cancer Cell Survival and Metastasis Development. *Cancer Research*, *67*(20), 9817–9824.

Mosher, D. F., Fogerty, F. J., Chernousov, M. a, & Barry, E. L. (1991). Assembly of fibronectin into extracellular matrix. *Annals of the New York Academy of Sciences*, *614*(V), 167–80.

Muratoglu, S. C., Mikhailenko, I., Newton, C., Migliorini, M., & Strickland, D. K. (2010). Low Density Lipoprotein Receptor-related Protein 1 (LRP1) Forms a Signaling Complex with Platelet-derived Growth Factor Receptor- in Endosomes and Regulates Activation of the MAPK Pathway. *Journal of Biological Chemistry*, *285*(19), 14308–14317.

Nemoto, T., & Sato, N. (1998). Oligomeric forms of the 90-kDa heat shock protein. *The Biochemical Journal*, *330 (Pt 2*, 989–95.

Nykjaer, A., Petersen, C.M., Moller, B. (1992). Purified α2-macroglobulin receptor/LDL receptor-related protein binds urokinase:plasminogen activator inhibitor type- 1 complex. *J. Biol. Chem.* 267:14543–14546.

Obermann, W. M. J., Sondermann, H., Russo, A. A., Pavletich, N. P., & Hartl, F. U. (1998). In Vivo Function of Hsp90 Is Dependent on ATP Binding and ATP Hydrolysis, *143*(4), 901–910.

Obermoeller-McCormick, L. M., Li, Y., Osaka, H., Fitzgerald, D. J., Schwartz, A. L., & Bu, G. (2000). Dissection of receptor folding and ligand-binding property with functional minireceptors of LDL receptor-related protein. *Journal of Cell Science*, *114*, 899–908.

Ohashi, T., & Erickson, H. P. (2009). Revisiting the mystery of fibronectin multimers: the fibronectin matrix is composed of fibronectin dimers cross-linked by non-covalent bonds. *Matrix Biology : Journal of the International Society for Matrix Biology*, *28*(3), 170–5.

Orr, a W., Elzie, C. a, Kucik, D. F., & Murphy-Ullrich, J. E. (2003). Thrombospondin signaling through the calreticulin/LDL receptor-related protein co-complex stimulates random and directed cell migration. *Journal of Cell Science*, *116*(Pt 14), 2917–27.

Pearl, L. H., Prodromou, C., & Workman, P. (2008). The Hsp90 molecular chaperone: an open and shut case for treatment. *The Biochemical Journal*, *410*(3), 439–53.

Pepin, K., Momose, F., Ishida, N., & Nagata, K. (2000). Molecular Cloning of Horse Hsp90 cDNA and Its Comparative Analysis with Other Vertebrate Hsp90 Sequences. *J.Vet. Med. Sci.*, *63*(2), 115–124.

Pickup, M. W., Mouw, J. K., & Weaver, V. M. (2014). The extracellular matrix modulates the hallmarks of cancer. *EMBO Reports*, *15*(12), 1243–53.

Piper, P. W., & Millson, S. H. (2011). Mechanisms of Resistance to Hsp90 Inhibitor Drugs: A Complex Mosaic Emerges. *Pharmaceuticals*, *4*, 1400–1422.

Polavarapu, R., An, J., Zhang, C., & Yepes, M. (2008). Regulated Intramembrane Proteolysis of the Low-Density Lipoprotein Receptor-Related Protein Mediates Ischemic Cell Death. *The American Journal of Pathology*, *172*(5), 1355–1362.

Ponti, A., Machacek, M., Gupton, S., Waterman-Storer, C., & Danuser, G. (2004). Two Distinct Actin Networks Drive the Protrusion of Migrating Cells. *Science*, *305*, 1782–1787.

Pratt, B. (1998). The hsp90-based Chaperone System : Involvement in Signal Transduction from a variety of hormone and growth factor receptors. *Society for Experimental Biology and Medicin*, *217*.

Prodromou, C., Roe, S. M., Brien, R. O., Ladbury, J. E., Piper, P. W., & Pearl, L. H. (1997). Identification and Structural Characterization of the ATP / ADP-Binding Site in the Hsp90 Molecular Chaperone. *Cell*, *90*, 65–75.

Qin, D., Zhang, G.-M., Xu, X., & Wang, L.-Y. (2015). The PI3K/Akt signaling pathway mediates the high glucose-induced expression of extracellular matrix molecules in human retinal pigment epithelial cells. *Journal of Diabetes Research*, 1–11.

Quinn, K. A., Pye, V. J., Dai, Y., Chesterman, C. N., Owensby, D. A., & Al, Q. E. T. (1999). Characterization of the Soluble Form of the Low Density Lipoprotein Receptor-Related Protein (LRP). *Experimental Cell Research*, *251*, 433–441.

Ranganathan, S., Cao, C., Migliorini, M., Zhang, L., & Strickland, D. K. (2011). Molecular Basis for the Interaction of Low Density Lipoprotein Receptor-related Protein 1 (LRP1) with integrin αMbeta2: IDENTIFICATION OF BINDING SITES WITHIN αMbeta2 FOR LRP1. *Journal of Biological Chemistry*, *286*(35), 30535–30541.

Richter, K. & Buchner, J. (2001). Hsp90:Chaperoning Signal Transduction. *Journal of Cell. Phys.*, 188: 281-290.

Ridley, A. J., Schwartz, M. A., Burridge, K., Firtel, R. A., Ginsberg, M. H., Borisy, G., & Horwitz, A. R. (2003). Cell Migration : Integrating Signals from Front to Back. *Science*, *302*, 1704–1710.

Riebold, M., Paez-pereda, M., Kozany, C., Freiburger, L., Sattler, M., Buchfelder, M., … Stalla, G. K. (2015). A C-terminal HSP90 inhibitor restores glucocorticoid sensitivity and relieves a mouse allograft model of Cushing disease A C-terminal HSP90 inhibitor restores glucocorticoid sensitivity and relieves a mouse allograft model of Cushing disease. *Nature Medicine*, *12*, 1–7.

Ritossa, F. (1962). A new puffing pattern induced by temperature shock and DNP in drosophila. *Experientia*, *18*(12), 571–573.

Röhl, A., Rohrberg, J., & Buchner, J. (2013). The chaperone Hsp90: changing partners for demanding clients. *Trends in Biochemical Sciences*, *38*(5), 253–62.

Rozario, T., & DeSimone, D. W. (2010). The extracellular matrix in development and morphogenesis: a dynamic view. *Developmental Biology*, *341*(1), 126–40.

Ruckova, E. V. A., Muller, P., & Nenutil, R. (2012). Alterations of the Hsp70/Hsp90 chaperone and the HOP/CHIP co-chaperone system in cancer. *Celluar and Molecular Biology Letters*, *17*, 446–458.

Ryu, S., Jimi, S., Eura, Y., Kato, T., & Takebayashi, S. (1999). Strong intracellular and negative peripheral expression of fibronectin in tumor cells contribute to invasion and metastasis in papillary thyroid carcinoma. *Cancer Letters*, *146*, 103–109.

Salicioni, A. M., Mizelle, K. S., Loukinova, E., Mikhailenko, I., Strickland, D. K., & Gonias, S. L. (2002). The low density lipoprotein receptor-related protein mediates fibronectin catabolism and inhibits fibronectin accumulation on cell surfaces. *The Journal of Biological Chemistry*, *277*(18), 16160–6.

Schedin, P., Strange, R., Mitrenga, T., Wolfe, P., & Kaeck, M. (2000). Fibronectin fragments induce MMP activity in mouse mammary epithelial cells: evidence for a role in mammary tissue remodeling. *Journal of Cell Science*, *113 (Pt 5*, 795–806.

Schlesinger, P. H., Krogstad, D. J., & Herwaldt, B. L. (1988). Antimalarial agents: Mechanisms of action. *Antimicrobial Agents and Chemotherapy*, *32*(6), 793–798.

Schwarzbauer, J. E. (1991). Fibronectin: from gene to protein. *Current Opinion in Cell Biology*, *3*(5), 786–91.

Schwarzbauer, J. E., & DeSimone, D. W. (2011). Fibronectins, their fibrillogenesis, and in vivo functions. *Cold Spring Harbor Perspectives in Biology*, *3*(7), 1–19.

Schwarzbauer, J. E., & Sechler, J. L. (1999). Fibronectin fibrillogenesis: a paradigm for extracellular matrix assembly. *Current Opinion in Cell Biology*, *11*(5), 622–627.

Schweinfest, C. W., Graber, M. W., Henderson, K. W., Papas, T. S., Baron, P. L., & Watson, D. K. (1998). Cloning and sequence analysis of Hsp89 αN, a new member of the Hsp90 gene family. *Biochimica et Biophysica Acta*, 18–24.

Shi, F., & Sottile, J. (2008). Caveolin-1-dependent beta1 integrin endocytosis is a critical regulator of fibronectin turnover. *Journal of Cell Science*, *121*(Pt 14), 2360–2371.

Sidera, K., El Hamidieh, A., Mamalaki, A., & Patsavoudi, E. (2011). The 4C5 cell-impermeable anti-HSP90 antibody with anti-cancer activity, is composed of a single light chain dimer. *PloS One*, *6*(9), e23906.

Sidera, K., Gaitanou, M., Stellas, D., Matsas, R., & Patsavoudi, E. (2008). A critical role for HSP90 in cancer cell invasion involves interaction with the extracellular domain of HER-2. *The Journal of Biological Chemistry*, *283*(4), 2031–41.

Sidera, K., & Patsavoudi, E. (2014). HSP90 inhibitors: current development and potential in cancer therapy. *Recent Patents on Anti-Cancer Drug Discovery*, *9*(1), 1–20.

Sidera, K., Samiotaki, M., Yfanti, E., Panayotou, G., & Patsavoudi, E. (2004). Involvement of cell surface HSP90 in cell migration reveals a novel role in the developing nervous system. *The Journal of Biological Chemistry*, *279*(44), 45379–88.

Siegel, R. L., Miller, K. D., & Jemal, A. (2015). Cancer Statistics, 2015. *CA Cancer J Clin*, *65*(1), 5–29.

Sims, J. D., McCready, J., & Jay, D. G. (2011). Extracellular heat shock protein (Hsp)70 and Hsp90α assist in matrix metalloproteinase-2 activation and breast cancer cell migration and invasion. *PloS One*, *6*(4), e18848.

Solit, D. B., & Chiosis, G. (2008). Development and application of Hsp90 inhibitors. *Drug Discovery Today*, *13*(1-2), 38–43.

Somanath, P. R., Kandel, E. S., Hay, N., & Byzova, T. V. (2007). Akt1 Signaling Regulates Integrin Activation, Matrix Recognition, and Fibronectin Assembly. *Journal of Biological Chemistry*, *282*(31), 22964–22976.

Song, H., Li, Y., Lee, J., Schwartz, A. L., & Bu, G. (2009). Low-Density Lipoprotein Receptor-Related Protein 1 Promotes Cancer Cell Migration and Invasion by Inducing the Expression of Matrix Metalloproteinases 2 and 9. *Cancer Research*, *69*(3), 879–887.

Song, X., Wang, X., Zhuo, W., Shi, H., Feng, D., Sun, Y., & Luo, Y. (2010). The regulatory mechanism of extracellular Hsp90{alpha} on matrix metalloproteinase-2 processing and tumor angiogenesis. *The Journal of Biological Chemistry*, *285*(51), 40039–49.

Sottile, J., & Chandler, J. (2005). Fibronectin matrix turnover occurs through a caveolin-1-dependent process. *Molecular Biology of the Cell*, *16*(2), 757–68.

Spuch, C., Ortolano, S., & Navarro, C. (2012). LRP-1 and LRP-2 receptors function in the membrane neuron . Trafficking mechanisms and proteolytic processing in Alzheimer ' s disease. *Frontiers in Membrane Physiology and Biophysics*, *3*(269), 1–14.

Sreedhar, A. S., Kalmár, É., Csermely, P., & Shen, Y.-F. (2004). Hsp90 isoforms: functions, expression and clinical importance. *FEBS Letters*, *562*(1-3), 11–15.

Steeg, P. S. (2006). Tumor metastasis: mechanistic insights and clinical challenges. *Nature Medicine*, *12*(8), 895–904.

Stellas, D., El Hamidieh, A., & Patsavoudi, E. (2010). Monoclonal antibody 4C5 prevents activation of MMP2 and MMP9 by disrupting their interaction with extracellular HSP90 and inhibits formation of metastatic breast cancer cell deposits. *BMC Cell Biology*, *11*, 51.

Stellas, D., Karameris, A., & Patsavoudi, E. (2007). Monoclonal antibody 4C5 immunostains human melanomas and inhibits melanoma cell invasion and metastasis. *Clinical Cancer Research : An Official Journal of the American Association for Cancer Research*, *13*(6), 1831–8.

Strickland, D. K., Ashcorns, J. D., Williams, S., Burgessq, W. H., Migliorinis, M., & Argraves, W. S. (1990). Communication Sequence Identity between the α2- Macroglobulin Receptor and Low Density Lipoprotein Receptor- related Protein Suggests That This Molecule Is a Multifunctional Receptor*. *Journal of Biological Chemistry*, *265*(29), 17401–17405.

Strickland, K.D., Kounnas, Maria.Z., Argraves, S. (1995). LDL receptor-related for lipoprotein protein : a multiligand catabolism receptor and proteinase. *FASEB Journal*, *9*, 890–898.

Stringa, E., Knäuper, V., Murphy, G., & Gavrilovic, J. (2000). Collagen degradation and platelet-derived growth factor stimulate the migration of vascular smooth muscle cells. *J Cell Sci*, *113*, 2055–2064.

Swiatoniowski, G., Matkowski, R., Suder, E., Bruzewicz, S., Setta, M., & Kornafel, J. A. N. (2005). E-cadherin and Fibronectin Expressions Have No Prognostic Role in Stage II Ductal Breast Cancer. *Anticancer Research*, *25*, 2879–2883.

Taipale, M., Krykbaev, I., Koeva, M., Kayatekin, C., Westover, D. ., Karras, G. I., & Lindquist, S. (2012). Quantitative Analysis of Hsp90-Client Interactions Reveals Principles of substrate recognition. *Cell*, *150*(5), 987–1001.

Takada, Y., Ye, X., & Simon, S. (2007). The integrins. *Genome Biology*, *8*(5), 215.

Theocharis, A. D., Skandalis, S. S., Gialeli, C., & Karamanos, N. K. (2015). Extracellular matrix structure. *Advanced Drug Delivery Reviews*.

Tissières, A, Mitchell, H. K., & Tracy, U. M. (1974). Protein synthesis in salivary glands of Drosophila melanogaster: relation to chromosome puffs. *Journal of Molecular Biology*, *84*(3), 389–398.

To, W. S., & Midwood, K. S. (2011). Plasma and cellular fibronectin: distinct and independent functions during tissue repair. *Fibrogenesis & Tissue Repair*, *4*(1), 21. doi:10.1186/1755-1536-4-21

Tomasini-Johansson, B. R., Kaufman, N. R., Ensenberger, M. G., Ozeri, V., Hanski, E., & Mosher, D. F. (2001). A 49-Residue Peptide from Adhesin F1 of Streptococcus pyogenes Inhibits Fibronectin Matrix Assembly. *Journal of Biological Chemistry*, *276*(26), 23430–23439.

Trepel, J., Mollapour, M., Giaccone, G., & Neckers, L. (2010). Targeting the dynamic HSP90 complex in cancer. *Nature Reviews. Cancer*, *10*(8), 537–49.

Triantafilou, M., & Triantafilou, K. (2004). Heat-shock protein 70 and heat-shock protein 90 associate with Toll-like receptor 4 in response to bacterial lipopolysaccharide. *Biochem Soc Trans*, *32*(Pt 4), 636–639.

Tsen, F., Bhatia, A., O'Brien, K., Cheng, C.-F., Chen, M., Hay, N., Li, W. (2013). Extracellular heat shock protein 90 signals through subdomain II and the NPVY motif of LRP-1 receptor to Akt1 and Akt2: a circuit essential for promoting skin cell migration in vitro and wound healing in vivo. *Molecular and Cellular Biology*, *33*(24), 4947–59.

Tsutsumi, S., Beebe, K., & Neckers, L. (2009). Impact of heat-shock protein 90 on cancer metastasis. *Future Oncology*, *5*(5), 679–88.

Tsutsumi, S., & Neckers, L. (2007). Extracellular heat shock protein 90: a role for a molecular chaperone in cell motility and cancer metastasis. *Cancer Science*, *98*(10), 1536–1539.

Ullrich, S. J., Robinson, E. A., Law, L. W., Willinghamt, M., & Appella, E. (1986). A mouse tumor-specific transplantation antigen is a heat shock related protein. *Proc Natl Acad. Sci*, *83*, 3121–3125.

Vasko, R. C., Rodriguez, R. A., Cunningham, C. N., Ardi, V. C., Agard, D. A., & McAlpine, S. R. (2010). Mechanistic Studies of Sansalvamide A-Amide: An Allosteric Modulator of Hsp90.

ACS Medicinal Chemistry Letters, *1*(1), 4–8.

Villiger, B., Kelley, D. G., Engleman, W., Kuhn, C., & McDonald, J. a. (1981). Human alveolar macrophage fibronectin: synthesis, secretion, and ultrastructural localization during gelatin-coated latex particle binding. *The Journal of Cell Biology*, *90*(3), 711–20.

Voss, A., Thomas, T., & Gruss, P. (2000). Mice lacking HSP90beta fail to develop a placental labyrinth. *Development*, *127*(1), 1–11.

Wandinger, S. K., Richter, K., & Buchner, J. (2008). The Hsp90 chaperone machinery. *The Journal of Biological Chemistry*, *283*(27), 18473–7.

Wang, X., Song, X., Zhuo, W., Fu, Y., Shi, H., Liang, Y., Luo, Y. (2009). The regulatory mechanism of Hsp90alpha secretion and its function in tumor malignancy. *Proceedings of the National Academy of Sciences of the United States of America*, *106*(50), 21288–21293.

Weaver, A. M., Hussaini, I. M., Mazar, A., Henkin, J., & Gonias, S. L. (1997). Embryonic Fibroblasts That Are Genetically Deficient in Low Density Lipoprotein Receptor-related Protein Demonstrate Increased Activity of the Urokinase Receptor System and Accelerated Migration on Vitronectin. *Journal of Biological Chemistry*, *272*(22), 14372–14379.

Webb, D. J., Nguyen, D. H., & Gonias, S. L. (2000). Extracellular signal-regulated kinase functions in the urokinase receptor-dependent pathway by which neutralization of low density lipoprotein receptor-related protein promotes fibrosarcoma cell migration and matrigel invasion. *Journal of Cell Science*, *113 (1)*, 123–134.

Webb, D. J., Parsons, J. T., & Horwitz, A. F. (2002). Adhesion assembly , disassembly and turnover in migrating cells – over and over and over again. *Nature Cell Biology*, *4*, 1–4.

Wegele, H., Muller, L., & Buchner, J. (2004). Hsp70 and Hsp90—a relay team for protein folding. *Rev Physiol Biochem Pharmacol*, 151:1–44.

Whitesell, L., & Lindquist, S. L. (2005). HSP90 AND THE CHAPERONING OF CANCER. *Nature Reviews*, *5*, 761–772.

Wierzbicka-Patynowski, I., & Schwarzbauer, J. E. (2003). The ins and outs of fibronectin matrix assembly. *Journal of Cell Science*, *116*(Pt 16), 3269–76.

Williams, S. E., Ashcom, J. D., Argraves, W. S., & Strickland, D. K. (1992). A Novel Mechanism for Controlling the Activity of α2-Macroglobulin Receptor / Low Density Lipoprotein Receptor-related Protein. *Journal of Biological Chemistry*, *267*(13), 9035–9040.

Willnow, T. E., & Herz, J. (1994). Genetic deficiency in low density lipoprotein receptor-related protein confers cellular resistance to Pseudomonas exotoxin A. Evidence that this protein is required for uptake and degradation of multiple ligands. *Journal of Cell Science*, *107*, 719–726.

Willnow, T. E., Orth, K., & Herz, J. (1994). Molecular dissection of ligand binding sites on the low density lipoprotein receptor-related protein. *Journal of Biological Chemistry*, *269*(22), 15827–15832.

Xu, J., Rodriguez, D., Petitclerc, E., Kim, J. J., Hangai, M., Yuen, S. M., Brooks, P. C. (2001).

Proteolytic exposure of a cryptic site within collagen type IV is required for angiogenesis and tumor growth in vivo. *Journal of Cell Biology*, *154*(5), 1069–1079.

Zhang, F., Snead, C. M., & Catravas, J. D. (2012). Hsp90 regulates O -linked beta-N -acetylglucosamine transferase : a novel mechanism of modulation of protein O -linked beta-N -acetylglucosamine modification in endothelial cells. *American Journal of Physiology Cell Physiology*, *302*, 1786–1796.

Zhang, X., Chen, C. T., Bhargava, M., & Torzilli, P. A. (2013). A Comparative Study of Fibronectin Cleavage by MMP-1, -3, -13, and -14. *Cartilage*, *3*(3), 267–277.

Zügel, U., & Kaufmann, S. H. (1999). Role of heat shock proteins in protection from and pathogenesis of infectious diseases. *Clinical Microbiology Reviews*, *12*(1), 19–39.

Zurawska, A., Urbanski, J., & Bieganowski, P. (2008). Hsp90n - An accidental product of a fortuitous chromosomal translocation rather than a regular Hsp90 family member of human proteome. *Biochimica et Biophysica Acta*, *1784*(11), 1844–6.

Zurhove, K., Nakajima, C., Herz, J., Bock, H. H., & May, P. (2008). Gamma-secretase limits the inflammatory response through the processing of LRP1. *Science Signaling*, *1*(47), 1–24.

Chapter 6. APPENDIX

6.1 PTZ57R-FN standard curves for quantification of FN mRNA in MEF-1 and PEA-13 NOV treated samples

The pTZ-FN construct as described in Methods of known concentration (301 ng/µl), served as the FN standard with which we generated a standard curve. The concentrations of test samples were calculated directly from this standard curve. Varying concentrations (10 ng - 1 x 10^{-6} ng) of the FN standard were prepared by diluting with nuclease free water. FN standards were run alongside test mRNA samples to generate a standard curve for the absolute quantification of FN mRNA levels from MEF-1 and PEA-13 cells (Figure 16).

A)

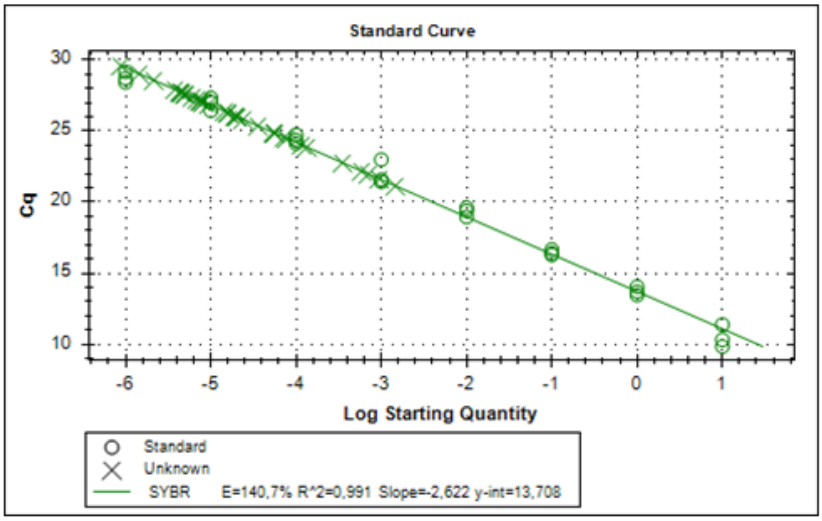

B)

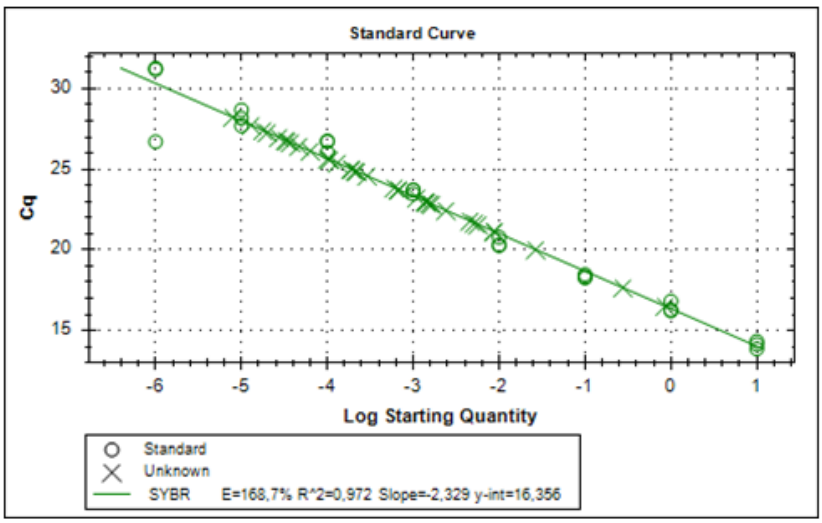

Figure 16: FN standard curves for absolute quantification of FN mRNA levels

Standard curves were generated from the pTZ-FN vector and mRNA levels of **A)** MEF-1 and **B)** PEA-13 treatments were quantified against known concentrations of the FN plasmid. qRT-PCR parameters are outlined in Methods. Graphs were generated using Bio-Rad™ CFX Manager 3.0 Software.

6.2 Overexpression and solubilisation of LRP1 inhibitor, RAP1

The partial colocalisation observed between FN and LRP1 as well as the gradual loss in levels of extracellular FN matrix observed in MEF-1 cells upon NOV treatment prompted us to want to investigate whether inhibiting LRP1 would diminish the observed colocalisation upon NOV treatment and abrogate the loss of FN matrix in MEF-1 cells. Because the site of the interaction between Hsp90, LRP1 and FN is unknown, and rather than using an epitope specific antibody (which is also limited to only 1 ligand binding domain), we aimed to use RAP1 (receptor associated protein 1) which is known to block all interactions of ligands with LRP1 (Willnow & Herz, 1994). The pQTEV-LRPAP1 plasmid, a gift from Konrad Buessow (Addgene plasmid #31327), encoding N-terminal His-tagged RAP1 was used for expression and purification using an adapted protocol from Herz *et al.,* (1991). The plasmid was transformed in *E.coli* BL21 competent cells and an induction study was carried out to determine the optimal time required for protein expression. Expression was induced by addition of 1 mM isopropyl β-D-1-thiogalactopyranoside (IPTG) at 37 ˚C and samples collected at hourly intervals and overnight were resolved by SDS-PAGE (Figure 17A). The arrow indicates the band at the predicted molecular weight of His-tagged RAP1 (41 kDa). The band intensity increased from time indicated 0-8 hours post induction. Induction fractions were also analysed by immunoblotting for His-tagged RAP1 using rabbit anti-His primary antibody (Figure 17B). A faint band is observed at the predicted MW of RAP1 which appears to increase with induction time. Non-specific lower molecular weight bands are observed at 25 kDa in all fractions (Figure 17B). From these data, we decided to use the 4 hour post induction sample as the optimal time point for harvesting RAP1 expressing BL21 cells.

After a 4 hour induction with IPTG, RAP1 expressing BL21 cells were used in affinity purification with MagReSyn™-NTA beads and fractions collected throughout the purification were resolved by SDS-PAGE (Figure 18A). The band at the predicted size of RAP1 appears faint in both elution fractions (E1 and E2) with several other bands of contaminating proteins still present. We suspected that either there was insufficient lysis of cells to release expressed RAP1 or that RAP1 was largely insoluble, owing to the presence of a thick band still in the pellet and cleared lysate fractions (Figure 18A, lane P and CL). We decided to conduct a solubility study to determine whether incorporating a specific detergent into the lysis buffer would assist in solubilising the protein and/or releasing it from cells. pQTEV-LRPAP1

transformed BL21 cells were induced for 4 hours and harvested cell pellets were resuspended in lysis buffer (10 mM Tris-Cl pH 7.5, 300 mM NaCl, 50 mM imidazole) containing different detergents (numbered i-vii). Lysis buffer was supplemented with (i) 0.2% [v/v] Triton-X-100, (ii) 0.4% [v/v] Tween-20, (iii) 0.2% [v/v] Triton-X-100 & 0.4% [v/v] Tween-20, (iv) 1% [v/v] NP40, (v) 6% [w/v] sarcosyl, (vi) 0.1% [v/v] TBS-Tween, (vii) 4% [v/v] Triton-X-100. Pellet (P) and supernatant (SN) fractions in each of the seven alternative treatments were resolved by SDS-PAGE (Figure 18B) and analysed by immunoblotting (Figure 18C). The ability of these detergents to solubilise RAP1 was compared to lysis buffer without any added detergent (UNT). The arrows alongside indicate the band position of the expected size of RAP1. Expression of protein was observed in all samples but the highest band intensity was observed in treatments (iv) and (v) (Figure 18B). Treatment with 6% [w/v] sarcosyl (v) appeared to greatly increase the proportion of RAP1 protein in the supernatant fraction (lane SN) compared to the pellet (lane P). Immunoblot analysis of the His-tagged RAP1 samples from the solubility study (Figure 18C) revealed several lower molecular weight non-specific bands. Faint bands (indicated by the arrow) were observed at the predicted size of RAP1 across all treatments, but the 6% [w/v] sarcosyl treatment (v) was the only sample which produced a distinct band at the predicted molecular weight (~41 kDa). From these data, sarcosyl appeared to provide the most favourable conditions for solubilising RAP1 and thus we decided to include this detergent in all subsequent purifications.

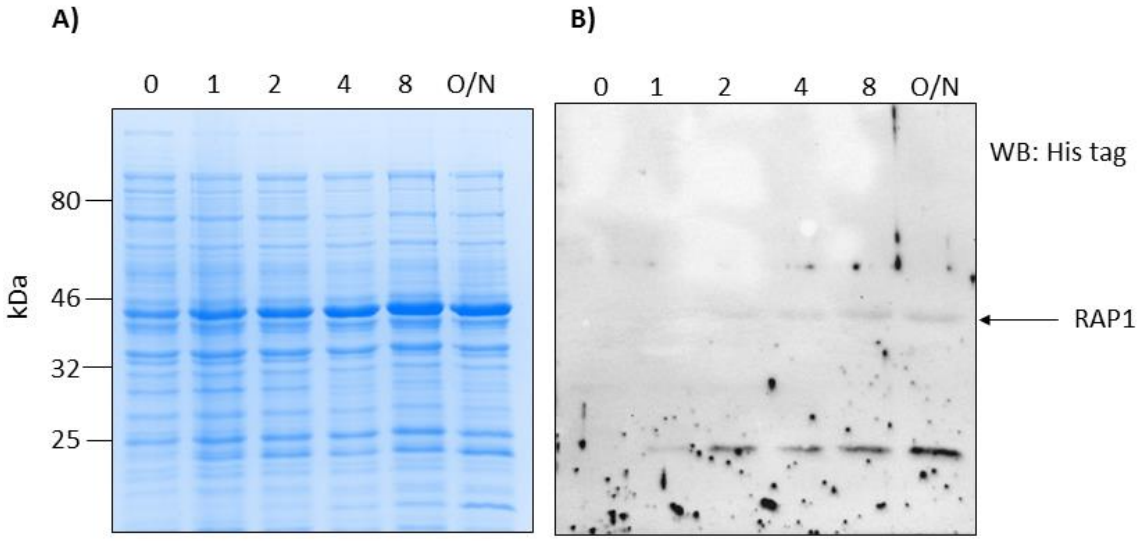

Figure 17: Induction study of RAP1

RAP1 was induced with 1 mM IPTG in *E.coli* BL21 cells and samples collected at various time points over 24 hours. Samples were resolved on a 4-10% SDS-PAGE gel and **A)** stained with Coomassie Brilliant Blue and **B)** Western blot probed for RAP1 with rabbit antibody against the His tag. Numbers above the figure indicate hours post induction. Arrow indicates the predicted size of His-tagged RAP1 (41 kDa).

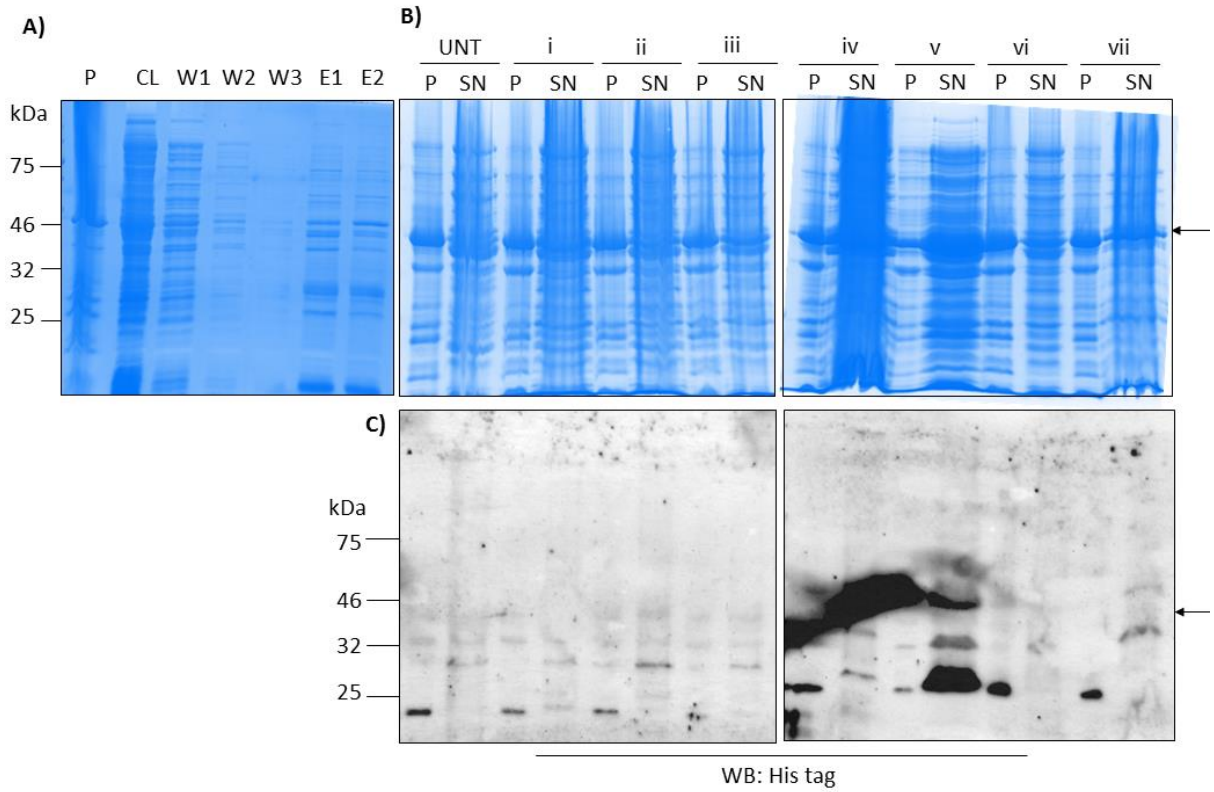

Figure 18: Solubility study of RAP1

A) RAP1 was induced for 4 hours with 1 mM IPTG at 37 ˚C in *E.coli* BL21 cells. RAP1 was purified using MagReSyn NTA beads and samples collected throughout the purification process were resolved by 4-10% SDS-PAGE. Letters above indicate the pellet (P), cleared lysate (CL), wash (W), and elution fractions (E). To determine optimal conditions for solubility of RAP1, following induction as described previously, samples were treated with various detergents and resolved on **B)** SDS-PAGE and **C)** probed for His tag. Numbering above indicates the detergent i) 0.2% Triton-X, ii) 0.4% Tween-20, iii) 0.2% Triton & 0.4% Tween-20, iv) 1% NP40, (v) 6% sarcosyl, vi) 0.1% TBST, (vii) 4% Triton-X. Letters (P) and (SN) denotes the pellet and supernatant fractions respectively. Arrows indicate RAP1.

6.3 Optimisation of RAP1 purification conditions

The induced RAP1 protein was affinity purified from *E.coli* cell lysates using either MagReSyn™-NTA beads or Nickel charged Sepharose fast flow beads. Samples were collected at each stage of the purification process and resolved by SDS-PAGE (Figure 19A). The presence of contaminating bands in both elution fractions were observed although much fewer were present in the MagReSyn elution compared to the Sepharose elutions. Interestingly, the MagReSyn wash (W) appeared to contain the fewest contaminating bands. Immunoblotting of purification fractions with anti-His antibody revealed faint bands at the predicted size of RAP1 (41 kDa, indicated by arrow) in all lanes except MagReSyn wash (W) and elution (E) fractions (Figure 19B). Again, non-specific bands were detected by the anti-His antibody which may represent degradation fragments of RAP1.

Given the high degree of contaminating bands present in the Sepharose purification, we decided the MagReSyn purification protocol was superior as it provided a more pure elution product.

Then, contaminating endotoxin (ET) was removed from elution fractions. This was done in two alternative approaches. In Figure 19C and D (ii), the eluted fraction was buffer exchanged using a Zeba spin desalting column and passed through an ET-removal column (lane E). In (iii), RAP1 cleared lysate was first passed through an ET-removal column overnight and subsequently buffer exchanged. A faint band representing the resulting RAP1 purified protein is represented in lane E (Figure 19C, iii). The flow through (FT), wash (W) and elution (E) fractions of MagReSyn purification without ET-removal were also resolved alongside the treated fractions (Figure 19C and D, i). The immunoblot of these fractions with anti-His tag antibody revealed intense bands in FT lanes and fainter bands in wash lanes. Very little to no protein was detected in elution lanes (Figure 19C and D, i). The protein levels were quantified using a NanoDrop 2000 spectrophotometer, however, very low yields of protein in each of the different elution fractions were obtained (i: 0.15 mg/ml, ii: 0.06 mg/ml, 0.12 mg/ml) and thus neither were usable. Due to time constraints further optimization of RAP1 purification was halted for future study.

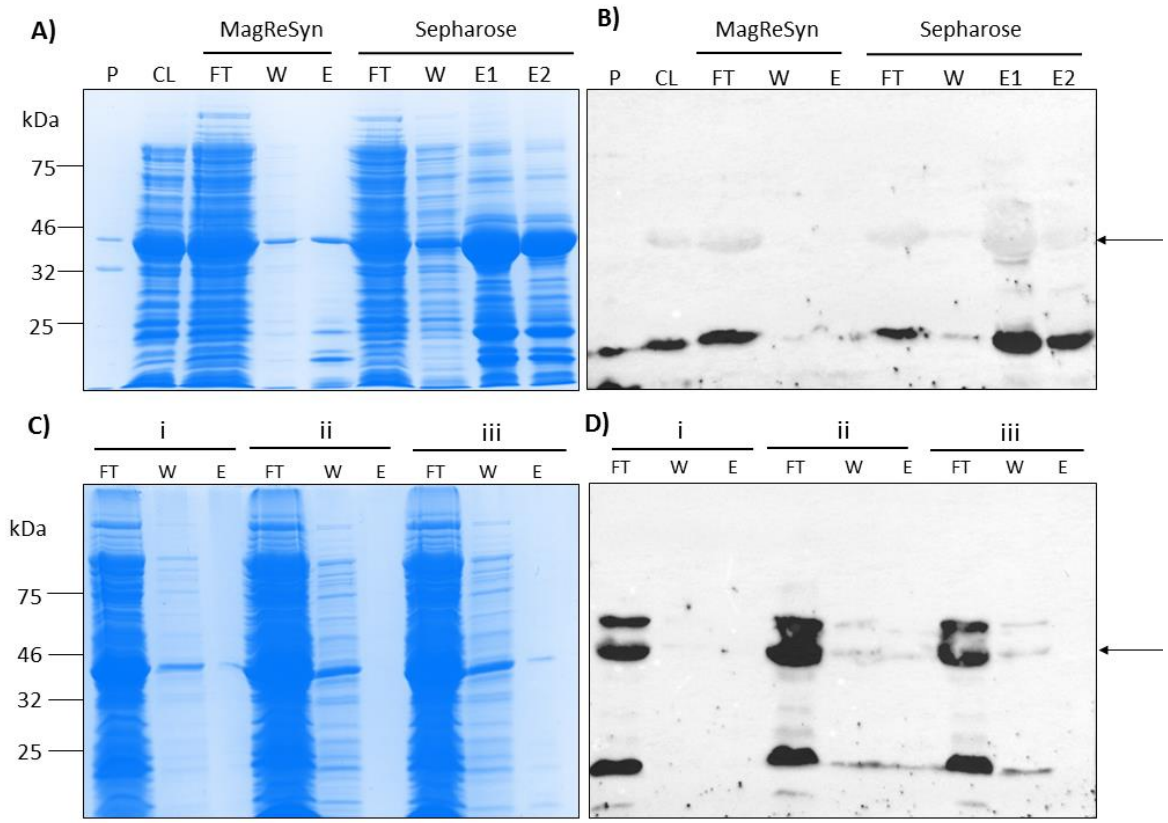

Figure 19: Optimisation of RAP1 purification conditions

A) Following 4 hour induction of RAP1 with 1 mM IPTG at 37 ˚C cells were lysed in resuspension buffer containing 6% [w/v] sarcosyl. After centrifugation at 16000 xg for 30 min at 4 ˚C the supernatant was added to either MagReSyn-NTA beads or nickel charged Sepharose beads. Fractions were collected throughout the purification and analysed on SDS-PAGE and **B)** western blot analysis with anti-His tag. RAP1 was induced as previously described and samples collected from the various downstream processing to yield purified endotoxin free RAP1 protein were analysed by **C)** SDS-PAGE and **D)** western blot. i) RAP1 purified with MagReSyn-NTA beads, ii) RAP1 eluted from MagResyn-NTA was buffer exchanged using a Zeba Spin desalting column followed by endotoxin (ET) removal using a Pierce high capacity ET removal resin. iii) The cleared lysate of RAP1 was incubated overnight with ET removal resin followed by purification with MagReSyn-NTA and elution fraction was buffer exchanged. Letters above each lane indicate pellet (P), cleared lysate (CL), flow through (FT), wash (W) and elution (E) fractions. Arrows indicate purified RAP1.

6.4 Determination of the affinity and binding domain on LRP1 for FN *in vitro*

To determine the role of LRP1 and Hsp90 in modulating FN turnover, it is necessary to define the interaction between these two molecules by mapping out the region on LRP1 to which FN and Hsp90 binds. A series of soluble recombinant receptor fragments were kindly provided by Dr Dudley Strickland (University of Maryland, USA) and are represented in Figure 20 alongside full length LRP1 (Mikhailenko *et al.,* 2001). Each of these soluble receptor fragments (sLRP1) contain various clusters of ligand-binding type repeats from the extracellular heavy chain of LRP1 and will be tested in future study for their ability to bind FN *in vitro*.

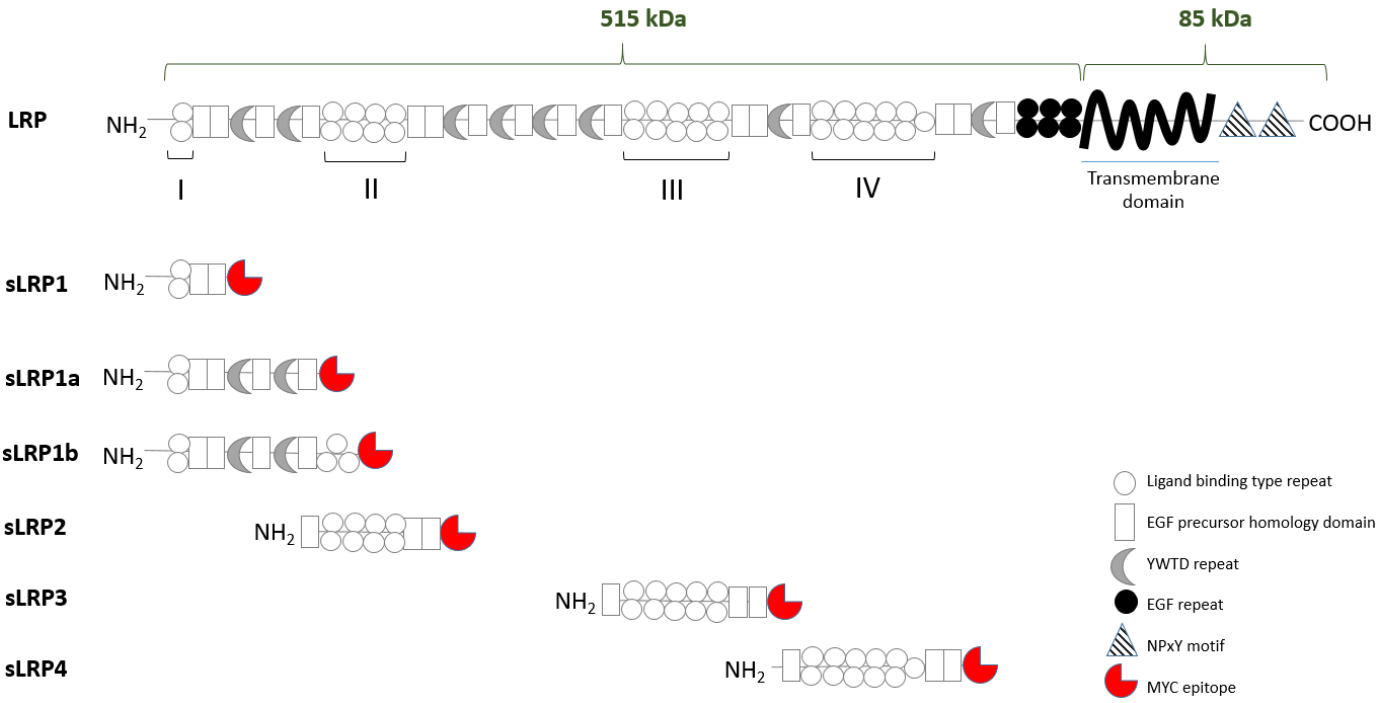

Figure 20: Secreted LRP1 fragments alongside full length LRP1 used for mapping of fibronectin and Hsp90 binding domain studies.

Each of the sLRP1 fragments contains only regions of the extracellular domain and is named according to the cluster (I-IV) of ligand binding type repeat which they comprise. Each contains a c-MYC epitope as indicated which is recognised by an anti-c-MYC antibody.